The Aurora B-dependent NoCut checkpoint prevents damage of anaphase bridges after DNA replication stress

Nuno Amaral

TESI DOCTORAL UPF / 2015

Thesis supervisor

Dr. Manuel Mendoza

CHROMOSOME SEGREGATION AND CYTOKINESIS LABORATORY

CELL AND DEVELOPMENTAL BIOLOGY PROGRAM

CENTER FOR GENOMIC REGULATION (CRG)

Els resultats de la tesi poden consultar-se també en l'article:

Amaral N, Vendrell A, Funaya C, Idrissi FZ, Maier M, Kumar A, Neurohr G,Colomina N, Torres-Rosell J, Geli MI, Mendoza M. The Aurora-B-dependent NoCut checkpoint prevents damage of anaphase bridges after DNA replication stress. Nat Cell Biol. 2016 May;18(5):516-26. doi: 10.1038/ncb3343.

Abstract

Coordination of cytokinesis with chromosome segregation is essential to maintain genome stability during cell proliferation. In yeast and animal cells, anaphase chromatin bridges induce an abscission delay through the Aurora B-dependent NoCut checkpoint. However, it is not known whether inhibition of abscission prevents damage of chromatin bridges and how these bridges are detected. We find that chromatin bridges induced by DNA replication stress or by defects in condensin or topoisomerase II delay abscission through the NoCut checkpoint. This delay prevents cytokinesis-dependent DNA damage and promotes cellular viability, after replication stress. Surprisingly, chromatin bridges from dicentric chromosomes are not sufficient to trigger NoCut. Additionally, we find that anaphase spindle stabilization, through APC-Cdh1, is essential for the NoCut response and can trigger NoCut in cells with dicentric bridges. We propose that chromosomal structural defects, from replication stress, decondensation or persistent catenations, trigger NoCut through impairment of APC-Cdh1 activity. This stabilizes the mitotic spindle and allows midzone-bound Aurora B to detect chromatin bridges and inhibit abscission.

Resum

La coordinació de la citocinesis amb la segregació cromosòmica és essencial per mantenir l'estabilitat cromosòmica durant la proliferació cel·lular. Tant en llevat com en cèl·lules animals, els ponts de cromatina en anafase indueixen un retard en l'absició promogut pel "NoCut checkpoint" dependent d'Aurora B.

No obstant això, es desconeix si la inhibició de l'abscisió protegeix del dany derivat dels ponts de cromatina i com aquests ponts son detectats. Hem descobert que els ponts de cromatina induïts per estrès replicatiu de l'ADN, defectes en condensació o en la topoisomerasa II atracen l'abscisió per mitjà del "NoCut checkpoint". Aquest retard prevé el dany al DNA citocinesis-dependent i promou la viabilitat cel·lular, després de l'estrès replicatiu. Sorprenentment, el ponts de cromatina dels cromosomes dicèntrics no són suficients per desencadenar un "NoCut checkpoint". A més a més, hem vist que l'estabilització del fus mitòtic en anafase, a través de APC-Cdh1, és essencial per la resposta NoCut i pot activar el NoCut en cèl·lules amb ponts dicentrics. Proposem que defectes estructurals dels cromosomes deguts a estrès replicatiu, descondensació o catenacions persistents, activen el NoCut a través d'una deficiència en l'activitat de la APC-Cdh1. Això estabilitza el fus mitòtic i permet a l'aurora B present a la "midzone" detectar els ponts de cromatina i inhibir l'abscisió.

Preface

In the work presented in this thesis, we show that, during anaphase, DNA bridges of different origins lead to different cellular responses, with different consequences to the cells. Anaphase DNA bridges can affect chromosome segregation and activate the NoCut checkpoint, which has been proposed to protect segregating chromosomes from damage caused by cytokinesis. However, some DNA bridges seem to evade detection by the NoCut checkpoint and are damaged. The reason for this difference was not known.

Our results suggest that anaphase bridges with under-replicated DNA, decondensed DNA and persistent DNA catenations activate the NoCut checkpoint, which delays the completion of cytokinesis to prevent damage of mis-segregated chromosomes. Moreover, inhibition of cytokinesis by the NoCut checkpoint requires the stabilization of the anaphase spindle, which we propose to allow for the detection of DNA bridges at the site of division. However, anaphase bridges from dicentric chromosomes, which presumably are properly replicated, condensed and decatenated, do not activate NoCut. Therefore, our work suggests that, by detecting specific chromosomal defects during DNA segregation, the NoCut checkpoint acts as a last safeguard mechanism to the cells.

Contents

1. Introduction

Accurate chromosome segregation is essential to maintain the genomic stability of all organisms. To ensure correct partitioning of the genome between the dividing cells this process must be tightly coordinated with cell division. In this study I have focused on understanding the mechanism behind such coordination. Before presenting the results of this work I will briefly introduce the relevant aspects of the eukaryotic cell cycle, with a special focus on cytokinesis.

1.1. Cell cycle

To divide and proliferate cells go through cycles of division. Each of these cycles is composed of a series of sequential processes with the final aim of producing two independent cells. In a proliferative cell each phase of the cell cycle prepares the cell for division, initially by synthesizing and duplicating its components and later by distributing those components into two daughter cells to finally individualize them. At the end of the cycle the cell is divided into two genetically identical cells by the process of cytokinesis.

1.1.1. Cell cycle phases

The cell cycle is broadly separated into two main phases: Mitosis and Interphase (Fig. **1**). Mitosis was initially viewed as the central process of the cycle, mainly because visually it is easily distinguishable as a dynamic phase, whereas interphase was simply viewed as the time separating each mitotic event. Nevertheless, interphase occupies most of the cycle and includes the necessary preparation stages for proper cell division. Interphase is divided in three sub-phases: gap phase 1 (G1), the synthesis phase (S) and gap phase 2 (G2).

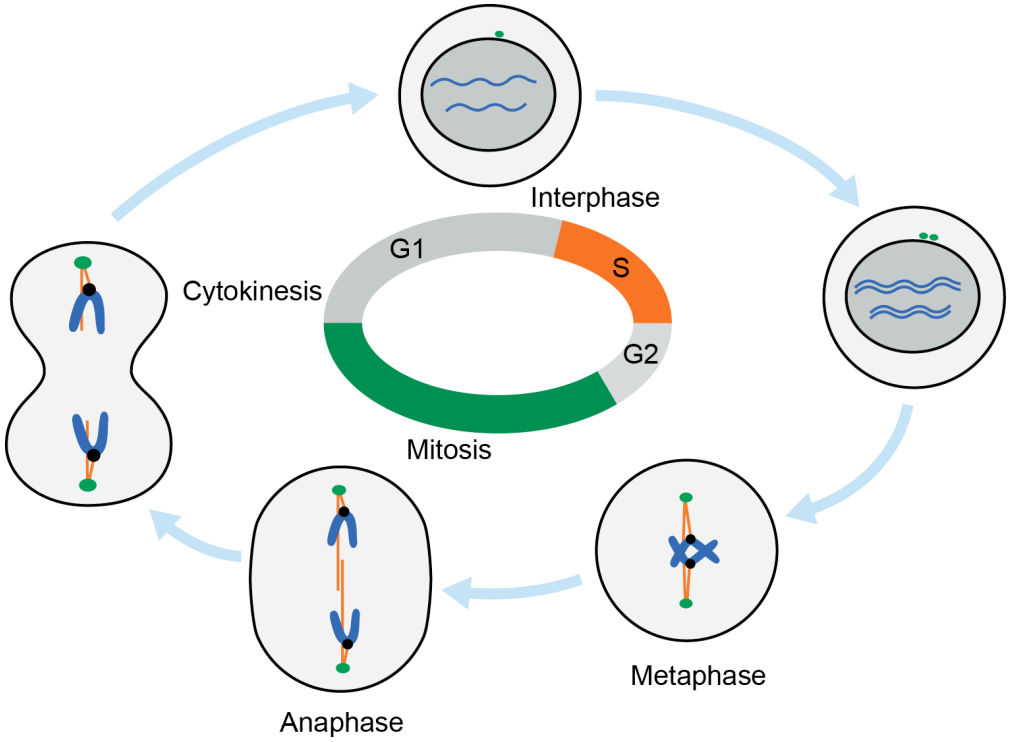

Figure 1: The cell cycle. Representation of the main phases of the cell cycle. During S phase chromosomes are replicated, and a copy of each chromosome is then segregated during mitosis. At the end of the cycle cytokinesis separates the diving cells, two independent cells are formed and a new cycle begins. Chromosomes are in blue, centrosomes in green and mitotic spindle in orange. Adapted from (Morgan, 2007).

G1 is a critical phase in which cells decide whether or not to divide. To enter the cycle cells have to meet certain requirements in terms of size and nutrient availability. This is controlled at the restriction point or START, and once cells pass this point they are committed to go through the cycle. This phase acts as a transition phase between the previous cycle and the new one. For example, cytokinesis in mammalian culture cells is completed only when the two daughter cells are already in G1 (Gershony et al., 2014) and the machinery for DNA replication starts to assemble at this stage too (Diffley et al., 1994).

During S phase, the cell creates an exact copy of its genome (Fig. **1**). In a process termed DNA replication, DNA polymerases and helicases work together to replicate of each chromosome. A large protein complex called the kinetochore assembles on the centromere as soon as it is replicated. This then works as the interface between spindle microtubules and chromosomes for their segregation later in mitosis. During replication, another protein complex called cohesin is loaded onto chromosomes.

Cohesin encircles the two copies of each chromosome - the sister chromatids - keeping them paired until separation in mitosis. This facilitate their segregation to each daughter cell. The microtubule organizing center - the centrosome or spindle pole body - is also duplicated during S phase. This allows a bipolar mitotic spindle to be assembled during mitosis, which is essential for proper chromosome segregation.

Between S phase and Mitosis there is the G2 phase, with a variable length in different organisms. In the fission yeast *Schizosaccharomyces pombe* the G2 phase is the longest of all phases whereas in the budding yeast *Saccharomyces cerevisiae* there is no clearly defined G2 phase as S phase is prolonged until Mitosis (Morgan, 2007).

Interphase is then followed by Mitosis when duplicated chromosomes, along with other cellular organelles, are segregated to each of the daughter cells (Fig. **1**). During this short but very dynamic phase the cell reorganizes its cytoskeleton to form the mitotic spindle, the chromosomes compact, align and bi-orient at the metaphase plate, segregate to opposite poles of the diving cell and two identical nuclei are formed. The newly originated cells are then physically separated into independent units through the process of cytokinesis.

1.2. DNA replication

To generate a copy of each chromosome during S phase, replication of the DNA molecule starts at thousands of different origins of replication in a bidirectional manner. Each of these origins needs to be licensed by proteins that assemble at specific sequences.

1.2.1. Mechanism

In *S. cerevisiae* the origin recognition complex (ORC) is loaded onto conserved replicator sequences, with the help of the Cdc6 ATPase to confer sequence specificity (Speck and Stillman, 2007). Loading of these complexes occurs early in G1 and together with the protein Cdt1 and the replicative DNA helicase Mcm2-7 a

pre-replication complex is assembled licensing the replication origin (Masai et al., 2010).
At the G1/S transition the kinases CDK and Cdc7-Dbf4 (also referred to as the Cdc7-dependent kinase - DDK) promote origin firing by activating the MCM helicase and DNA polymerases (Labib, 2010).
CDK also promotes Cdt1 and Cdc6 degradation during S phase, which not only stabilizes the binding of MCM to DNA but more importantly prevents relicensing of replication origins and therefore reduplication of the genome (Piatti et al., 1996; Petersen et al., 1999; Perkins et al., 2001; Arias and Walter, 2005).
The active replication complex or replisome is composed of many other factors. The CMG complex, which is composed of Cdc45 and the MCM and GINS complexes, associates with Ctf4 which in turn interacts with the DNA polymerase alpha to coordinate progression of the helicase with chain elongation by the polymerase (Tanaka et al., 2009).

To aid in the progression of replication, topological remodeling enzymes such as topoisomerase I (topo 1) and topoisomerase II (topo 2) are also required. During replication fork progression the DNA double helix is unwound which introduces topological stress on the DNA due to accumulation positive supercoiled DNA in front of the replication fork. This supercoiling is diminished by the rotation of the fork, but introduces catenanes in the replicated DNA. Topo 1 and topo 2 contribute to diminishing the topological stress by catalyzing the relaxation of the supercoiled DNA (Wang, 2002).

1.2.2. Replication stress

Replication forks can encounter several obstacles to their progression such as DNA-binding proteins, chromatin proteins, unusual secondary structures or an insufficient supply of nucleotides. These obstacles can lead to uncoupling between the helicase and the polymerase resulting in replication fork stalling. In order to prevent the genomic instability that could result from having unreplicated regions of DNA these stalled forks are stabilized by the S phase or replication checkpoint.

This checkpoint detects damaged DNA and/or stalled replication forks and prevents firing of new origins of replication and entry into mitosis to allow for proper completion of DNA replication. However, in budding yeast, unlike in other eukaryotes, entry into mitosis is not prevented by the DNA damage checkpoint, rather it is the transition of metaphase to anaphase that is inhibited by preventing the degradation of the cohesin complex that holds the sister chromatids together (Sanchez et al., 1999; Wang et al., 2001).

1.2.3. DNA damage checkpoint

The DNA damage checkpoint requires the activity of two central kinases - ATM and ATR (*S. cerevisiae* Tel1 and Mec1, respectively). ATM is specialized in the response to double-stranded breaks whereas ATR in addition to recognizing double-stranded breaks responds to other types of damage such as nucleotide damage and stalled replication forks. The common factor in the ATR response to different types of damage seems to be the generation of single-stranded DNA (ssDNA). Whether due to accumulation of ssDNA in stalled forks, or its generation during nucleotide excision repair or resection of a double-stranded DNA break, the single-strand binding protein RPA binds to it and promotes the recruitment and activation of ATR to these sites through interaction with the ATR adaptor ATRIP (Ddc2). Factors involved in homologous recombination are then recruited, promoting damage repair and/or replication fork restart (Dungrawala et al., 2015).

Upstream of ATM and ATR the MRN complex (budding yeast MRX) is one of the first to be recruited to sites of DNA double-strand breaks to hold the ends together. One of its components - the nuclease Mre11 - promotes the resection of the break to generate a stretch of single-stranded DNA, possibly to elicit a stronger checkpoint response (D'Amours and Jackson, 2002). The complex also localizes to replication foci during S phase and promotes replication fork stability during replication stress (Stracker and Petrini, 2011).

Ultimately, whether it’s directly activated by damaged DNA or by problems during DNA replication the DNA damage checkpoint will block cell cycle progression and

promote repair of the damage, which can happen in a variety of ways. In the case of double-strand breaks there are two main pathways that promote their repair: the non-homologous end joining (NHEJ) and the homologous recombination (HR). The choice between these pathways seems to be related to when in the cycle the break occurs. In G1, the absence of a sister chromatid containing an homologous sequence for repair and the low CDK activity directs the repair through the NHEJ pathway. Because this repair occurs by simply rejoining the two broken ends with DNA ligases it is prone to mistakes. However, if the break occurs in S or G2, high CDK activity promotes resection of the break by Mre11 and HR becomes the preferential repair pathway (Ira et al., 2004; Simoneau et al., 2014). This allows for a more accurate repair by recombination with the undamaged sister chromatid.

1.3. Mitosis

1.3.1. Phases of mitosis

The mitotic phase of the cell cycle is characterized by high mitotic CDK (Cdk1-Cyclin B) activity and by numerous changes at the structural level of the cell. A dramatic re-arrangement of cellular architecture occurs through changes of its cytoskeleton and of its many organelles, among which most importantly is the nucleus.

Changes in nuclear morphology during mitosis allow for the distinction of 5 mitotic phases. Chromosome condensation is the first observable change when cells enter mitosis and marks the onset of the first phase - Prophase. In systems with open mitosis, such as mammalian cells, the nuclear envelope starts disassembling at this phase allowing for accessibility of chromosomes to the mitotic spindle. In organisms with closed mitosis, such as budding yeast, the nuclear envelope remains assembled throughout the entire cell cycle and a mitotic spindle is assembled inside the nucleus.

As cells progress through Prometaphase chromosomes continue to condense and begin to congress at the center of the cell. Cells reach Metaphase once a perfect alignment of the chromosomes is achieved, forming the metaphase plate. Each of the sister chromatids is oriented to opposite poles of the cell, cohesion between sisters is lost and its decatenation begins to allow for correct chromosome segregation.

Anaphase entry begins with elongation of spindle microtubules which pull on the attached chromosomes, bringing each sister chromatid to opposite poles of the dividing cell. This is done in two sequential steps: firstly, during Anaphase A, the kinetochore microtubules shorten, bringing the kinetochores closer to the spindle poles; secondly, in Anaphase B, the interpolar microtubules slide in opposite directions to elongate the mitotic spindle. Biochemically, Cyclin B/Clb2 degradation begins at this stage, decreasing mitotic CDK activity to drive the cells out of mitosis.

Finally, when cells complete segregation Telophase starts. Chromosomes decondense and in the case of open mitosis a nuclear envelope is formed on each daughter nuclei to individualize them.

At this point mitosis is considered finished, leaving the two daughter cells to be physically separated. This is achieved by the process of cytokinesis which brings together the plasma membranes at the site of division to cleave them off. This process will be introduced in more detail in chapter 1.4

1.3.2. The mitotic spindle

In mammalian cells the cytoskeleton is drastically reorganized during mitosis with the main purpose of promoting genome partition. Microtubules that are organized in a network covering almost the entire cell during most of the cycle are reorganized into a mitotic spindle to capture chromosomes and segregate them into the future daughter cells. In this section I will briefly describe the components and mechanisms involved in spindle assembly, elongation and disassembly.

1.3.2.1. Spindle assembly

In budding yeast microtubules are attached to kinetochores throughout the cell cycle, and only transiently detach, when kinetochores disassemble during replication of the centromeric regions in S phase (Kitamura et al., 2007). Afterwards, kinetochores reassemble and once the spindle pole body (SPB) duplicates a mitotic spindle is formed.

The spindle is composed of polarized microtubules formed mainly by α- and β-tubulin dimers. The minus ends are oriented towards the SPBs and the plus ends in the opposite direction, towards the other half of the spindle or attached to the kinetochores (Desai and Mitchison, 1997).

The mitotic spindle is constituted by functionally distinct microtubules. In budding yeast, astral microtubules link the SPBs embedded in the nuclear envelope to the cell cortex, to help achieving the correct spindle orientation; 32 kinetochore microtubules tether the kinetochores in each chromosome to the SPBs, with only one microtubule binding to each kinetochore; and interpolar microtubules connect the two SPBs forming an antiparallel array of about 4 microtubules that constitutes the spindle midzone (Winey et al., 1995). The midzone is essential for spindle

elongation during anaphase as it is bound by proteins that stabilize the spindle and proteins that promote the sliding of the overlapping microtubules.

1.3.2.2. Spindle elongation

Spindle dynamics are regulated by motor proteins that localize at the microtubules. These microtubule motors comprise two distinct families: kinesins and kinesin-related proteins, which move towards the plus ends; and dyneins which move towards the minus ends. It is the balance of these proteins that contributes to a functional and dynamic mitotic spindle. As an example of this balance, the *S. cerevisiae* kinesin-related protein Kip3 moves towards the plus ends to promote depolymerization of microtubules (Gupta et al., 2006) and the presumptive microtubule polymerase Stu2 counteracts the activity of Kip3 (Severin et al., 2001) and together with the kinesins Cin8 and Kip1 promotes spindle elongation (Saunders and Hoyt, 1992).
Additionally, microtubule dynamics are regulated by non-motor proteins such as Ase1 (human PRC1) that localize to the spindle midzone. This protein is recruited to the midzone early in mitosis where it acts as a microtubule bundler and contributes to spindle stability and elongation (Schuyler et al., 2003; Kotwaliwale et al., 2007).

As mentioned before, spindle elongation occurs during Anaphase B, as interpolar microtubules slide apart extending the spindle in length. This elongation is biphasic, with an initial, fast phase of antiparallel microtubule sliding, with an elongation rate of 1 μm/min. Once a 4-6 μm spindle is reached, starts a second phase of microtubule sliding and polymerization at the midzone. During this phase the elongation rate drops down to half or less of the previous one, until the spindle reaches its maximal length of approximately 10 μm (Winey and O'Toole, 2001).

1.3.2.3. Spindle disassembly

Spindle disassembly begins after spindle elongation reaches its maxima. However, the timing for spindle disassembly has to be precisely coordinated with two cell cycle events: chromosome segregation and cytokinesis. These happen only after chromosome segregation is complete and before cytokinesis. Spindle disassembly happens by depolymerization at the plus ends of the microtubules which results in

shortening of the spindle halves towards their respective SPB (Maddox et al., 2000). This is promoted by a combination of three different pathways that involve the microtubule depolymerase Kip3, the ubiquitin ligase complex APC-Cdh1, and the Aurora B kinase Ipl1 (Buvelot et al., 2003; Woodruff et al., 2010). The APC-Cdh1 complex promotes the degradation of several spindle-associated proteins required for spindle stability, such as Cin8, Kip1, Fin1 and Ase1. Ipl1 directly phosphorylates the microtubule stabilizing protein Bim1 (human EB1), reducing its affinity for microtubule plus ends and thus promoting spindle disassembly (Zimniak et al., 2009).

The timing of spindle disassembly is regulated at least in part by the mitotic exit network, through the activity of the Cdc14 phosphatase. In agreement with this, *cdc15* and *cdc14* mutants of this pathway cause an arrest in late anaphase with fully elongated spindles (Wood and Hartwell, 1982). Specifically, Cdc14 dephosphorylates Ipl1 allowing for its interaction with and phosphorylation of Bim1 (Zimniak et al., 2012), on one side; and it dephosphorylates the APC activator Cdh1 (Visintin et al., 1998; Jaspersen et al., 1999) on the other side, controlling a second independent pathway for spindle disassembly.

1.3.3. Chromosome segregation

The process of chromosome segregation involves separating the two copies of each chromosome (sister chromatid) in order to segregate them to opposite poles of the dividing cell.

The fidelity of this process requires both correct orientation of each pair of sister chromatids, achieved through regulation of microtubule and kinetochore interactions; and resolution of each chromatid into individual units, which is accomplished by dissolution of cohesion, condensation and decatenation.

1.3.3.1. Chromosome bi-orientation

Correct chromosome orientation at the metaphase plate is achieved by ensuring that each pair of sister chromatids is attached by microtubules from opposite poles of the cell, through their kinetochores. This amphitelic attachment establishes chromosome

bi-orientation and it is accomplished by the combined actions of the spindle assembly checkpoint (SAC) and the Aurora B kinase (Ipl1 in budding yeast).

When the spindle microtubules pull on the kinetochores, bi-oriented sister kinetochores become under tension. In the absence of such tension, the SAC prevents the onset of anaphase. At this stage, Aurora B is localized at kinetochores and promotes bi-orientation by destabilizing the interactions between microtubules and kinetochores that are not under tension (Tanaka et al., 2002; Pinsky et al., 2005).
Experiments in human cells have shown that the phosphorylation of Aurora B substrates at the kinetochore decreases in response to tension and distance (Liu et al., 2009). This suggests that spatial proximity between Aurora B localized at the inner kinetochore and its substrates at the outer kinetochore is sufficient to regulate microtubule-kinetochore attachments. Therefore, tension-generating attachments become stabilized by moving away from the sphere of Aurora B activity, and bi-orientation is established (Akiyoshi et al., 2010).

Unattached kinetochores promote maintenance of the mitotic checkpoint complex where Mad2, Mad3/BubR1 and Bub3 sequester Cdc20 and block APC activation (Sacristan and Kops, 2015). Once all kinetochores have formed a stable attachment, the complex is disassembled releasing Cdc20. Cdc20 then activates the APC and targets several proteins for degradation to allow for the metaphase to anaphase transition. Among the APC-Cdc20 substrates are securin/Pds1 which prevents degradation of the Scc1 subunit of the cohesin complex by the separase Esp1 (Cohen-Fix et al., 1996; Ciosk et al., 1998; Uhlmann et al., 2000). Therefore, once the SAC is silenced cohesin is released from sister chromatids allowing for their separation.

1.3.3.2. Chromosome condensation

Chromosome condensation allows for the packaging of the genome into units of manageable size to facilitate their segregation. In most organisms chromosome condensation is observable from the beginning of prophase and is completed by metaphase. In budding yeast, the small nuclear size and inability to see individual

chromosomes does not obviate condensation. However, analysis of distances between chromosomal loci in the same chromosome arm have shown not only increased compaction during anaphase but also the existence of a midzone-based mechanism capable of regulating the level of this compaction (Neurohr et al., 2011). Moreover, inactivation of condensin, a multisubunit protein complex required for condensation, significantly affects chromosome compaction during anaphase (Renshaw et al., 2010) leading to chromatin bridges that are damaged by cytokinesis (Cuylen et al., 2013).

Condensin activity is regulated by phosphorylation. Besides being a target of CDK1, condensin is specifically phosphorylated in anaphase by Ipl1 and Cdc5 independently (Lavoie, 2004; St-Pierre et al., 2009). These phosphorylations are required for Condensin's DNA supercoiling activity *in vitro* and for proper compaction of the ribosomal DNA (rDNA) locus *in vivo* (Kimura et al., 2001; St-Pierre et al., 2009).

1.3.3.3. Chromosome decatenation

During DNA replication, intertwines arise between the replicating sister chromatids, due to its double-stranded structure. These topologically intertwined strands of DNA - catenanes - are resolved by the enzyme topoisomerase II (topo 2). In an ATP-dependent reaction, this enzyme produces a transient double-strand break and passes an intact double-strand of DNA through the gap (Wang, 2002). This unlinks the DNA strands, resolving the catenane.

Topo 2 actively decatenates during DNA replication and its activity is essential for replication termination (Baxter and Diffley, 2008). However, the enzyme is still required during mitosis for proper chromosome segregation and cell viability (Holm et al., 1985; Titos et al., 2014).

1.3.4. Defects in chromosome segregation

Interfering with any of the above processes can lead to anaphase DNA bridges, which challenge genomic integrity if not properly resolved. DNA bridges can have different origins but are of two main types. Chromatin bridges can be visualized with DNA dyes, such as DAPI or Hoechst, and are considered to be chromatinized.

Howver, some bridges are only detected by nucleotide labelling and by the localization of certain proteins that coat these bridges. These are considered de-chromatinized bridges and are called ultrafine DNA bridges (UFBs) (Chan et al., 2007). UFBs are generally associated with replication, particularly unfinished replication due to replication stress; unresolved replication intermediates; or defective decatenation (Baxter, 2015).

1.3.4.1. Resolution of DNA intermediates

Besides catenations unfinished replication or unresolved replication intermediates are also sources of sister chromatid intertwines (SCIs). Failure to resolve any SCI leads to the formation of DNA bridges during mitosis potentially resulting in defective chromosome segregation. In fact, interfering with DNA replication genetically or chemically has been shown to lead to anaphase bridges and in many cases genomic instability (Chan et al., 2009; Germann et al., 2013).

Additionally, repair of DNA damaged during replication can generate DNA intermediates that must be processed. Repair of double-stranded DNA breaks occurs in many cases by homologous recombination. This process occurs through strand invasion of one chromatid into its sister to use as template for repair, which generates a joint molecule of the two sister chromatids called double Holliday junction (Baxter, 2015).

Three distinct pathways contribute to Holliday junction processing. The main one relies on the functions of topoisomerase III and the BLM/Sgs1 RecQ helicase, which work together in a complex that is able to process intertwined unreplicated regions of DNA and hemicatenanes in a reaction termed dissolution.

The other two pathways rely one on the structure-specific nucleases SLX1-4 and MUS81-EME1 (*S. cerevisiae* Mus81-Mms4) of the SLX-MUS pathway, and the other on the Holliday junction resolvase GEN1/Yen1. This last enzyme introduces two symmetric nicks in the junction to produce nicked duplexes and then allows for their ligation. The activity of Yen1 is cell cycle regulated and was shown to be specifically activated in anaphase through dephosphorylation by Cdc14. Interestingly, both its inactivation or earlier activation in the cell cycle lead to genomic instability (Blanco et al., 2014; Eissler et al., 2014).

DNA bridges are common in cancer cells, many of which are due to elevated replication stress caused by oncogene deregulation. Some oncogenes reduce the number of replication origins firing whereas others increase it, but in both cases progression through replication is affected and leads to increased SCIs (Hills and Diffley, 2014). If the appropriate resolution mechanisms are not functional this results in genomic instability. This is the case when DNA processing enzymes like BLM are mutated, which results in in the condition known as Bloom's syndrome, characterized by loss of heterozygosity and cancer susceptibility.

1.3.4.2. Chromatin bridges

Apart from SCIs other types of chromosome segregation defects can occur. Misattachments between microtubules and kinetochores can go unnoticed by the spindle assembly checkpoint. This is the case when one kinetochore is attached by microtubules from opposite poles, since it can still be under tension with its sister. This type of attachment, termed merotelic, results in a full chromosome lagging behind the main segregating DNA masses (Cimini et al., 2001). Lagging chromosomes can be chemically induced by the use of microtubule destabilizing drugs such as Nocodazole and Monastrol. This however does not occur in budding yeast, as each kinetochore is only attached by a single microtubule.
In addition, syntelic attachments can also occur if a defective SAC response is established or if correction mechanisms are not fully functional. In these cases sister chromatids can be segregated to the same pole, generating aneuploid cells, which contribute to genomic instability and are frequently observed in cancer (Holland and Cleveland, 2009; Sheltzer et al., 2011).

Finally, one particularly interesting type of segregation defect comes from dicentric chromosomes. These originate from inappropriate DNA repair or the fusion of two chromosome ends as a result of telomere erosion (Stewénius et al., 2005). The cell is therefore presented with the challenge of segregating one chromosome with two centromeres. As a consequence a chromatin bridge will form in half of the cases due to attachment of those two kinetochores by microtubules from opposite poles of the cell. Because a dicentric chromosomal bridge is broken by cytokinesis at the end of mitosis (Pobiega and Marcand, 2010; Lopez et al., 2015), these chromosomes

undergo a breakage-fusion-bridge cycle which is potentially very deleterious to the cells carrying these chromosomes (McClintock, 1941).

1.3.5. Exit from mitosis

The complexity of the processes involved in chromosome segregation underscores the importance of robust mechanisms regulating the progression through mitosis. Besides the spindle assembly checkpoint (described in chapter 1.3.3.1), which ensures proper microtubule-kinetochore attachments, two additional mechanisms come into play once the cells enter anaphase and drive their progression through and exit from mitosis.

Essentially this regulation happens by reverting the phosphorylation state of Cdk1 substrates. The initial step in this direction is given by the inactivation of the Cdk1-Clb2 complex through the degradation of Clb2 promoted by APC-Cdc20. Complete Cdk inhibition and dephosphorylation of its substrates is then done by the phosphatase Cdc14, the essential driver of mitotic exit.

1.3.5.1. The mechanism of mitotic exit

During most of the cell cycle, Cdc14 is kept inactive in the nucleolus, where it is bound to its inhibitor Net1 (Visintin et al., 1999; Shou et al., 1999). This inhibitory complex is stably maintained as long as Net1 is in a hypophosphorylated state, which is ensured by the phosphatase PP2A-Cdc55 that counteracts the activity of Cdk1 and the polo kinase Cdc5 on Net1 (Fig. **2**). Therefore, Cdc14 release from the complex occurs by phosphorylation of Net1.

The release of Cdc14 coincides with its activation, which occurs in two phases. An initial release of Cdc14 from the nucleolus to the nucleus through the fourteen early anaphase release (FEAR) network is then followed by a sustained release from the nucleus to the cytoplasm, through the mitotic exit network (MEN).

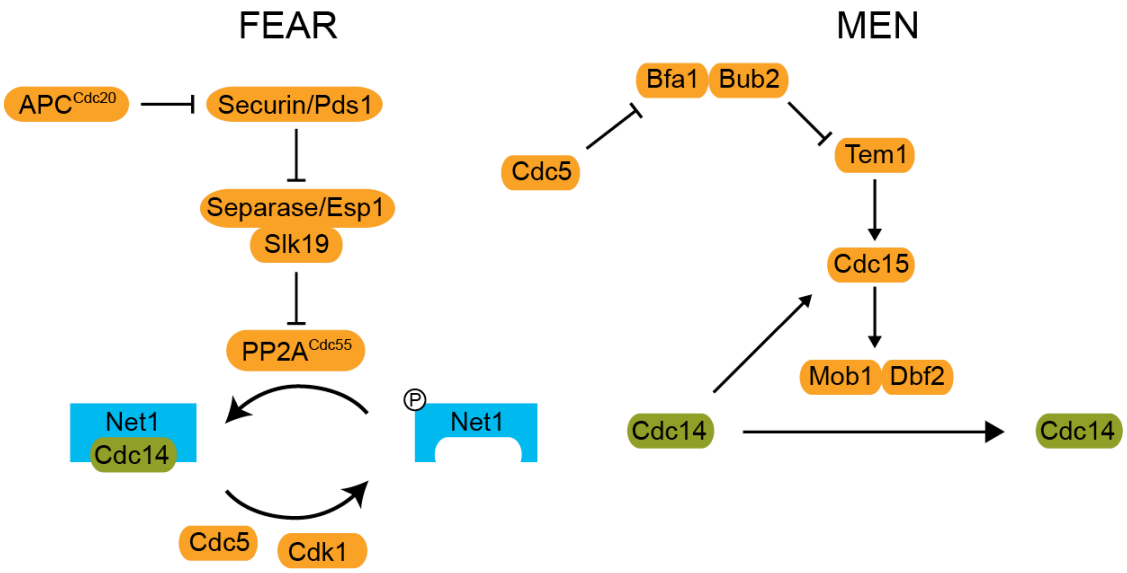

Figure 2: Regulation of exit from mitosis in *S. cerevisiae*. The FEAR and MEN networks regulate activation of the Cdc14 phosphatase. At the onset of anaphase, degradation of Securin/Pds1 induces the transient release of Cdc14 from the nucleolus through the FEAR (Fourteen Early Anaphase Release) pathway. After one spindle pole entes the bud the MEN (Mitotic Exit Network) pathway becomes activated. The small GTPase Tem1 induces a sustained release of Cdc14 from the nucleus to the cytoplasm. Figure adapted from (Neurohr, 2012).

The initial, FEAR-mediated release of Cdc14 begins once the spindle assembly checkpoint is satisfied. Through the release of Esp1 (separase), and together with the proteins Slk19, Spo12 and Bns1, PP2A-Cdc55 is downregulated and allows for Cdk1 and Cdc5 to phosphorylate Net1 and promote the release of Cdc14 (Stegmeier et al., 2002; Queralt et al., 2006) (Fig. **2**).

The full activation of Cdc14 is brought about by the MEN network. At the top of the pathway the spindle pole body-localized GTPase Tem1 activates the kinase Cdc15, which in turn activates the Dbf2-Mob1 complex to phosphorylate Cdc14 (Fig. **2**). This kinase cascade leads to the inactivation of the nuclear localization signal of Cdc14 allowing for its translocation to the cytoplasm (Mohl et al., 2009).

Tem1 is kept in the inactive GDP-bound state by its GTPase activating protein (GAP) Bub2-Bfa1, which is inactivated by Cdc5 when one SPB enters the daughter cell (Fig. **2**) (Hu et al., 2001). Altogether the mechanisms involved in activation of Cdc14 combine temporal and spatial regulation to drive the cells through the late stages of mitosis.

1.3.5.2. Cdc14 regulation of mitotic exit

The functions of Cdc14 are broad, promoting a variety of cellular events in a relatively short time span. At the metaphase to anaphase transition Cdc14 promotes the translocation of the chromosomal passenger complex (CPC) from kinetochores to the spindle midzone. By dephosphorylating the CPC component Sli15/INCENP, Cdc14 further contributes to the stabilization of kinetochore-microtubule attachments and anaphase progression (Pereira, 2003; Mirchenko and Uhlmann, 2010). Also, during anaphase it promotes transcriptional repression of the ribosomal DNA (rDNA) and condensin recruitment to this particular region for proper chromosome segregation (Clemente-Blanco et al., 2009).

Cdc14 further promotes inhibition of mitotic Cdk activity through dephosphorylation of the Cdk inhibitor Sic1, and also through dephosphorylation of Swi5 which leads to increased Sic1 transcription (Visintin et al., 1998). Additionally, Clb2 degradation proceeds promoted by the activity of the ubiquitin ligase APC-Cdh1, further contributing to a decrease in Cdk activity.

Activation of the APC co-factor Cdh1 by Cdc14 confers a different substrate specificity to the ligase (Schwab et al., 1997; Jaspersen et al., 1999). Among its targets are also the polo kinase Cdc5; the IQGAP-related protein Iqg1 whose degradation promotes completion of cytokinesis (Tully et al., 2009); the chitin synthase Chs2, essential for primary septum formation (Chin et al., 2011); and in mammalian cells Aurora B has also been shown to be a direct target of the ligase (Floyd et al., 2013). Lastly, APC-Cdh1 promotes the degradation of the spindle stabilizing proteins Ase1, Cin8, Kip1 and Fin1 (Juang, 1997; Hildebrandt and Hoyt, 2001; Woodbury and Morgan, 2006), contributing to the disassembly of the mitotic spindle at the end of mitosis. In parallel, Cdc14 contributes to the spindle disassembly pathway promoted by Ipl1 by dephosphorylating specific residues on the kinase that allow for its interaction with and destabilization of the microtubule bundler Bim1 (human EB1) (Zimniak et al., 2009; 2012).

1.4. Cytokinesis

The purpose of cytokinesis is the physical separation of the diving cell into two independent units. An apparently simple process however requires the assembly of a complex machinery that has to be both spatially and temporally regulated. The spatial regulation determines the site of separation, which affects the symmetry of the division, important in developmental contexts and for cell size. The temporal regulation ensures that cytokinesis occurs only after all the other events required for the formation of fully functional daughter cells.
In this section I will describe the components and the mechanisms involved in budding yeast cytokinesis and in abscission of human cells.

1.4.1. Budding yeast cytokinesis

1.4.1.1. Division site selection.

Budding yeast cells form a bud axially to the their previous site of budding. The budding site determines their site of division at the end of the cycle, and depends on the BUD1-5 genes (Chant and Herskowitz, 1991). Mutants of the Ras GTPase Bud1 and its GAP (Bud2) or GEF (Bud5) have random budding patterns, whereas Bud3 or Bud4 mutants show bipolar budding patterns (Chant and Herskowitz, 1991).
Bud emergence requires polarization of the actin network at these sites, which depends on the small Rho-GTPase Cdc42, its GEF Cdc24 and on the scaffold protein Bem1 (Sloat et al., 1981; Adams et al., 1990; Chant et al., 1991). These polarity-establishment proteins localize to the emerging bud site (Ziman et al., 1993) and local regulation of Bud1 by Bud2/Bud5 promotes the interaction of these different complexes, possibly helping to direct actin organization to the growth site (Casamayor and Snyder, 2002).

1.4.1.2. Septins

Septins also contribute to the process of budding, since mutations in septin proteins make random budding patterns (Flescher et al., 1993). Of the seven septin proteins in yeast, five of them are involved in vegetative growth - Cdc3, Cdc10, Cdc11, Cdc12

and Shs1. These are structural components of the septin ring that forms at the mother-bud junction (commonly referred to as the bud neck) and they work as a scaffold for cytokinesis proteins, essential for the localization of many of them. Septins localize to the budding site before bud emergence where they interact directly with membranes (Fig. **3**) through the lipid-binding motif, a polybasic region that binds phosphatidylinositol 4,5-biphosphate (PIP2) (Zhang et al., 1999). Assembly and organization of the septin ring depends on Cdc42, Cdc24, and its effectors Cla4 and Ste20 (Cvrcková et al., 1995; Richman et al., 1999; Cid et al., 2001).

Even though septins localize to the bud neck throughout most of the cycle, they form dynamic structures and with variable mobility states (Dobbelaere et al., 2003). During bud growth the septin ring expands to form a collar - an hourglass structure of 10 nm filaments (Lippincott et al., 2001). At the onset of cytokinesis a structural rearrangement splits the collar into two rings, presumably to allow for contraction of the actomyosin ring. The small GTPase and MEN activator Tem1 is required for septin ring splitting (Lippincott et al., 2001). The fact that Tem1 inactivation also prevents actomyosin ring contraction (Lippincott et al., 2001) suggests that actomyosin ring contraction is coupled to septin ring splitting. Afterwards, each septin ring extends to mark the new bud site and is removed from the old site as the new bud emerges (Lippincott and Li, 1998b). Accordingly, defective septum disassembly results in delayed emergence of the new bud.

The chromosomal passenger complex component Bir1/Survivin also has a role in the regulation of septin dynamics. Bir1 regulates the timing of septin ring splitting and promotes septin disassembly at the end of cytokinesis through interaction with Sli15/ INCENP and the kinetochore complex CBF3 (Gillis et al., 2005; Thomas and Kaplan, 2007).
In addition to and independently of their role in cytokinesis, septins form a diffusion barrier between mother and daughter cell, possibly by preventing the lateral diffusion of membrane-bound proteins (Barral et al., 2000).

The disassembly of septins occurs in G1 and although not very well understood several players seem to promote it. Phosphorylation of Cdc3 by Cdk1 is required for septin disassembly (Tang and Reed, 2002). Additionally, septin filament dissociation was recently proposed to be promoted by the binding of Cdc42 in its GDP-bound form (Sadian et al., 2013). Finally, the regulatory subunit of PP2A, Rts1, promotes septin disassembly in G1 (Dobbelaere et al., 2003). Interestingly, *rts1* mutant cells are also defective in a late step of cytokinesis but do not affect actomyosin ring dynamics. This defect was unable to be resolved by zymolyase treatment to digest the cell wall suggesting a specific defect in abscission (Dobbelaere et al., 2003).

1.4.1.3. Actomyosin ring assembly

A contractile actomyosin ring is assembled at the site of cytokinesis to drive the ingression of the plasma membrane to separate the two daughter cells. The ring is essentially constituted by myosin type II (Myo1) and actin filaments that localize to the bud neck. The recruitment of myosin happens just before bud appearance - at the onset of S phase - where it remains as a ring throughout the rest of the cycle until the completion of cytokinesis.

Like for many cytokinetic proteins, assembly and stability of the myosin ring depends on septins (Lippincott and Li, 1998a; Bi et al., 1998). Myo1 is recruited to the bud neck and stabilized by the septin-binding protein Bni5 (Fang et al., 2010). Bni5 is in turn recruited to the bud neck by the septins Cdc11 and Shs1, through their C-terminal extensions (Lee et al., 2002; Finnigan et al., 2015).

Actin is recruited to the bud neck later in the cycle, during anaphase (Bi et al., 1998), by the protein Iqg1 (Lippincott and Li, 1998a). During most of the cell cycle an actin cytoskeleton consisting of actin patches and cables of filamentous actin (F-actin) is polarized towards the growing bud. At the time of cytokinesis, F-actin is then repolarized towards the bud neck and forms an actin ring that co-localizes with myosin.
Assembly of the actin cables that form the ring is promoted by the formins Bni1 and Bnr1 (Sagot et al., 2002); the regulator of actin polymerization Profilin; and by the F-actin binding tropomyosins (Tolliday et al., 2002). The Rho-like GTPases Rho3,

Rho4 and to some extent also Rho1 regulate Bni1 and Bnr1 functions for the assembly of actin cables (Tolliday et al., 2002; Dong, 2003). Additionally, the activity of Bnr1 has been proposed to be regulated by the protein Hof1, to which it binds directly in a Rho4-dependent manner (Kamei et al., 1998). Hof1 was recently found to affect actin cable organization (Graziano et al., 2014), but a direct role in assembly of the actin ring has not been shown. However, since both proteins localize to the bud neck it is likely that Hof1 promotes actin ring assembly through Bnr1.

Both myosin and actin are essential for proficient cytokinesis. However, at least in some backgrounds Myo1 is not essential for viability, since these cells seem to have evolved alternative mechanisms to compensate for its loss and still divide (Tolliday et al., 2003; Rancati et al., 2008). Actin on the other hand is an essential molecule. Treatment of cells with Latrunculin A, which sequesters actin monomers, leads to rapid actin depolymerization and blocks ring contraction (Bi et al., 1998).

1.4.1.4. Actomyosin ring contraction

A few studies have shown that myosin motor activity and actin dynamics have a major role in the regulation of ring contraction. *In vitro* experiments showed that the minimal requirements for ring contraction are myosin II and ATP and that neither actin polymerization nor its disassembly are required (Mishra et al., 2013). However, *in vivo* stabilization of actin or inhibition of actin severing by Cofilin significantly affects the rate of contraction (Pinto et al., 2012).
Nevertheless, other proteins that localize to the bud neck contribute to the stability and contraction of the ring. The complex formed by Hof1, Inn1 and Cyk3 is central to this process.

Hof1 contains a membrane-binding F-BAR domain. Its localization to the bud neck depends on septins and co-localization between them is observed throughout most of the cycle (Vallen et al., 2000). Hof1 presumably interacts with the septin Cdc10 (Oh et al., 2013) and at the time of contraction shuttles from the septin double-ring to the myosin ring.
These dynamics are regulated during mitotic exit. Hof1 is initially phosphorylated by the polo kinase Cdc5 and subsequently by the MEN kinase complex Dbf2-Mob1.

This promotes its release from septins and the transition to the actomyosin ring (Vallen et al., 2000; Meitinger et al., 2011). There Hof1 interacts with Iqg1 (Tian et al., 2014) and contributes to Myo1 stability, preventing its disassembly before complete contraction (Lippincott and Li, 1998b). However, Hof1 only remains associated with Myo1 during the onset of contraction. It then returns to a double-ring conformation and extends towards the new bud site (Lippincott and Li, 1998b), similar to septins.

Inn1, although not directly involved in actomyosin ring assembly or contraction, is required for plasma membrane ingression and proper primary septum formation (Sanchez-Diaz et al., 2008; Nishihama et al., 2009). Inn1 is recruited to the bud neck by the MEN network (Nishihama et al., 2009). It contains a C2 domain at its amino terminal, which is required for membrane ingression and is known for binding phospholipids weakly and mediating interactions with other proteins (Sanchez-Diaz et al., 2008). In addition, Inn1 interacts with the SH3 domains of Hof1, via its C terminus (Sanchez-Diaz et al., 2008), which leads to stabilization and symmetric localization of Hof1 along the ring (Nishihama et al., 2009). Inn1 also binds Cyk3 at the ring. This interaction occurs during mitotic exit when the C terminus of Inn1 is dephosphorylated by Cdc14 and promotes the interaction with and recruitment of Cyk3 to the neck (Palani et al., 2012). This interaction presumably activates Cyk3 and promotes the catalytic activity of the chitin synthase Chs2 to induce primary septum formation (Nishihama et al., 2009). Therefore, through Inn1 the Hof1-Inn1-Cyk3 complex couples actomyosin ring contraction with ingression of the plasma membrane and septum formation.

1.4.1.5. Septum formation

As part of the cytokinetic process in budding yeast a septum is formed at the bud neck. Initially, a primary septum follows the contraction of the actomyosin ring and once completed a secondary septum is deposited on both sides of the primary septum (Fig. **3**).

The primary septum is mainly constituted of chitin, which is primarily synthesized by the chitin synthase enzyme Chs2 (Shaw et al., 1991). Chs2 is delivered to the bud neck through the exocytic pathway just before the onset of actomyosin ring contraction and continuously throughout - a process that is dependent on its

dephosphorylation by the Cdc14 phosphatase (Chin et al., 2011). In fact, septum formation and ring contraction are interdependent processes. Chs2 is necessary for actomyosin ring stability during contraction and couples the assembly of the septum with the dynamics of ring contraction. Preventing the delivery of Chs2 to the bud neck impairs myosin ring contraction leading to an apparent breakage of the ring and myosin disassembly before contraction is completed (VerPlank and Li, 2005). Moreover, much like in Myo1 mutants, lack of Chs2 leads to defects in cell separation with no observable membrane ingression or primary septum formation. However, both mutants are able to complete cytokinesis due to the formation of a remedial septum that depends on the activity of the chitin synthase Chs3 (Schmidt et al., 2002).

The secondary septum has a molecular structure similar to the cell wall, mainly composed by β(1,3)- and β(1,6)-glucans and chitin, but its synthesis and assembly are poorly studied (Bowers et al., 1974).

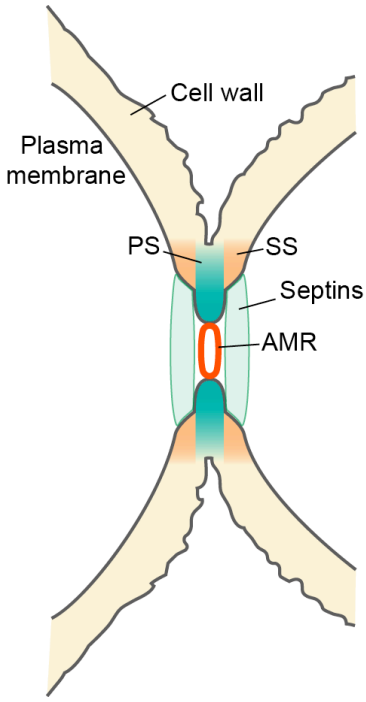

Figure 3: Cytokinesis in *S. cerevisiae*. Actomyosin ring (AMR) contraction drives the ingression of the plasma membrane during cytokinesis. This is coupled with primary and secondary septum (PS and SS, respectively) formation. After AMR disassembly the PS is degraded to allow for the final separation of the two daughter cells. The SS is then remodeled and becomes part of the cell wall. Adapted from (Weiss, 2012).

1.4.1.6. Abscission

The resolution of the plasma membrane - abscission - is tightly coupled to actomyosin ring contraction and septum formation. Studies focusing on abscission use plasma membrane proteins or membrane binding domains as reporters for its dynamics. However, apart from a few cases no specific mechanisms are known to control exclusively abscission in budding yeast cytokinesis. These include the protein Cyk3 and Rts1, which when inactivated have apparently normal ring contraction but show defects in cytokinesis that are independent of septum degradation (Dobbelaere et al., 2003; Norden et al., 2006).

1.4.1.7. Cell separation

After cytokinesis is completed cell separation is the final step to obtain an individualized yeast cell. This step is specific to yeasts due to presence of the cell wall and occurs by degradation of the septum that was built during cytokinesis.

Septum degradation is promoted by a daughter cell-specific transcription factor controlled by the RAM network. This transcription factor - Ace2 - is specifically expressed in the daughter cell nucleus and activates transcription of genes involved in septum degradation. Ace2 is restricted to the daughter cell nucleus through phosphorylation by the Mob2-Cbk1 kinase complex, which additionally promotes its activation (Weiss, 2002). The mechanism of nuclear localization of these proteins requires MEN signaling and regulated nuclear export (Weiss, 2002).

Ace2 promotes expression of several genes essential for septum degradation, among which the endochitinase-coding gene CTS1. This enzyme is incorporated into the cell wall to hydrolyze the chitin composing the primary septum (Kuranda and Robbins, 1991). In addition to Cts1, hydrolytic enzymes such as Dse4/Eng1 - a specific cell separation endoglucanase - localizes to the daughter side of the septum to promote cell separation (Baladron et al., 2002).
A current model for septum degradation hypothesizes that once septation is completed an unknown signal triggers exocytic delivery of chitinase and glucanases to the periplasmic space between the plasma membrane and the secondary septum (Weiss, 2012). From there these enzymes diffuse aided by cell wall rearrangements

by glucanases and new cell wall synthesis by transmembrane enzymes. Once chitinase reaches the primary septum digestion happens and mother and daughter cells separate.

1.4.2. Human cytokinesis

Cytokinesis in human cells depends on the same basic processes that are involved in yeast cytokinesis. Contraction of an actomyosin ring drives ingression of the plasma membrane to promote the fusion and separation of the membranes. However, these occur with some particular differences and additional complexity.

To begin with, unlike in budding yeast, the division of human culture cells is symmetric. The selection of the division site is determined by the position of the mitotic spindle during anaphase, particularly of its midzone and astral microtubules (Burgess and Chang, 2005), and by chromosome-derived signals to the plasma membrane (Kiyomitsu and Cheeseman, 2013).
Cytokinesis is dependent on an actomyosin ring that drives ingression of the plasma membrane. This generates a cleavage furrow that evolves into an intercellular bridge of approximately 1 µm diameter. Abscission is the very last step of cytokinesis, which allows for the final scission of the plasma membrane and the separation of the daughter cells. Through a combination of active membrane remodeling mechanisms and delivery and fusion of vesicles, the connection between the two daughter cells is dissolved and cellular individualization is achieved.

The intercellular bridge contains microtubules from the spindle midzone that connect the two daughter cells. It has a central dense region called the midbody where a disc-shaped structure, called the Flemming body, is surrounded by the midbody arms (Fig. **4i**). Besides microtubules the midbody contains several proteins which are involved in stabilization and constriction of the bridge.
The central spindlin subunit mitotic kinesin-like protein 1 (Mklp1) localizes to the midzone early on as it's essential for its assembly. As the midzone matures into the midbody Mklp1 contributes to the stabilization of the intercellular bridge, where

phosphorylation by Aurora B is essential to prevent furrow regression and binucleation (Guse et al., 2005).

The centrosomal protein Cep55 binds to Mklp1 at the midbody, after phosphorylation by Cdk1 and Plk1, and is required for midbody structure (Fabbro et al., 2005; Zhao et al., 2006). Cep55 also interacts with ESCRTs (endosomal sorting complexes required for transport). By interacting with the ESCRT-I subunit Tsg101 and the ESCRT-related protein Alix, Cep55 further recruits the ESCRT-III subunit CHMP4B to the midbody (Carlton and Martin-Serrano, 2007; Elia et al., 2011). All of these are essential for completion of cytokinesis.

Aurora B also localizes to the midbody during cytokinesis. Its translocation from the centromeres to the spindle midzone is promoted by the kinesin Mklp2 where it remains associated to microtubules and accompanies the formation of the midbody (Guse et al., 2005). During cytokinesis Aurora B is observed at the midbody arms (Elia et al., 2011) and plays an inhibitory role on abscission (Steigemann et al., 2009).

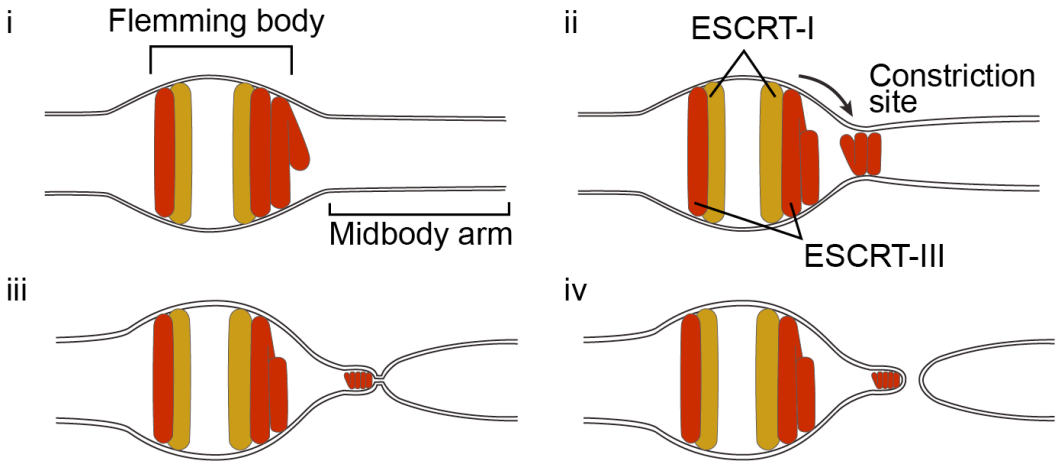

Figure 4: Abscission in human cells. A model for abscission driven by ESCRT complexes. Midbody-localized ESCRT-III subunits polymerize and remodel into helical spirals. These proteins move to one of the sides of the Flemming body, creating a constriction site which brings the plasma membranes close together to allow for abscission. Adapted from (Elia et al., 2013).

Two essential steps need to take place for abscission to occur: severing and depolymerization of microtubules present at the bridge followed by sealing of the membranes.
The microtubule severing enzyme Spastin is recruited to the midbody by the ESCRT-III subunit CHMP1B (Yang et al., 2008) and has been proposed to clear the site of abscission to allow for membrane constriction (Connell et al., 2008). Moreover, cryo-EM analysis have shown increased microtubule depolymerization and buckling at the constriction sites (Schiel et al., 2011). However, contrary to the generally accepted role of Spastin in this process, the authors of the latter study have shown that depletion of the enzyme did not lead to an increased mass of microtubules at the bridge and suggest that the enzyme is not essential for microtubule severing at the bridge. Rather Spastin seems to be required for organization of microtubule bundles and efficient trafficking of vesicles to the bridge. They observed that as cells approach the later stages of cytokinesis, the plasma membrane becomes more dynamic due to vesicle fusions (Schiel et al., 2011), which was proposed to contribute to the constriction of the membrane.

The sealing of the membranes by constriction occurs adjacent to the Flemming body, on one of its sides. The ESCRT-III subunit CHMP4B assembles as a helical filament and is recruited from the Flemming body to the constriction site where abscission occurs (Fig. **4ii**). The colocalization of the AAA-ATPase (ATPase associated with diverse cellular activities) Vps4 with CHMP4B and its recruitment to the constriction site just 20 minutes before separation of the intercellular bridge suggests it could induce a conformational change on the ESCRT-III helix mediating constriction of the plasma membrane (Fig. **4iii**) (Elia et al., 2011), finally leading to abscission (Fig. **4iv**).

1.5. The NoCut checkpoint

Coordination of the segregation of chromosomes with the process of cytokinesis is of extreme importance for the fidelity of mitosis. Ensuring that all chromosomes have been properly segregated prior to completion of cytokinesis is essential in promoting the correct transmission of genomic information to future generations and therefore essential for genomic stability.
To some extent, this coordination is done already at the transition from metaphase to anaphase. The spindle assembly checkpoint prevents cytokinesis from occurring before the onset of anaphase, by controlling exit from mitosis. However, during anaphase problems in chromosome segregation might still occur. This makes essential the existence of a mechanism capable of regulating the two processes - chromosome segregation and cytokinesis - later in the cell cycle.

The NoCut checkpoint was discovered almost 10 years ago as the mechanism proposed to coordinate those two events (Norden et al., 2006; Mendoza et al., 2009; Steigemann et al., 2009). Along with a desire to fully understand the process and regulation of cytokinesis the NoCut checkpoint has generated much interest and discussion with a significant number of studies focusing on it. Below I will review the contribution of these studies to our understanding of NoCut and the regulation of cytokinesis in budding yeast and in human cells.

1.5.1. NoCut in budding yeast

The initial studies of the NoCut checkpoint showed a strong correlation between defects during chromosome segregation and inhibition of abscission. Specifically, defective stabilization of the spindle midzone, as in ase1 mutants, and mutants of the kinetochore components ndc10 and ndc80, induce an abscission delay that is dependent on the function of the kinase Aurora B/Ipl1 (Norden et al., 2006). Depolymerization of spindle microtubules was shown to activate an Ipl1-dependent abscission delay, which further suggested a specific requirement for a stable spindle midzone for completion of cytokinesis.

These perturbations also interfered with chromosome segregation. And in fact, spontaneous chromatin bridges in human cells (Steigemann et al., 2009) and budding yeast cells with defective resolution of cohesion or catenated sister chromatids (Norden et al., 2006; Mendoza et al., 2009) induced delays in the completion of cytokinesis through NoCut activation.

This led to the proposal that the spindle midzone allows for the NoCut checkpoint to monitor the clearance of chromatin from the cleavage plane. Consequently, during anaphase progression the spindle midzone would sequester Ipl1 away from the segregating chromatin, inactivating it and allowing for abscission to occur (Fig. **5**).

In all cases the inhibition of abscission was dependent on the function of the yeast Aurora B kinase Ipl1, as well as on its spindle midzone localization. By perturbing the FEAR network, which affects Ipl1 spindle localization, NoCut could not be activated in response to chromosome segregation or spindle defects (Mendoza et al., 2009).

In addition to Aurora B three other proteins were identified as essential for the NoCut response: Ahc1, Boi1 and Boi2. The Ahc1 protein is a component of the ADA acetyltransferase complex and although its specific function on NoCut is not known it was proposed to be required upstream of Ipl1 for proper NoCut activation (Mendoza et al., 2009).

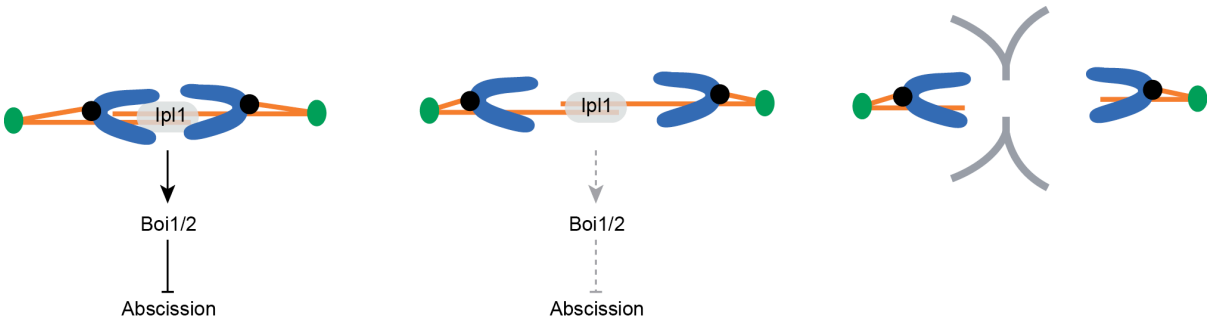

Figure 5: Model for the NoCut checkpoint in budding yeast. During anaphase Aurora B/Ipl1 localizes to the spindle midzone. There it is able to detect the presence of chromatin bridges and inhibit abscission by regulating Boi1/2 function. Once chromosomes are cleared away from the midzone Ipl1 becomes inactive and no longer inhibits abscission. Adapted from (Norden et al., 2006).

Boi1 and Boi2 are redundant proteins involved in polarized growth that translocate from the bud cortex to the bud neck at the time of cytokinesis (Hallett et al., 2002). Interestingly, their bud neck localization was observed to be dependent on Ahc1 and on Ipl1 (Norden et al., 2006; Mendoza et al., 2009) suggesting they work as effectors of Ipl1's function on NoCut (Fig. **5**). Importantly, the function of Boi1 and Boi2 on NoCut is essential to prevent damage of unsegregated DNA (Norden et al., 2006).

1.5.2. NoCut in human cells

The NoCut checkpoint (also referred to as the Aurora B-mediated abscission checkpoint) has also been shown to exist in higher eukaryotes. Spontaneous chromatin bridges in several human cell lines occur in low frequency and affect the progression of cytokinesis. In particular two responses have been observed: regression of the cleavage furrow or intercellular bridge stabilization. What determines the type of response to chromatin bridges is not known. The outcomes however are significantly different. In the first case cleavage furrow regression leads to cytokinesis failure and binucleation, resulting in tetraploidy, which hampers proliferation (Steigemann et al., 2009). In the second case, the intercellular bridge eventually resolves leading to two independent cells each with its own nucleus where segregation was seemingly completed and cells resumed normal proliferation (Steigemann et al., 2009).

Aurora B localizes to the midbody during telophase and remains on the midbody remnant after disassembly of midbody microtubules. Based on antibody detection of its phosphosite in Threonine 232, in an unperturbed cycle the kinase remains active until telophase. However, cells with stable intercellular bridges showed Aurora B activity persisting at the midbody to post-telophase stages, which appears to induce a delay in abscission (Steigemann et al., 2009).
Interestingly, besides chromatin bridges, defects in nuclear pore assembly or tension between the dividing cells influences the timing of abscission in an Aurora B-dependent manner (Mackay et al., 2010; Lafaurie-Janvore et al., 2013).

More recently, Aurora B was showed to control abscission timing by regulating one of the subunits of the membrane-remodeling complex ESCRT-III (Fig. **6**). The CHMP4C subunit has an inhibitory role on abscission (Carlton et al., 2012; Capalbo et al., 2012) and its regulation is done by direct phosphorylation on Serine 210 by the Aurora B kinase (Carlton et al., 2012). CHMP4C S210 phosphorylation is required for its translocation from the midbody arms to the Flemming body in late cytokinesis (Carlton et al., 2012). In response to chromatin bridges, CHMP4C together with the ANCHR protein were proposed to cooperate and retain the AAA-ATPase Vps4 at the midbody ring (Fig. **6**), preventing its localization to the abscission zone and thereby delaying abscission (Thoresen et al., 2014). Additionally, also the Ist1 subunit of ESCRT-III regulates abscission downstream of Aurora B. This regulation is mediated by the serine/threonine kinase Ulk3 after chromatin bridges, nuclear pore assembly defects or tension forces at the midbody (Caballe et al., 2015) and similarly to CHMP4C and ANCHR, enhances the interaction between Ist1 and Vps4.

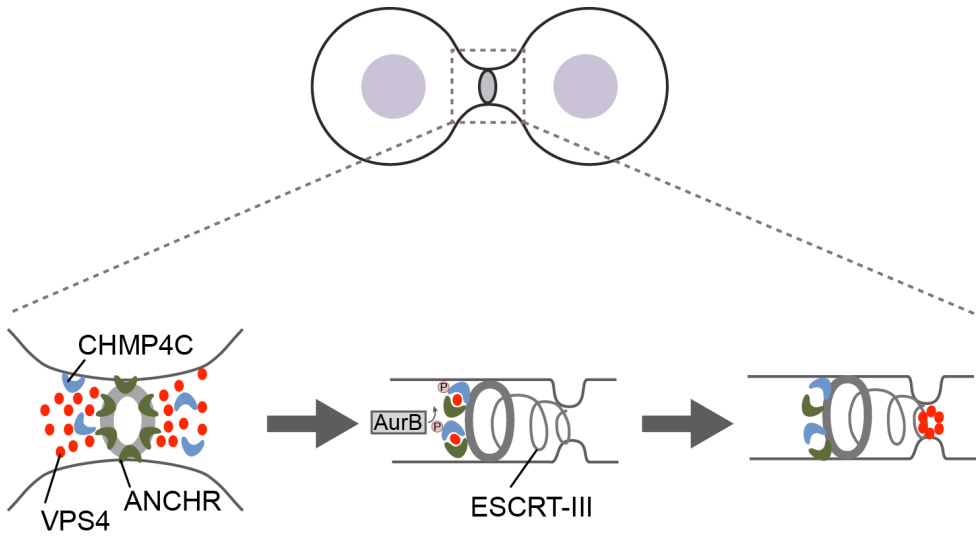

Figure 6: Model for the NoCut checkpoint in human cells. The ESCRT-III subunit CHMP4C forms a complex with ANCHR upon phosphorylation by Aurora B (AurB). This complex sequesters the ATPase VPS4 away from the constriction site, preventing it from promoting remodeling and/or disassembly of ESCRT complexes to allow for abscission to occur. Adapted from (Thoresen et al., 2014).

1.5.3. The physiological relevance of the NoCut checkpoint

The studies on the NoCut checkpoint suggest a correlation between chromosome segregation defects and delayed completion of cytokinesis. However, it has been shown that lagging chromosomes and chromatin bridges caused by dicentric chromosomes and by inactivation of condensin or topoisomerase II lead to cytokinesis-dependent DNA damage, in yeast (Baxter and Diffley, 2008; Cuylen et al., 2013; Lopez et al., 2015), as in human cells (Hoffelder et al., 2004) (Janssen et al., 2011). Therefore, it remains to be understood under which conditions is cytokinesis inhibited by the presence of chromatin bridges and whether this inhibition of cytokinesis prevents damage of unsegregated chromosomes. Moreover, good efforts have been made on understanding how is abscission regulated by NoCut, but it is not known how defects in chromosome segregation are detected by the checkpoint.

2. Objectives

From the initial studies on the NoCut checkpoint until now interesting observations have been made and significant advances have contributed to a better understanding of the mechanism behind the checkpoint. However, several questions remain open leaving new and exciting hypothesis to be tested.
In particular, with this study I have addressed the following questions:

- How are chromatin bridges detected by the NoCut checkpoint? Are there signals associated with specific types of chromatin bridges that trigger the checkpoint?

- How is the activity of the Aurora B kinase regulated in the context of the checkpoint?

- Does NoCut protect chromatin bridges from DNA damage by the cytokinetic machinery?

3. Methods

3.1. Strains and plasmids

Saccharomyces cerevisiae strains are derivatives of S288c. Gene deletions and taggings were generated by PCR-based methods (Janke et al., 2004); all fluorescently tagged proteins were expressed from the native promoter at the endogenous locus except GFP-Tub1 and mCherry-Tub1, which were inserted at the *URA3* locus after digestion of pRS306-based plasmids (gifts from Aaron Straight and Dimitris Liakopoulos) with StuI or ApaI respectively. DAPI staining (1 µg/ml) was performed as described (Norden et al., 2006). The conditional dicentric chromosome was previously described (Neurohr et al., 2011).

3.2. Cell growth

For G_1 arrest, cells were grown in YPDA (yeast extract, peptone, dextrose, and adenine) medium to logarithmic phase, synchronized with 15 µg/ml alpha-factor (purified from the in house proteomics facility) for 2 h at 25 ºC, and released in fresh YPDA medium at 30 °C or 37 ºC. *GAL1,10*-promoter driven GFP-CAAX expression was induced in glucose media in cell expressing the hybrid Gal1-ER-Vp16 protein (Louvion et al., 1993) by addition of 90 nM beta-estradiol 3 hours before imaging or by addition of galactose 3 hours before imaging to cells pregrown in YPRA (yeast extract, peptone, raffinose and adenine). Cells with the conditional dicentric chromosome were grown at 30 ºC in YPGA (yeast extract, peptone, galactose and adenine) medium before G1 arrest. To activate the dicentric chromosome, glucose was added to a final concentration of 2 % 1.5 hours after alpha-factor addition and cells were released from the G_1 arrest in fresh YPDA.

3.3. Fluorescence Microscopy

For time-lapse imaging, cells were plated in minimal synthetic medium on concanavalin A–coated (Sigma-Aldrich) Lab-Tek chambers (Thermo Fisher Scientific). Imaging was performed in a pre-equilibrated temperature-controlled microscopy chamber, using a spinning-disk confocal microscope (Revolution XD; Andor Technology) with a Plan Apochromat 100x, 1.45 NA objective equipped with a dual-mode electron-modifying charge-coupled device camera (iXon 897 E; Andor Technology). Time-lapse series of 4.5 µm stacks spaced 0.3 µm were acquired every 1.5 or 2 minutes. iQ Live Cell Imaging software (Andor Technology) was used for image acquisition. For quantification of abscission, images were analyzed on 4D hyperstacks and smoothed with the Gaussian blur function in ImageJ (National Institutes of Health). Only cells starting cytokinesis (membrane ingression) at least 45 minutes before the end of image acquisition were considered for the quantifications of abscission. Fluorescence intensities were measured from single sections of each cell to score membrane separation (abscission). Fluorescence analysis of fixed cells was performed in a wide-field microscope (Leica AF 600) with an Andor DU-885K-CSO-#VP camera. Images of 4.5 µm stacks spaced 0.3 µm apart were acquired.

3.4. Electron microscopy and tomography

Cells in Fig. 13c were fixed at 37 ºC using 4% formaldehyde and 0.4% glutaraldehyde, then processed as previously described (Idrissi et al., 2008). Ultrathin serial sections (60-70 nm) were collected on formvar-coated slot grids, post-stained with uranyl acetate (2% in water) over 30 min and lead citrate for 15 s and examined under a Tecnai Spirit transmission electron microscope (FEI Company) at 120 kV accelerating voltage. Micrographs were acquired at 26500x magnification using a CCD camera (MegaView III; Olympus) and the image acquisition analySIS software (Olympus) and processed for brightness and contrast using Photoshop (Adobe Systems). Cells in Fig. 13a, b were cryoimmobilized by high-pressure freezing with Leica EMPACT-2. High-pressure freezing and freeze substitution (-90 ˚C for 48 h in 0.1% glutaraldehyde, 0.2 % uranyl acetate and 1 % water in acetone) were performed on a EM-AFS2 device (Leica Microsystems,

Vienna, Austria). The temperature was then increased at a rate of 5 ˚C / hour to -45 ˚C followed by 5 h incubation. Samples were rinsed with acetone followed by stepwise lowicryl HM20 (Polysciences, Warrington, PA, USA) infiltration at -45 to -25 ˚C. UV polymerization was applied for 48 hours at -25 ˚C and the temperature was increased to 20 ˚C at a rate of 5 ˚C per hour. Finally the samples were left exposed to UV at room temperature for 48 h.

Sectioning was done on a Leica Ultra-cut UCT microtome (Leica Microsystems, Vienna, Austria) and serial sections were collected on Formvar-coated, palladium-copper slot grids. 70 nm thin sections were viewed using a CM120 biotwin electron microscope (FEI, Eindhoven, The Netherlands) operating at 120 kV. Digital acquisitions were made with a Keen View CCD camera (Soft Imaging System, Muenster, Germany). For tomography, 250 nm thick sections were placed in a high-tilt holder (Model 2020; Fischione Instruments; Corporate Circle, PA) and recorded on a Tecnai F30 EM (FEI, Eindhoven, The Netherlands) operating at 300kV using the SerialEM software package (Mastronarde 2005). Images were taken every degree over a ±60˚ range on an FEI Eagle 4K x 4K CCD camera at a magnification of 20000x and a binning of 2 (pixel size 1.179 nm). Tilted images were aligned using tilt series patch tracking. Tomograms were generated using the R-weighted back-projection algorithm and displayed as slices one voxel thick, modeled, and analyzed with the IMOD software package (Kremer et al., 1996).

3.5. Pulse-field gel electrophoresis

Cells growing in YPGA were arrested in G_1 with alpha factor (6 µg/ml). The culture was then split and glucose was added to one half to activate the dicentric chromosome. Cells were released 30 min later into a synchronous cell cycle. 3 ODs samples were taken at time 0; the same volume of culture was collected 2 and 3 hours after release from the G_1 arrest. Cells were washed with 50 mM EDTA twice, resuspended in 50 µl ice cold Solution 1 (1 M sorbitol, 0.1 M Sodium citrate, 60 mM EDTA, 0.5% β-mercaptoethanol, 1 mg/ml zymolyase 100T), and mixed with 75 µl molten 1 % LMP (1 % Low melting point agarose in 125 mM EDTA) before dispensing into plug molds. Plugs were incubated 2 hours at 37ºC in 400 µl Solution

2 (0.45M EDTA, 0.01M Tris HCl pH 7, 7.5 % β-mercaptoethanol, 10 µg/ml RNAse A), followed by overnight incubation in 400 µl of Solution 3 (0.25M EDTA, 0.01M Tris HCl pH 7, 1 % Sarkosyl, 1 mg/ml Proteinase K). Plugs were loaded in 0.8 % agarose gels and chromosomes separated in 0.5x TBE, recirculated at 14 ºC in a CHEF-DRII system (BioRad). The run time was 68 hours at 1.5 V/cm, followed by 48 hours at 2 V/cm. The switch time ramp was 300 to 900 seconds. The run time was 72 hours at 2 V/cm with a 1200 to 1800 seconds switch time ramp. Yeast chromosomes were visualized after staining with ethidium bromide and transferred onto positively charged membranes by saline upward capillary transfer. The dicentric chromosome was visualized using a 1.5 kb fluorescein-labelled probe within the *RDN1* gene in the rDNA array. Signals for broken and intact dicentrics were quantified from different unsaturated exposures of the same blot with Image Lab (Bio-Rad).

4. Results

4.1. The Ahc1 NoCut component promotes cell viability after DNA replication stress

Limited exposure to genotoxic agents causes mild DNA replication stress and increases the frequency of anaphase bridges in budding yeast, *Drosophila* and human cells (Germann et al., 2013; Fasulo et al., 2012; Chan et al., 2009). To assess whether NoCut is important for cell proliferation after DNA replication stress, yeast cells were grown to exponential phase and exposed to 100 mM hydroxyurea (HU) for 2 hours. Large budded cells were isolated after HU washout; after completion of cytokinesis, mother and daughter cells were separated and allowed to form colonies for 2 days (Fig. **7a**). Only 6-7% of wild-type cells failed to produce colonies, indicating that transient exposure to HU did not strongly impair their viability. In contrast, deletion of the previously described NoCut component *AHC1*, encoding a non-essential subunit of the ADA histone acetyltransferase (Mendoza et al., 2009), led to a 5-fold increase in cell lethality specifically after exposure to HU (Fig. **7b, c**). Furthermore, deletion of the non-essential cytokinesis gene *CYK3* which leads to delayed septum formation (Onishi et al., 2013) rescued the viability of HU-treated *ahc1*Δ mutants (Fig. **7c**). This suggests that an Ahc1-dependent cytokinesis delay promotes cell viability after DNA replication stress.

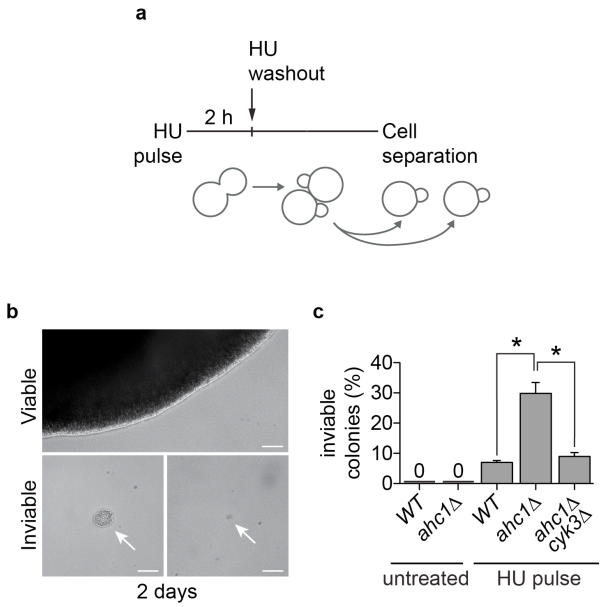

Figure 7: The Ahc1 NoCut component promotes cell viability after DNA replication stress. (**a**) Colony formation assay to determine cell viability after HU exposure. Log phase cells were treated with 100 mM HU for 2 hours at 30 ºC, washed with fresh medium and placed in YPD plates. Large-budded cells were isolated under a dissection microscope and upon entry in the next cycle (indicated by appearance of at least one bud) mother and daughter cells were separated and allowed to grow for 2 days at 30ºC. (**b**) Representative images of viable colonies and inviable micro-colonies (arrows) after 2 days of growth. Scale bars, 100 µm. (**c**) Percentage of inviable micro-colonies in the indicated cell types. Mean and SEM of 2-3 experiments are shown. Untreated: *n* = 98 (*WT*), 196 (*ahc1*Δ); HU pulse: *n* = 92, 78 (*WT*), 88, 80, 76 (*ahc1*Δ), 78, 78 (*ahc1*Δ *cyk3*Δ). Asterisks, p < 0.0001, Fisher's exact test.

4.2. NoCut prevents damage of chromatin bridges after replication stress

Cells were then stained with DAPI at time intervals after HU exposure and washout as above. Anaphase figures were not detected until 30 minutes after HU removal, reaching a maximum after 120 minutes. Thin DNA bridges containing histones (visualized via the core histone Htb2 fused to mCherry) connected the separated nuclei in most telophases (Fig. **8a**).

Nuclear and contractile ring components were next labeled with fluorescent reporters to follow anaphase and cytokinesis by time-lapse microscopy following HU exposure. Imaging of the nuclear envelope (NE) protein Nsg1-GFP showed that in untreated and HU-treated cells, the tube-like NE bridge connecting telophase nuclei was resolved during contraction of the actomyosin ring, which marks the onset of

cytokinesis (Lippincott, 2000) (Fig. **8b**). Untreated cells completed chromosome segregation before onset of Myo1 ring contraction. In contrast, cells exposed to 100 mM HU followed by washout, or to 60 mM HU without washout (which did not immediately prevent anaphase onset), displayed thin chromatin bridges labeled with Htb2-mCherry, which disappeared only after contraction of the Myo1 ring (Fig. **8c, d**).

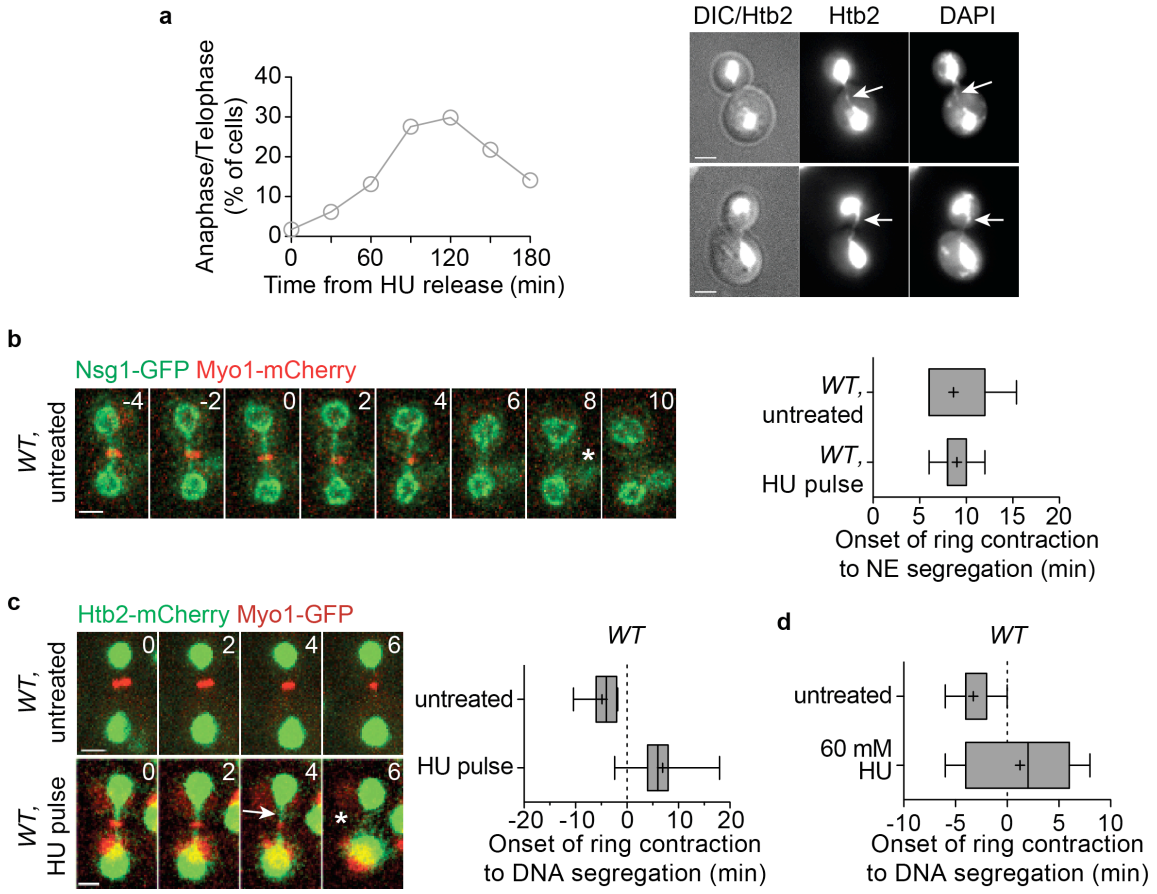

Figure 8: DNA replication stress induces formation of chromatin bridges. (a) Time-course of wild type cells after treatment with 100 mM HU for 2 hours. The Htb2-mCherry signal was used to estimate the frequency of anaphase (with elongated nuclei) or telophase (with separated nuclei) cells (left). More than 100 cells were analyzed for each time point in one experiment. The micrographs (right) show cells 120 min after HU washout stained with DAPI to visualize DNA. The arrows point to chromatin bridges. Scale bars, 2µm. **(b)** Kinetics of nuclear division (visualized with Nsg1) in wild type cells in log-phase or after exposure to HU at 30 ºC. Asterisk marks the time of nuclear division. Numbers indicate time in minutes. The graph shows the time of nuclear division relative to the onset of ring contraction (time 0). The kinetics between the two conditions were considered to be not statistically significant ($p > 0.05$, Mann-Whitney test). *n* = 22 untreated cells and 20 HU-treated cells. **(c,d)** Kinetics of chromosome segregation (Htb2-mCherry) relative to actomyosin ring contraction (Myo1-GFP) of wild type cells at 30 ºC, untreated or treated with HU. (c) Cells were treated with an HU pulse. An arrow points to a chromatin bridge, and an asterisk marks the time of chromosome segregation (separated nuclear masses) after HU treatment. The graph shows the time of chromosome segregation relative to the onset of ring contraction (time 0). In this and following graphs, boxes include 50% of data points, and whiskers are 90%. Median (lines) and mean (crosses) are shown. *n* = 28 untreated and 43 HU-treated cells. (d) cells in the absence or presence of 60 mM HU. *n* = 80 untreated cells and 66 HU-treated cells.

Contraction of the actomyosin ring drives the plasma membrane inward and guides deposition of the primary septum, followed by deposition of secondary septa. Fission of the contracted membrane ensues, in a process termed abscission (Dobbelaere and Barral, 2004). To monitor plasma membrane ingression and resolution after inducing DNA replication stress, GFP fused to the membrane-targeting CAAX motif of Ras2 was used as a reporter. The spindle pole marker Spc42-GFP allowed the simultaneous visualization of spindle elongation. In untreated cells, membrane ingression at the mother-bud neck was followed by its resolution after an average of 20 minutes, whereas deletion of *CYK3* significantly delayed the time between membrane ingression and resolution, confirming it plays a role in abscission (Fig. **9a-c**). Abscission was delayed in wild-type cells exposed to DNA replication stress, caused by either a 100 mM HU pulse or by the continued presence of 60 mM HU, at both 30 ºC and 37 ºC (Fig. **9a-e**), and this delay was rescued in *sml1* mutants with increased dNTP levels (Zhao et al., 1998) (Fig. **9f**), suggesting replication stress induces an abscission delay. To determine whether NoCut mediates this abscission delay, abscission kinetics were determined in *ahc1*Δ mutant cells and in cells impaired in Aurora B function by the *ipl1-321* temperature sensitive (ts) mutation. Ahc1 deletion and Aurora B inactivation restored abscission kinetics to wild-type levels (Fig. **9c, d** and **g**). Thus, DNA replication stress causes chromatin bridges and delays abscission in a manner depending on Ahc1 and Aurora B.

The DNA double strand break repair protein Mre11 forms nuclear foci indicative of DNA damage. Approximately 35% of wild type, *ipl1-321* and *ahc1*Δ cells exposed to 100 mM HU for 2 hours showed Mre11-GFP nuclear foci when examined by time-lapse microscopy (Fig. **10a**). In wild type and in mutant strains, the fraction of cells with foci diminished following HU removal to less than 10% during mitosis, and remained low even after prolonged arrest in late anaphase by the *cdc15-1* mutation (Fig. **10b**). Foci were again detected in 10-15% of wild-type cells in the next cycle; however, this fraction was increased to 30% in *ipl1-321* and *ahc1*Δ mutant cells (Fig. **10c, d**). Moreover, the fraction of cells with Mre11 foci in the *ipl1* and *ahc1* NoCut mutants was reduced back to wild-type levels by depletion of Cyk3, indicating that they depended on advanced abscission (Fig. **10c, d**). We conclude that NoCut prevents DNA damage in cells exposed to replication stress.

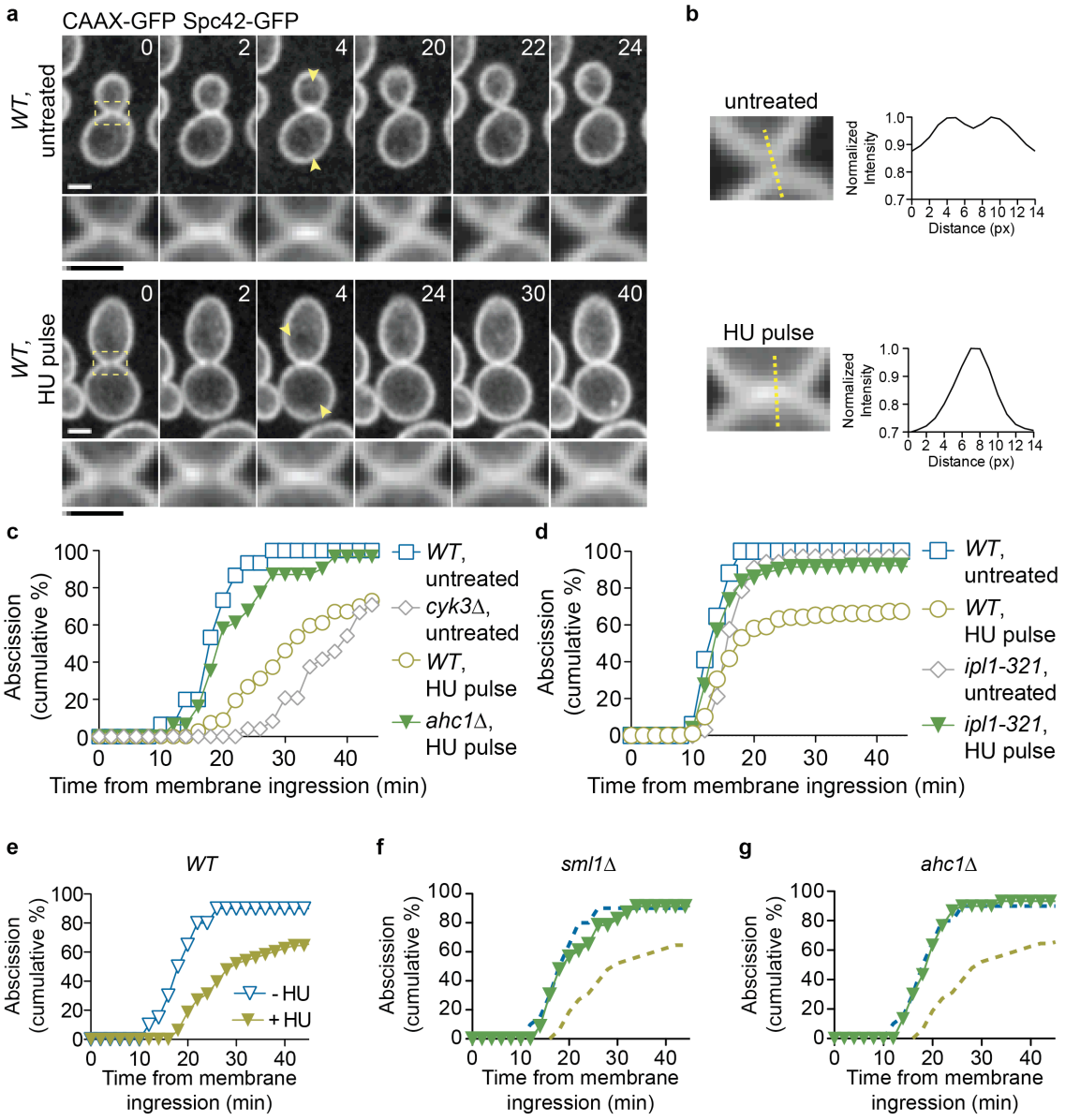

Figure 9: DNA replication stress induces a NoCut-dependent abscission delay. (a) Membrane ingression and abscission in control and HU-treated wild-type cells. Whole-cell images are shown on top, and enlargements of the bud neck region at the bottom. The position of spindle pole bodies labeled with Spc42-GFP is marked with arrowheads. Numbers indicate time in minutes; time 0 marks the frame before membrane ingression. (**b**) To analyze the status of the bud neck membrane, the GFP fluorescence intensity was measured across the cleavage plane in the central Z-plane (yellow lines). A drop in intensity marked membrane resolution and was scored as abscission (top); a single peak denoted the pre-abscission stage (bottom). (**c-g**) Graphs show the fraction of cells completing abscission relative to the time of membrane ingression at 30 ºC (c, f-g) and 37 ºC (d). Cells in (c,d) were treated with a 2 hour, 100 mM HU pulse, released and analyzed. Statistically significant delays in abscission relative to the *WT* untreated condition were only found in *cyk3*Δ and *WT* HU-treated cells ($p < 0.0001$, Mann-Whitney test). In (c) n = 19 cells (*WT* untreated); 24 (*cyk3*Δ); 88 (*WT* HU pulse); 31 (*ahc1*Δ HU pulse). In (e), n = 17 cells (*WT*, untreated); 98 (*WT*, HU pulse); 33 (*ipl1-321* untreated); 140 (*ipl1-321* HU pulse). Cells in **(e-g)** were either untreated or treated with 60mM HU and analyzed. A statistically significant difference was only observed between *WT* -HU and *WT* +HU (p = 0.0111, Mann-Whitney test). *WT* -HU and *WT* +HU from (e) are represented as dashed lines for comparison in (f-g). n = 20 (*WT* -HU); 48 (*WT* +HU); 23 (*sml1*Δ); 30 (*ahc1*Δ).

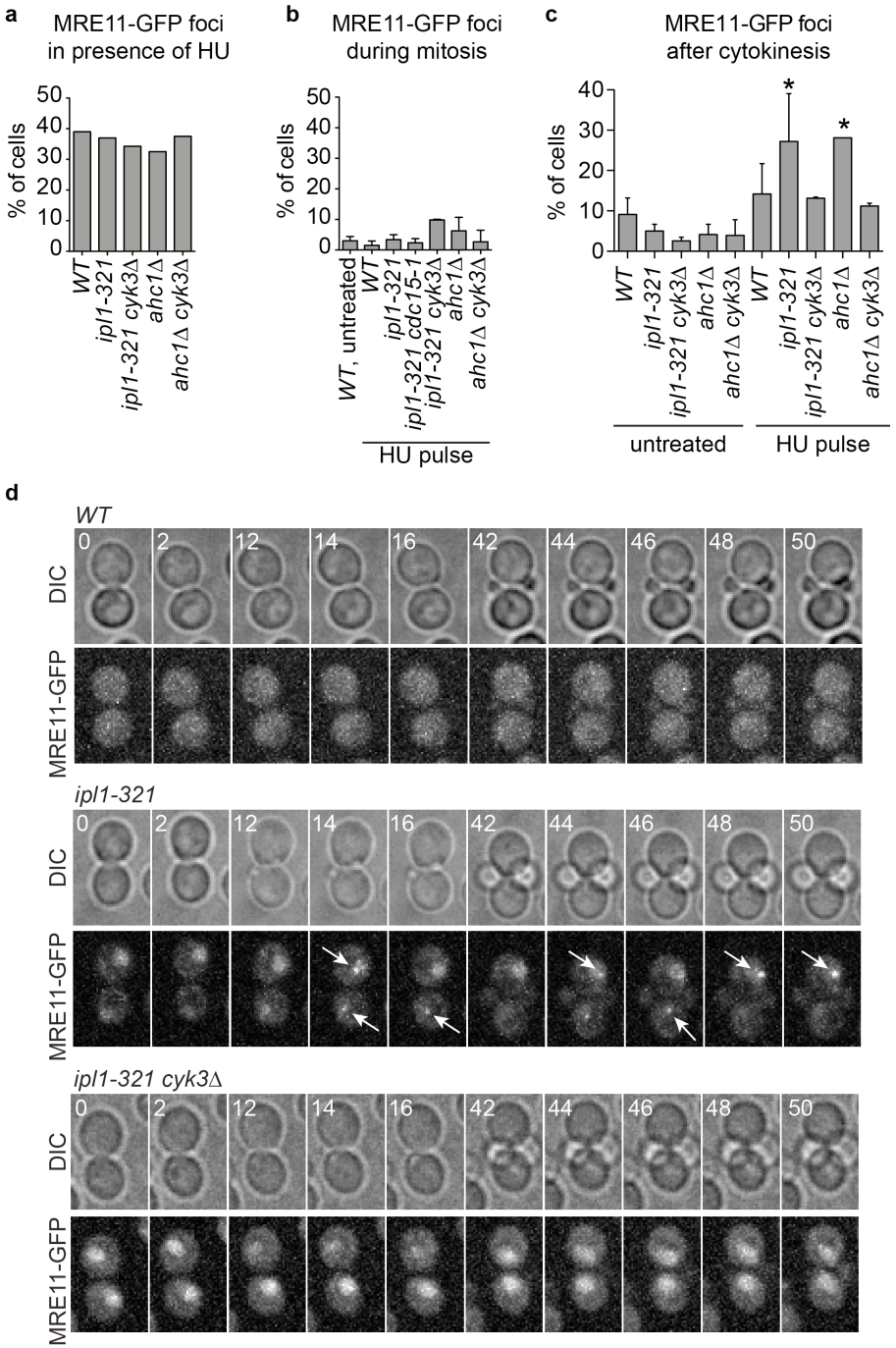

Figure 10: NoCut prevents DNA damage after DNA replication stress. (a-c) Percentage of cells with Mre11-GFP foci in HU (a), during mitosis (b) or after cytokinesis (c). **(a)** Cells of the indicated strains were treated with 100 mM HU for 2 hours and imaged for 20 minutes. *n* = 41 cells (wild type); 46 (*ipl1-321*); 35 (*ipl1-321 cyk3*Δ); 40 (*ahc1*Δ); 40 (*ahc1*Δ *cyk3*Δ). **(b)** After HU washout, cells were imaged during nuclear elongation. *n* = 98 (*WT,* untreated); HU-treated cells: 190 (wild type), 176 (*ipl1-321*), 134 (*ipl1-321 cdc15-1*), 122 (*ipl1-321 cyk3*Δ), 128 (*ahc1*Δ), 116 (*ahc1*Δ *cyk3*Δ). (c) Frequency of Mre11-GFP focus formation after cytokinesis. Asterisks represent statistically significant differences from wild type, HU pulse ($p < 0.005$, Fisher's exact test). Mean and SD of 2-3 experiments are represented. Untreated cells: *n* = 98 (*WT)*, 120 (*ipl1-321)*, 110 (*ipl1-321 cyk3*Δ*)*, 112 (*ahc1*Δ*)*, 112 (*ahc1*Δ *cyk3*Δ); HU pulse: 190 (*WT*), 176 (*ipl1-321*), 122 (*ipl1-321 cyk3*Δ), 128 (*ahc1*Δ), 116 (*ahc1*Δ *cyk3*Δ). **(c)** Time-lapse images of representative wild type, *ipl1-321* and *ipl1-321 cyk3*Δ cells expressing Mre11-GFP, after cytokinesis following a HU pulse. The arrows point to nuclear Mre11 foci. Numbers indicate time in minutes where time 0 is the frame before cytokinesis. Frames were selected to show Mre11-GFP foci in the *ipl1-321* mutant.

4.3. Aurora B inhibits abscission in cells with decondensed and catenated chromatin bridges

To evaluate if specific features of chromatin present at the division site contributed to inhibition of abscission, we characterized cytokinesis in cells with lagging chromatin due to ts mutations inactivating condensin (*ycg1-2*) and topoisomerase II (*top2-4*) (Holm et al., 1985; Lavoie et al., 2002). Cells were grown at 25 ºC, arrested in G_1 with mating pheromone, and released from the arrest at 37 ºC. Inactivation of condensin or topoisomerase II (Topo 2) did not delay the onset of Myo1-GFP ring contraction relative to the time of nuclear elongation (imaged with Htb2-mCherry), or the duration of the ring contraction period compared with wild-type cells, as reported (Cuylen et al., 2013) (Fig. **11a**). Chromosome segregation was completed before contraction of the actomyosin ring in wild-type cells, whereas *ycg1-2* and *top2-4* cells displayed prominent chromatin bridges that disappeared only after ring contraction (Fig. **11b**).

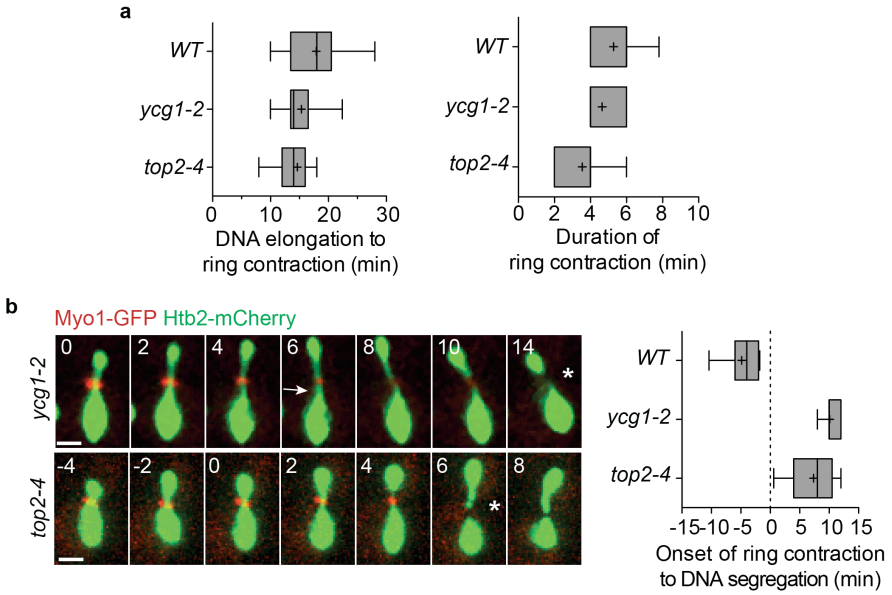

Figure 11: Chromosome segregation is delayed in *ycg1-2* and *top2-4* cells. (**a**) Time of actomyosin ring contraction relative to nuclear elongation (left) and the duration of contraction (right), in the indicated cell types. *n* = 42 cells (wild type), 18 (*ycg1-2*), 19 (*top2-4*). **(b)** Anaphase progression in *ycg1-2* and *top2-4* cells with fluorescently tagged histone (Htb2) and myosin (Myo1). The arrow points to a chromatin bridge. Numbers indicate time in minutes. Scale bar is 2 µm. Time 0 is before onset of myosin ring contraction. Asterisk marks the time of chromosome segregation (separated nuclear masses). The graph shows the time of segregation in wild type and mutant cells relative to ring contraction. *n* = 28 cells (*WT*); 19 (*ycg1-2*); 22 (*top2-4*).

Efficient plasma membrane ingression was also observed in *ycg1-2* and *top2-4* cells expressing the GFP-CAAX plasma membrane reporter. However membranes failed to resolve within 45 minutes in more than 75% of *ycg1-2* and *top2-4* cells (Fig. **12a-c**), indicating impairment of abscission. Initiation of the next cell cycle, as indicated by appearance of a new bud in the mother cell, was also delayed in condensin and Topo II mutants: 95% of wild type cells started a new bud within 30 minutes of cytokinesis membrane closure, compared to 27% of *ycg1-2* and 43% of *top2-4* cells (Fig. **12c**). The mechanism delaying entry into the next cell cycle is not known at this point.

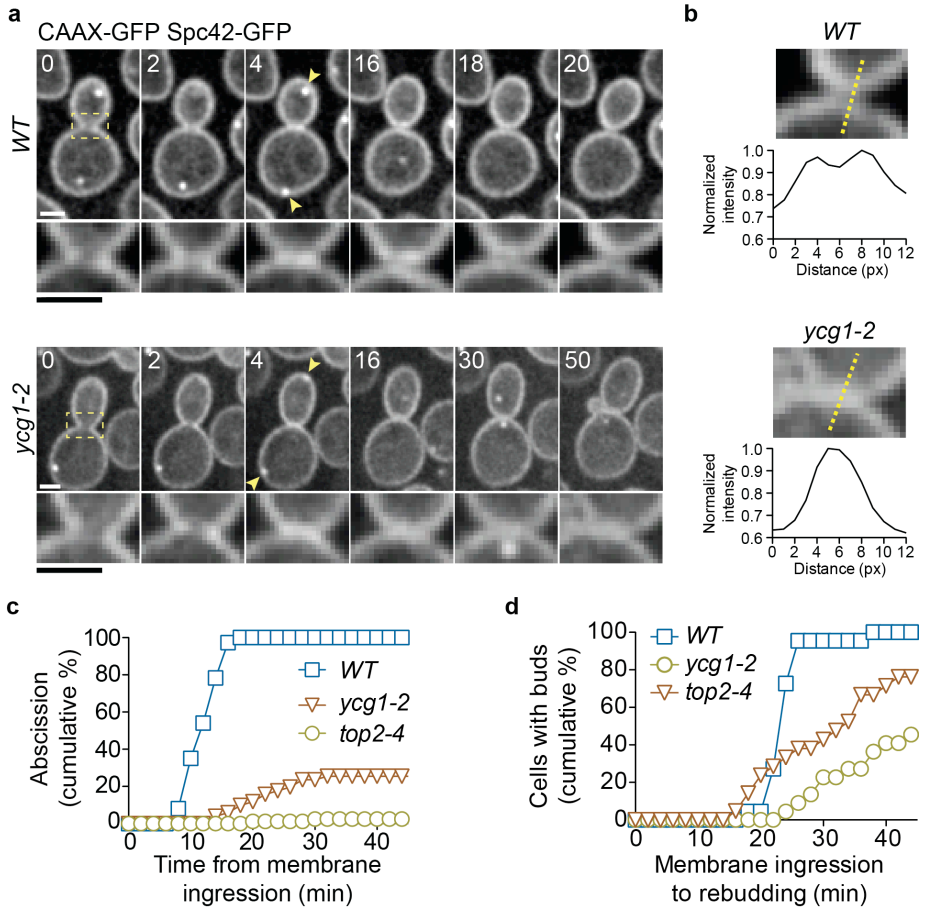

Figure 12: Abscission is delayed in *ycg1-2* and *top2-4* cells. (**a**) Membrane ingression and abscission in wild type and *ycg1-2* cells, visualized with GFP-CAAX. Whole-cell images are shown on top, and enlargements of the bud neck region at the bottom. The position of spindle pole bodies labeled with Spc42-GFP and determined by examining all optical sections is marked with arrowheads. Numbers indicate time in minutes; time 0 marks the frame before membrane ingression. (**b**) Bud neck membrane status in the indicated strains. GFP fluorescence intensity was measured across the cleavage plane in the middle optical section. **(c)** The graph shows the fraction of cells completing abscission relative to the time of membrane ingression. *n* = 37 cells (*WT*), 51 (*ycg1-2*); 80 (*top2-4*). Significant differences were observed in *WT* vs. *ycg1-2* and *WT* vs. *top2-4* ($p < 0.0001$, Mann-Whitney test). **(d)** Time of appearance of the next bud after cytokinesis (rebudding) relative to the time of membrane closure. *n* = 22 cells (wild type), 22 (*ycg1-2*), 21 (*top2-4*). The rebudding kinetics of wild type and mutant cells were considered significantly different ($p < 0.05$, Mann-Whitney test).

Thin-section electron microscopy was performed in wild type, *ycg1-2* and *top2-4* cells 90 minutes after release from the G_1 block. Septa with typical trilaminar structure were formed in cells of all strains; however, septa in *ycg1-2* and *top2-4* contained lacunae not observed in wild-type cells (Schmidt et al., 2002; Tully et al., 2009) (Fig. **13a**). Electron tomography further revealed that these lacunae formed a continuous “channel” across the septum connecting mother and daughter cells. Septum channels in *ycg1-2* and *top2-4* cells were delimited by plasma membrane, and enclosed nuclear envelope (tomograms of 6 *ycg1-2* and 6 *top2-4* cells) (Fig. **13a,b**). Membrane-bound vesicles of 60-100 nm in diameter were also found in close proximity to the division septa in *ycg1-2* cells, which also contained microtubule bundles traversing the septum (Fig. **13a**). Septum channels in *ycg1-2* and *top2-4* mutants occasionally contained amorphous electron-dense material (see Fig. **13a**, iii and iv and **13b**). Furthermore, analysis of ultra-thin serial sections showed that septum channels were present in all examined *ycg1-2* mutant cells 3 hours after release from the G_1 block (9 cells), whereas all wild-type cells showed intact septa (13 cells) (Fig. **13c**). The narrow diameter of septum channels in *ycg1* and *top2* mutants, and their close association with NE membranes may explain why these channels do not support the exchange of a cytoplasmic reporter between mother and daughter cells in the next cycle (Cuylen et al., 2013). Moreover because cytoplasmic continuity was assayed after rebudding, which is delayed in *ycg1* and *top2* mutants relative to wild-type cells (Fig. **12d**), this previous study does not rule out delayed abscission in cells with chromatin bridges. We thus conclude that membrane abscission is inhibited or strongly delayed in condensin and Topo II mutants.

We next tested the role of Ahc1 and Aurora B in this abscission delay. Deletion of Ahc1 slightly advanced abscission in *ycg1-2* and *top2-4* mutants; however, this effect was of a very small magnitude or did not reach statistical significance (Fig **14a**). In contrast, inactivation of Aurora B in *ipl1-321* cells significantly advanced abscission in condensin and Topo II mutants. Membrane resolution at the bud neck visualized by GFP-CAAX was completed within 45 minutes after onset of cytokinesis in more than 65% of *ycg1-2* and *top2-4* mutant cells with inactive Aurora B, compared to 25% in the *ycg1-2* and 2.5% *top2-4* single mutants (Fig. **14b, c**).

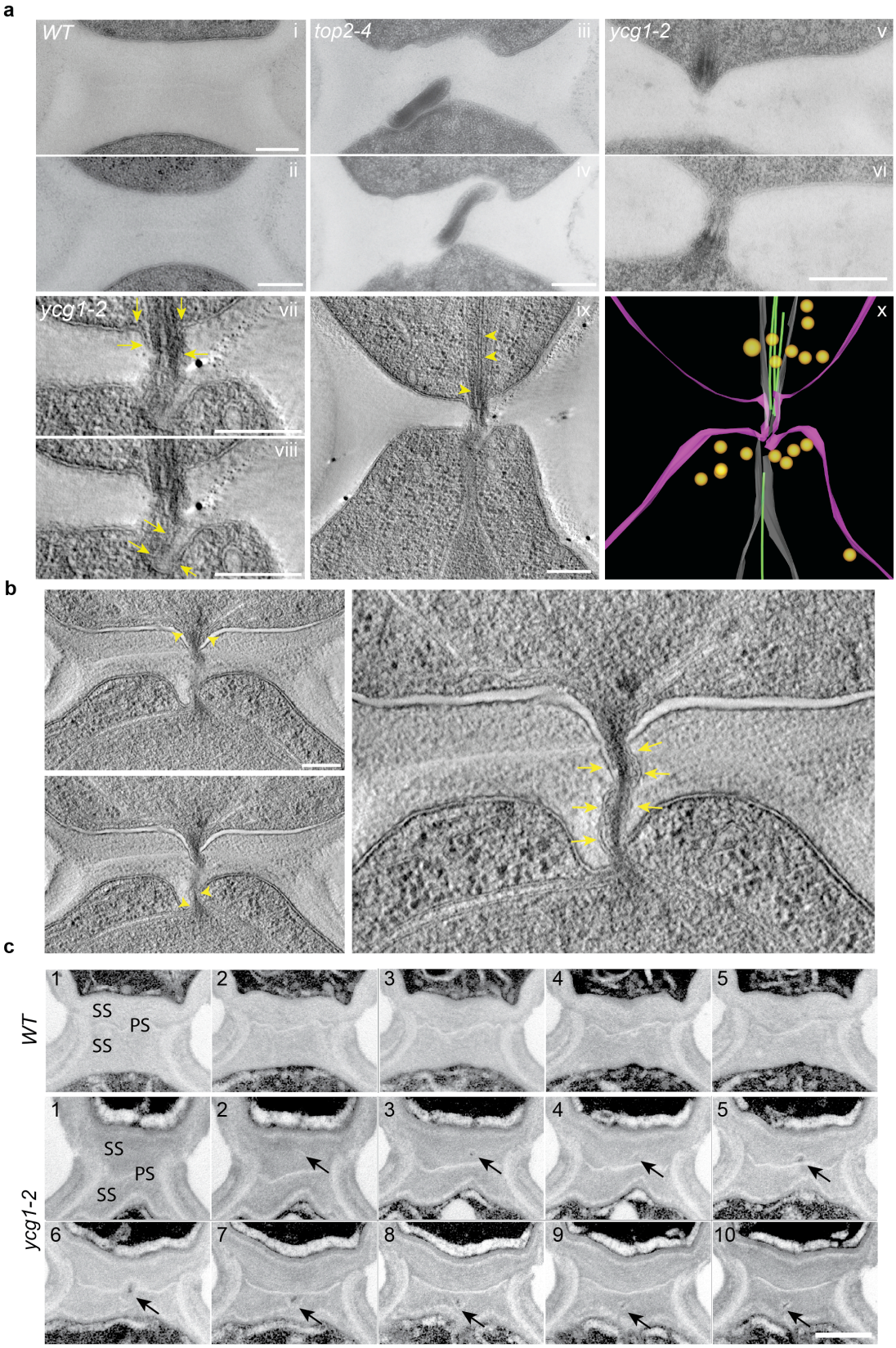

Figure 13: Septum channels are present in *ycg1-2* and *top2-4* cells. (a) Transmission electron microscopy of cells of the indicated strains. Images show the medial septum region of two wild type cells (i-ii), and two consecutive serial sections of *top2-4* (iii-iv) and *ycg1-2* cells (v-vi) 90 minutes after release from a G_1 block at 37 ºC. (vii-ix). Tomographical slices of the septum area of a *ycg1-2* cell. Arrows point to plasma membrane underlying the channel (vii-viii), arrowheads point to microtubules

(ix). A 3D model of the membrane organization at the medial septum is shown in (x). Plasma membrane is in purple, nuclear envelope in light gray, microtubules in green and vesicles in yellow. **(b)** Slices from a tomogram of the septum in a *top2-4* cell. Arrowheads point to nuclear membrane entering the channel (left); Arrows point to plasma membrane underlying the channel (right). **(c)** Electron micrographs of ultra-thin sections (60-70 nm) from cells of the indicated genotype. Arrows point to lacunae traversing the septum of the mutant. PS, primary septum, SS, secondary septum. Scale bars, 0.2 µm in (a-b) and 0.5 µm in (c).

Yet, chromatin bridges were present in Ipl1-deficient cells in these mutant backgrounds (Fig. **14d**). In addition, the anaphase function of Aurora B was perturbed by deletion of Slk19, which promotes Aurora B activity at the spindle midzone through its role in the early anaphase activation of the Cdc14 phosphatase (Pereira, 2003). The *slk19*∆ mutation restored abscission in the condensin mutant in spite of the presence of chromatin bridges during ring contraction (Fig. **14b, d**). The time of disappearance of Htb2-mCherry bridges after condensin inactivation was slightly advanced in *ipl1* and *slk19* mutants, suggesting that Aurora B increases the lifetime of the DNA bridge even in the absence of condensin function (Fig. **14d**). Additionally expression of Sli15-6A, a phosphomutant form of the chromosomal passenger complex component Sli15/INCENP that restores anaphase Ipl1 function in the absence of Slk19 (Mendoza et al., 2009; Neurohr et al., 2011), introduced an abscission delay in the *ycg1-2 slk19*∆ mutant (Fig. **14e**). Thus, Aurora B inhibits abscission in cells with chromatin bridges caused by lack of condensin or Topo II activity.

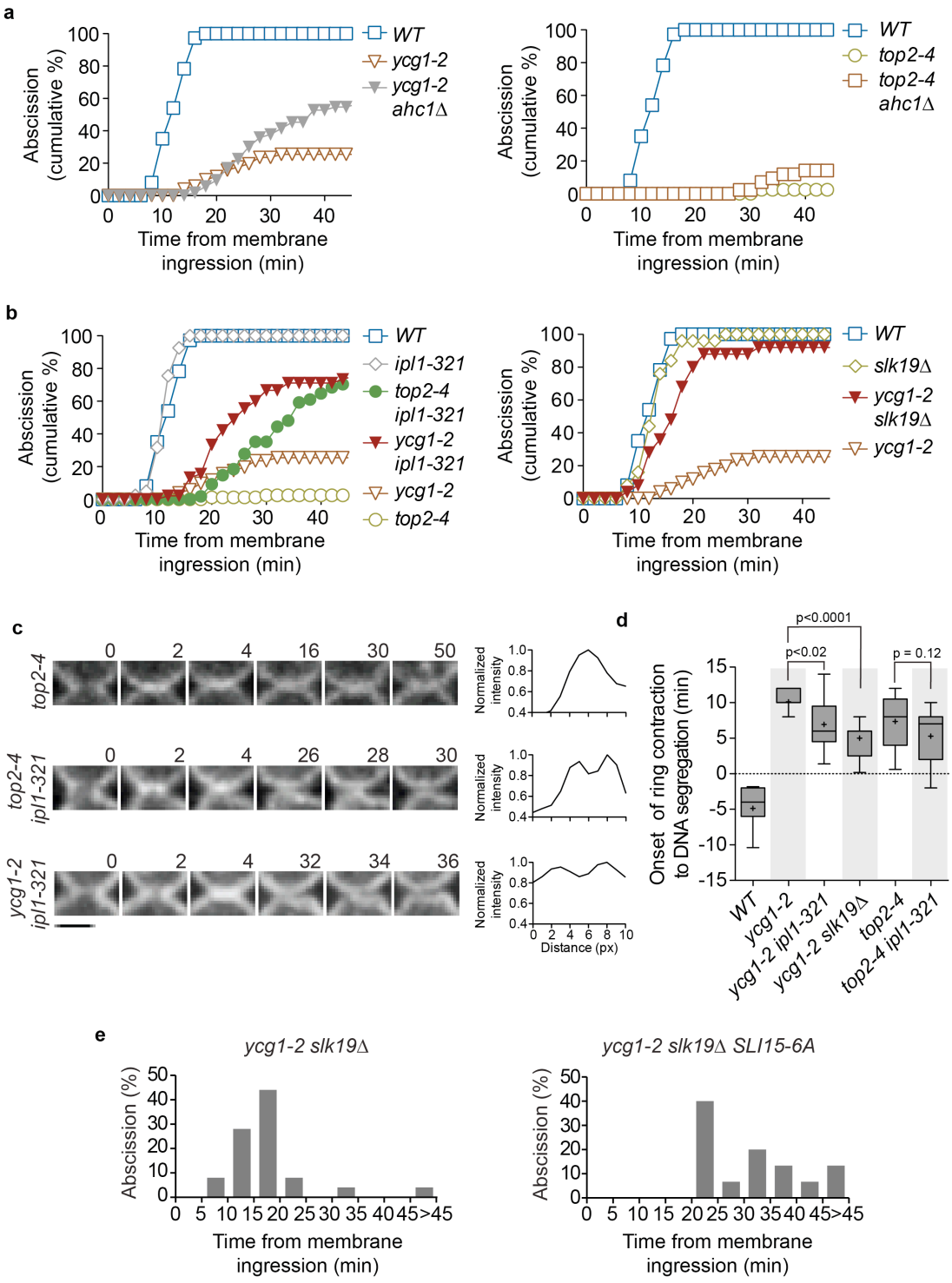

Figure 14: Aurora B inhibits abscission in response to condensin or topoisomerase II defects. **(a-b)** Cumulative percentage of abscission in the indicated strains. (a) *p* values (Mann-Whitney test) are: 0.31 (*ycg1-2* vs. *ycg1-2 ahc1*Δ) and 0.0253 (*top2-4* vs. *top2-4 ahc1*Δ). (b) Inactivation of Ipl1 or Slk19 advances abscission in *ycg1-2* and *top2-4* mutant cells ($p < 0.0001$, Mann-Whitney test). Data from: *n* = 53 cells (*ycg1-2 ahc1*Δ); 40 (*top2-4*); 42 (*top2-4 ahc1*Δ); 41 (*ipl1-321*), 45 (*ycg1-2 ipl1-321*); 54 (*top2-4 ipl1*-321); 25 (*slk19*Δ); 25 (*ycg1-2 slk19*Δ). Wild type, *ycg1-2* and *top2-4* data from Fig 12c are shown for comparison. (**c**) Time series of membrane ingression and resolution of the indicated strains. Scale bar is 2µm. The graphs show the GFP fluorescence intensity across the cleavage plane in the middle optical section. **(d)** Time of chromosome segregation in the indicated strains. Time 0 was defined as the frame before the onset of contraction of the myosin ring. *n* = 29 cells (*ycg1-2 ipl1-321*); 20 (*ycg1-2 slk19*Δ); 20 (*top2-4 ipl1-321*). *p* values are shown (Mann Whitney test). **(e)** Expression of

Sli15-6A delays abscission in *ycg1-2 slk19*Δ cells. 15 *ycg1-2 slk19*Δ *SLI15-6A* cells were analyzed and compared with *ycg1-2 slk19*Δ cells from (b) ($p < 0.001$, Mann-Whitney test).

4.4. Dicentric chromatin bridges do not inhibit abscission

Next, we investigated whether chromatin bridges inhibit abscission in the presence of condensin and Topoisomerase II activity, using a conditionally dicentric chromosome. End-to-end fusion of chromosomes IV and XII produced the conditional dicentric *LC(IV:XII)pGAL-CEN4*, in which centromere 4 is kept inactive thanks to activation of the strong *GAL1,10* promoter (Fig. **15a**). Upon activation of *CEN4* in glucose-containing media, the two kinetochores achieve biorientation independently, leading to formation of chromatin bridges in 50% of anaphases (Fig. **15b**). Accordingly, the conditional dicentric chromosome does not affect cell growth when *CEN4* is inactivated in media containing galactose, whereas it causes poor growth when cells are cultured in glucose (Neurohr et al., 2011) (Fig. **15c**).

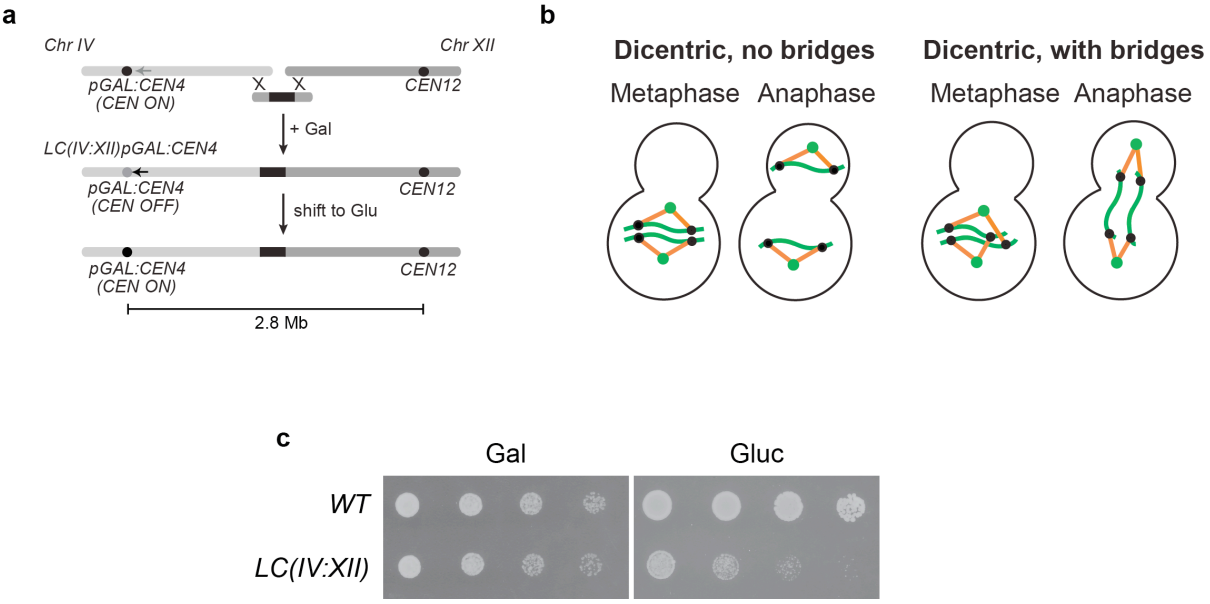

Figure 15: Generation of dicentric chromosomes. (a) Schematic representation of the generation and structure of the conditionally dicentric chromosome LC(IV:XII)pGAL-CEN4. The estimated distance between centromeres 4 and 12 is indicated, assuming 100 rDNA repeats. **(b)** Biorientation of kinetochores in a dicentric chromosome leads to lagging chromosomes in 50% of anaphases. Green circles, spindle pole bodies; orange bars, kinetochore microtubules; black circles, kinetochores; green lines, dicentric chromosomes. **(c)** Growth test of serial dilutions of the indicated cell types in rich medium plates with galactose (Gal) or glucose (Gluc).

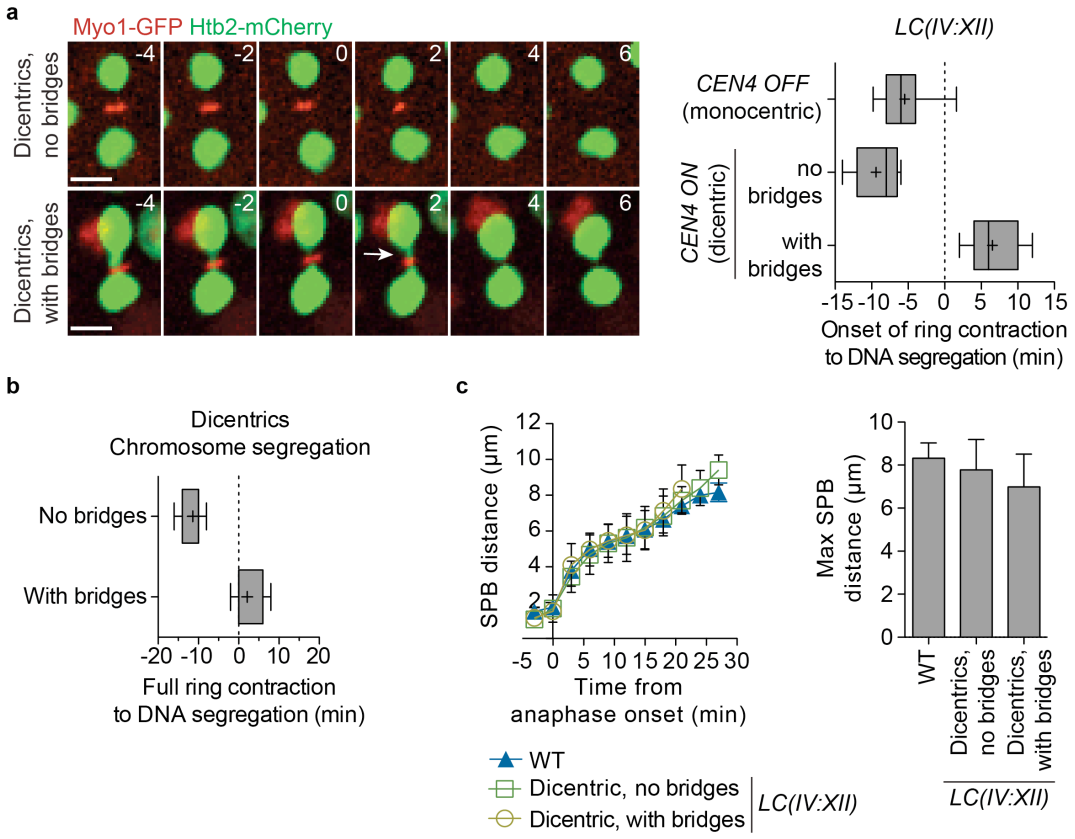

Figure 16: Dicentric chromosomes form anaphase bridges. (a) Anaphase progression in cells with the conditional dicentric chromosome expressing fluorescently tagged histone (Htb2) and myosin (Myo1). Arrow points to a chromatin bridge. The graph shows the time of chromosome segregation for cells with the conditional dicentric chromosome in either galactose medium (*CEN4 OFF* - monocentric condition) or after shift to glucose (*CEN4 ON* - dicentric condition). *n* = 50 cells (monocentric); 20 (dicentric, no bridges); 19 (dicentric, with bridges). **(b)** Time of chromosome segregation relative to full ring contraction in cells with dicentric chromosomes. **(c)** Spindle tracks (left) and maximal spindle length (right) of cells with wild type chromosomes (WT) and the two categories of cells with dicentrics chromosomes (*LC(IV:XII)*). SPB distance is the linear distance between the two spindle pole bodies (SPBs) at each time point. Both graphs show the mean and SD. Anaphase onset was defined when SPB distance was above 2.5 µm. *n* = 9 cells for each cell type or category.

Time-lapse microscopy of *MYO1-GFP HTB2-MCHERRY* cells with the conditional dicentric in galactose medium showed that chromosome segregation was completed prior to myosin ring contraction in 90% of cells (45/50) (Fig. **16a**). In contrast, after activation of *CEN4* in glucose-containing medium, nuclear division was completed before the onset of ring contraction in only 51% of cells (20/39), whereas chromatin bridges persisted during cytokinesis in 49% of cells (19/39) (Fig. **16a**). In most cases these bridges persisted after complete ring contraction (Fig. **16b**). Spindle elongation visualized with Spc42-GFP was similar in monocentric and *LC(IV:XII)* dicentric cells; both the time of spindle disassembly and the maximal spindle length were

comparable with those of wild-type cells (Fig. **16c**). Activation of conditional dicentrics based on chromosome III (Yang et al., 1997) or by fusion of chromosomes VI and VII (Lopez et al., 2015) causes defects in spindle elongation. The lack of such defects in the dicentric described here might be due to the longer distance between the centromeres in the *LC(IV:XII)* (2.8 Mb) compared to the previously described dicentrics (45 kb and 620 Kb respectively).

Abscission efficiency in the presence of dicentric bridges was then scored by inspection of the plasma membrane at the bud neck in *HTB2-MCHERRY GFP-CAAX* cells. Abscission occurred with nearly wild-type kinetics in all dicentric cells irrespective of the presence of chromatin bridges (Fig. **17a-c**). Breakage of the LC(IV:XII) dicentric after cytokinesis was confirmed by pulse-field gel electrophoresis showing fragmentation of the *RDN1* locus in the dicentric chromosome (Fig. **17d**), in agreement with similar observations in dicentrics formed by fusion of chromosome VI with chromosomes III, VII or XIV (Lopez et al., 2015). Thus dicentric chromosome bridges do not trigger the NoCut response.

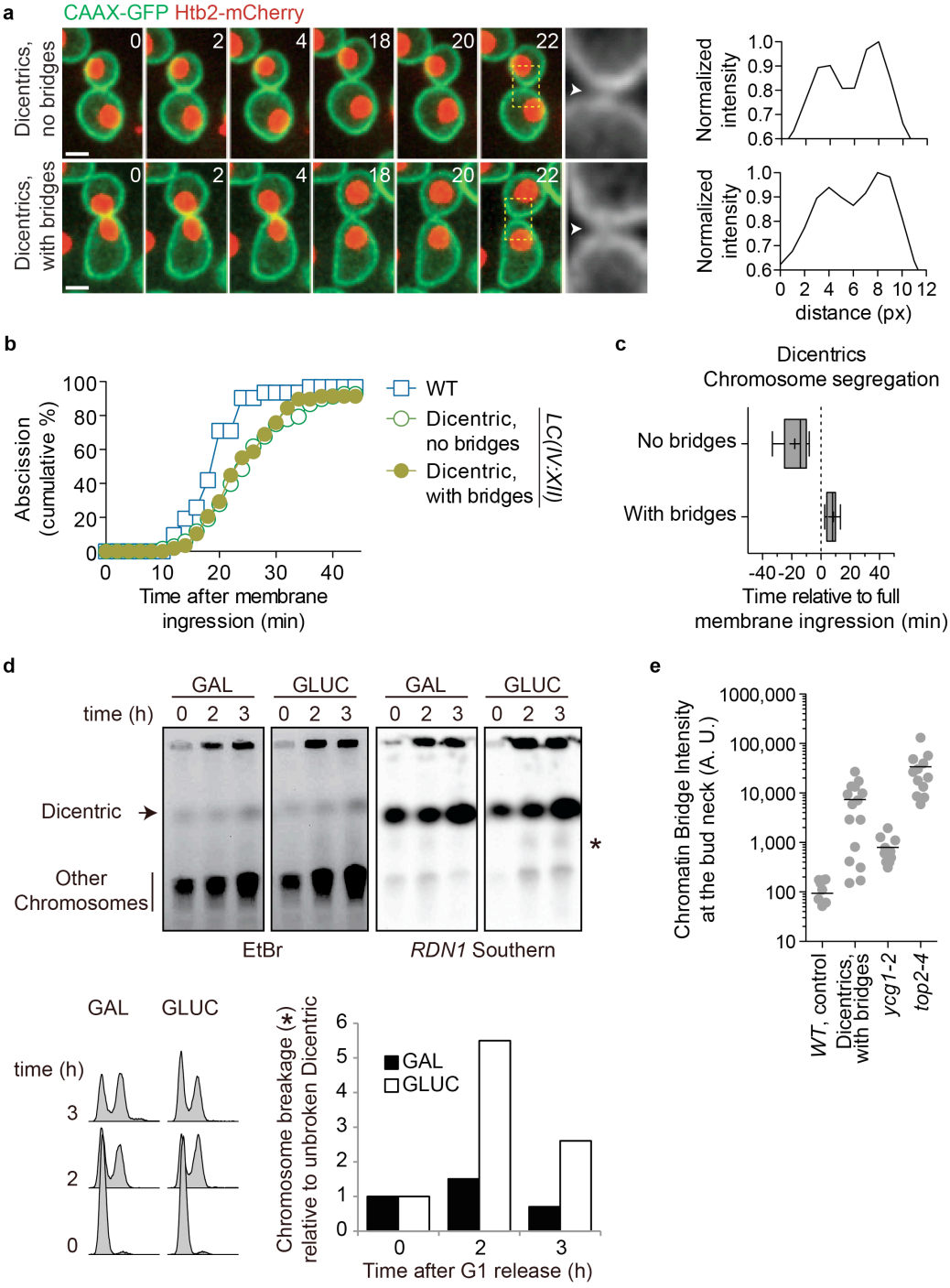

Figure 17: Dicentric chromatin bridges do not inhibit abscission. (a) Membrane ingression and abscission (GFP-CAAX) in cells with dicentric chromosomes (Htb2-mCherry). Arrowheads point to resolved membranes. GFP fluorescence intensities across the cleavage plane are shown for both dicentric categories. (**b**) Cumulative percentage of cells with resolved membranes (abscission) for cells of the indicated categories. Numbers indicate time in minutes; scale bar, 2 µm. Data from: *WT* = 31 cells; Dicentric, no bridges = 68; Dicentric, with bridges = 58. **(c)** Time of chromosome segregation relative to full membrane ingression for dicentric cells. *n* = 20 (dicentric, no bridges); 19 (dicentric, with bridges). **(d)** PFGE analysis of dicentric chromosomes. Asterisk marks position of broken dicentric molecules. The graph shows the amount of broken molecules in Southern blot, relative to intact dicentrics and arbitrarily set to 1 at time 0. **(e)** Fluorescence intensities of Htb2-mCherry in the bud neck region at the onset of myosin ring contraction (Myo1-GFP), for the indicated cell types and conditions. Values are in arbitrary units (A. U.) and background-subtracted. *n* = 10 cells (*WT*); 10 (Dicentrics, with bridges); 10 (*ycg1-2*); 12 (*top2-4*).

4.5. Anaphase spindle stabilization is required for inhibition of abscission

Why is abscission inhibited in response to replication stress-induced, decondensed and catenated chromatin bridges, but not to dicentric chromosomes? This was not due to differences in the amount of chromatin present at the cytokinesis site, since the intensity of fluorescently labeled histones at the bud neck was low in condensin-deficient bridges (which inhibit abscission), whereas it was 10-fold higher in both abscission-competent dicentric cells and in abscission-defective *top2-4* mutants (Fig. **17e**). We next considered the possibility that the DNA damage checkpoint could be involved in the NoCut response in cells with replication, condensation and decatenation defects. However, DNA damage checkpoint mutants (including *tel1*, *mec1*, *chk1*, *rad53*, *mrc1, rad9* and *mre11*) showed a similar abscission delay to that of wild type cells in response to replication stress (Fig. **18a, b**) or after inactivation of topoisomerase II (Fig. **18c**). Condensin inactivation also delayed abscission in *mec1* and *tel1* single and double mutants, but not in *rad53* and *mre11* checkpoint-deficient cells (Fig. **18d**). Together, these data indicate that Rad53 and Mre11 play a role in delaying abscission specifically in response to condensin defects, but that the canonical DNA damage checkpoint is not essential for NoCut.

It has been proposed that Aurora B at the spindle midzone monitors the presence of bridges (Mendoza et al., 2009). Therefore an alternative explanation for efficient cytokinesis in the presence of dicentric chromosomes could be that dicentric bridges are not properly detected by Aurora B. We reasoned that Aurora B mediated detection of chromatin bridges should require the persistence of spindle microtubules during at least the initial stages of cytokinesis. Spindle disassembly dynamics (Tub1-mCherry or Tub1-GFP) were determined relative to cytokinesis (Myo1-GFP) in cells with different types of chromatin bridges. In wild-type cells, disassembly of the spindle occurs shortly before the actomyosin ring fully contracts (Woodruff et al., 2010). In contrast, spindle disassembly occurred only after contraction of the Myo1 ring in the majority of HU-treated cells and in *ycg1-2* and *top2-4* mutants (Fig. **19a, b**).

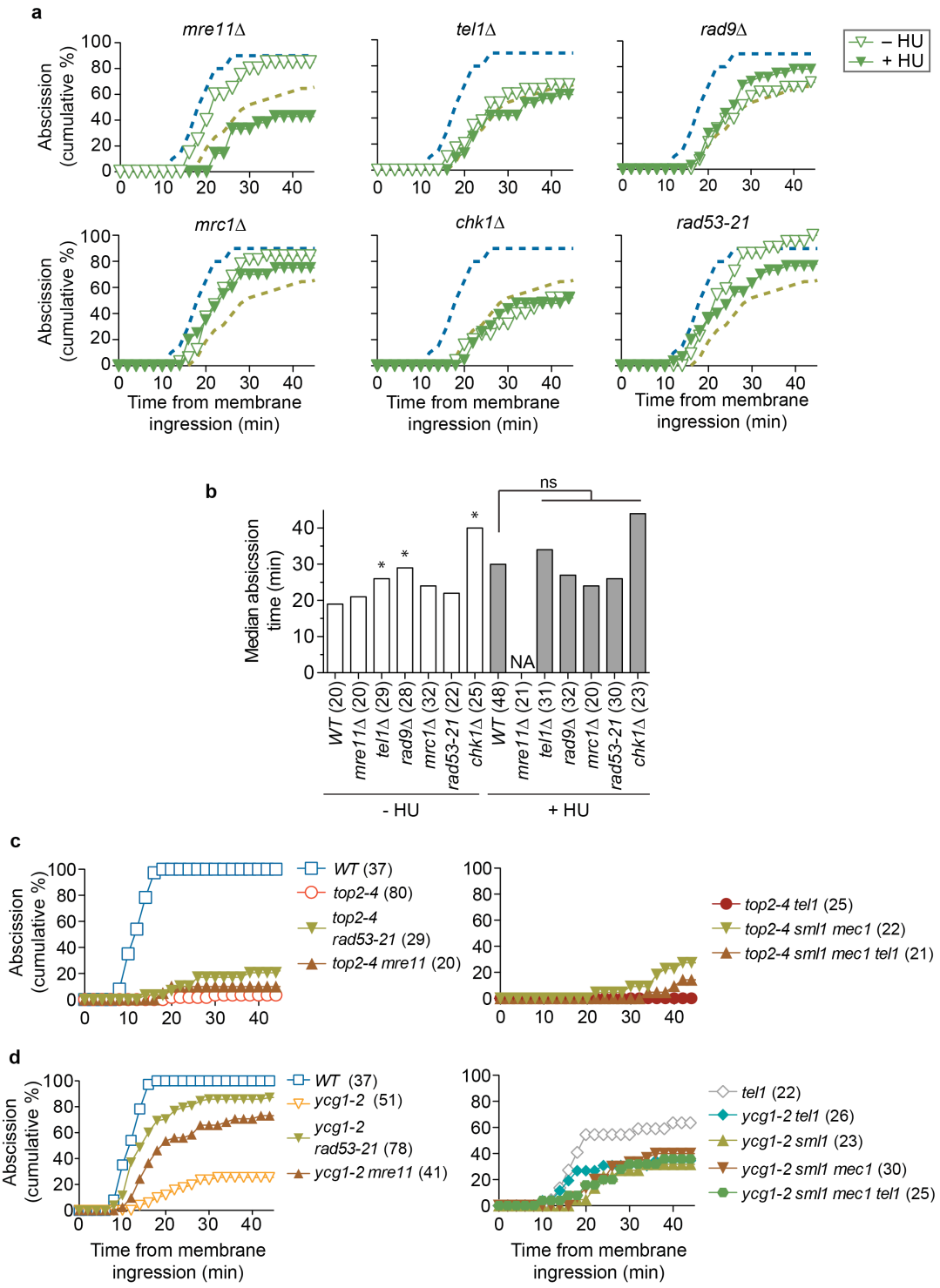

Figure 18: The role of DNA damage checkpoint in abscission dynamics. (**a**) Cumulative percentage of abscission in untreated and HU-treated cells of the indicated strains at 30 ºC. Cells were treated as in Fig. 9e, d. Open inverted triangles represent untreated cells and filled inverted triangles represent HU-treated cells. *WT* and *WT* +HU from Fig. 9e are represented as blue and green dashed lines for comparison. **(b)** The median values of the data in (a) are represented for the indicated strains and conditions. Asterisks represent significant differences relative to WT -HU ($p < 0.05$, Mann-Whitney test). **(c-d)** Abscission dynamics in the indicated strains at 37 ºC. *WT*, *ycg1-2* and *top2-4* data from Fig. 12c are represented for comparison. Significant differences were found only for *ycg1-2 rad53-21* and *ycg1-2 mre11*Δ relative to *ycg1-2* ($p < 0.0001$, Mann-Whitney test). The number of cells in each category is in brackets. ns, non significant.

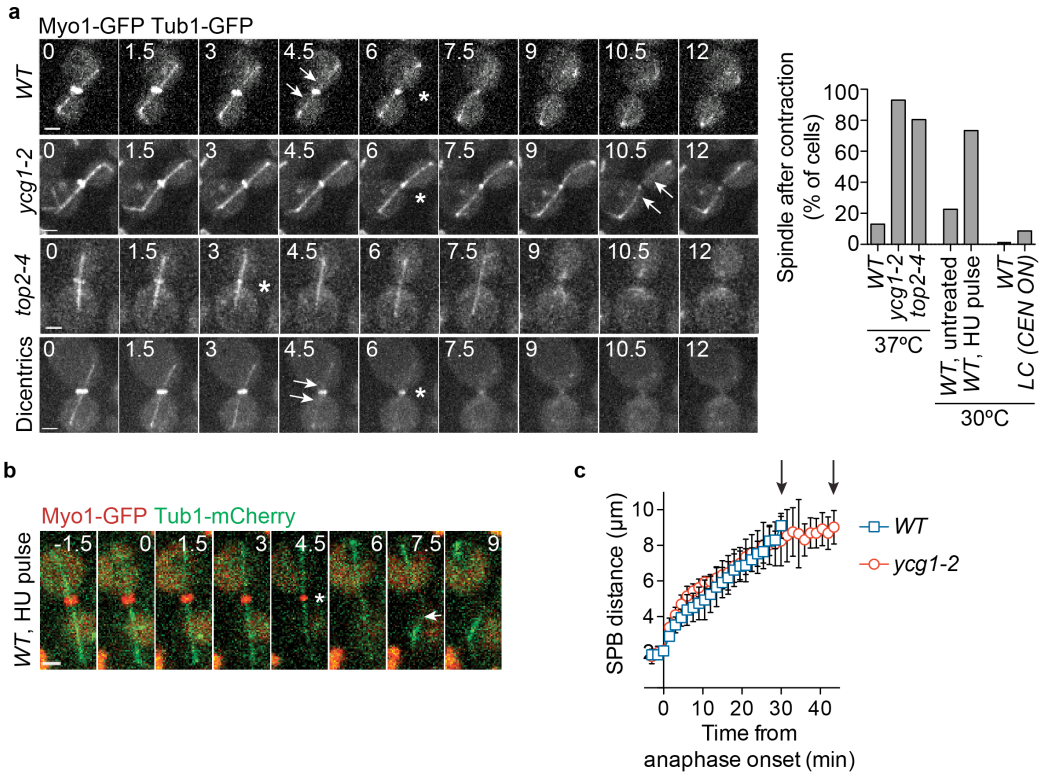

Figure 19: The mitotic spindle is stabilized by inactivation of condensin, topoisomerase II and replication stress, but not by dicentric chromosomes. (**a-b**) Actomyosin ring contraction and anaphase spindle disassembly were visualized through Myo1-GFP and Tub1-GFP in (a) and Tub1-mCherry in (b). Arrows point to spindle disassembly; asterisks mark full contraction of the myosin ring. Percentage of cells in which spindle disassembly occurs after full myosin ring contraction is shown for the indicated cells. Data from the following number of cells and independent experiments: *WT* 37ºC = 23 cells (1 experiment); *ycg1-2* = 59 (2); *top2-4* = 51 (2); *WT* 30ºC untreated = 88 (3); *WT* 30ºC HU pulse = 94 (3); *WT*, 30ºC = 42 (2); *LC (CEN ON)* = 23 (2). (**c**) Spindle tracks of wild type and *ycg1-2* cells. SPB distance is the linear distance between the two spindle pole bodies (SPBs) at each time point. Mean and SD are shown. Anaphase onset was defined when SPB distance was above 2.5 µm. Arrows mark the time of spindle disassembly. *n* = 7 cells (wild type); 6 (*ycg1-2*).

Inactivation of condensin also resulted in a delay in the time of spindle disassembly relative to anaphase onset (Fig. **19c**) and in delayed removal from spindles of the Prc1 homologue Ase1 and of the kinesin-5 motor protein Cin8, two midzone components supporting spindle integrity (Saunders and Hoyt, 1992; Juang, 1997) (Fig. **20a, b**). No spindle stabilization was observed in cells with dicentric chromosomes, which disassembled their spindles with wild-type kinetics (Fig. **19a**) consistent with previous analysis of spindle pole trajectories in these cells (Fig. **16c**). Thus, spindle stabilization and inhibition of abscission are associated with each other.

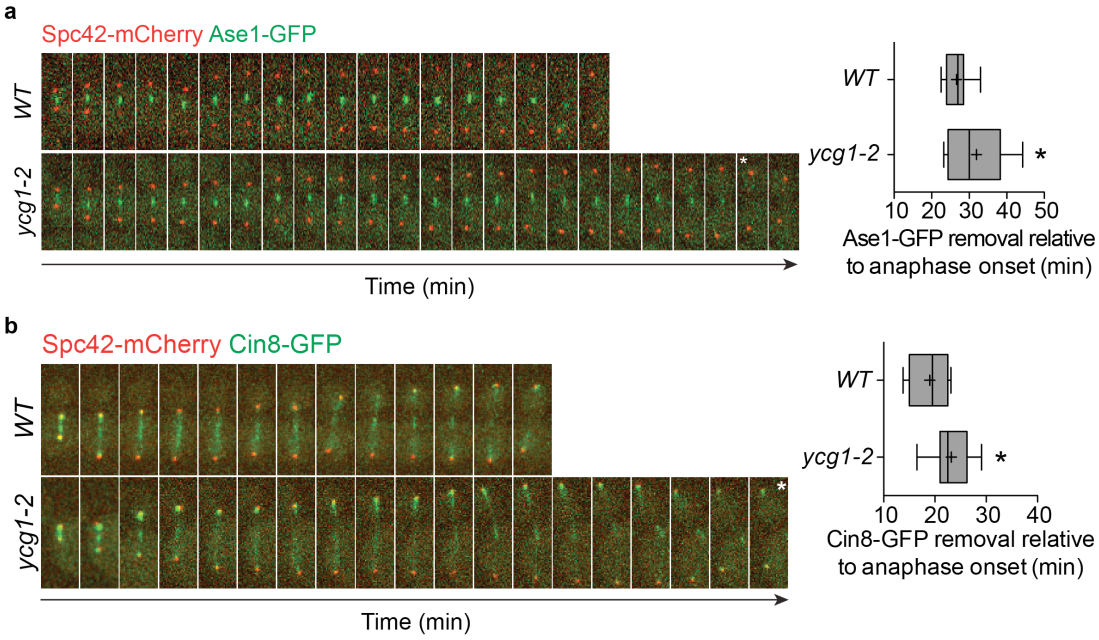

Figure 20: Spindle-associated APC substrates are stabilized in condensin mutant cells. (**a-b**) Visualization of Ase1-GFP (a) or Cin8-GFP (b) dynamics during spindle elongation (Spc42-mCherry) in wild type and *ycg1-2* cells; time interval is 1.5 minutes. The graphs show the time of disappearance from the spindle midzone relative to the start of spindle elongation. Asterisks indicate statistical significance ($p < 0.005$). Data from the following cell numbers: Ase1-GFP = 33 (*WT*); 24 (*ycg1-2*). Cin8-GFP = 15 (*WT*); 25 (*ycg1-2*).

To assess whether spindle stabilization during cytokinesis has a functional role in abscission inhibition, the microtubule-depolymerizing drug nocodazole was added to *top2-4* cells after anaphase spindle elongation but prior to ingression of the bud neck membrane. Spindles (visualized with Tub1-mCherry) efficiently disassembled within 6 minutes of nocodazole addition. Only cells that retained one spindle pole in the mother and one in the bud after membrane ingression were considered for further analysis. Imaging of GFP-CAAX showed that more than 70% of nocodazole-treated *top2-4* cells completed abscission within 40 minutes of membrane ingression, compared to only 20% of untreated *top2-4* cells (Fig. **21**). Therefore anaphase microtubules are essential for inhibition of abscission in response to catenated DNA bridges.

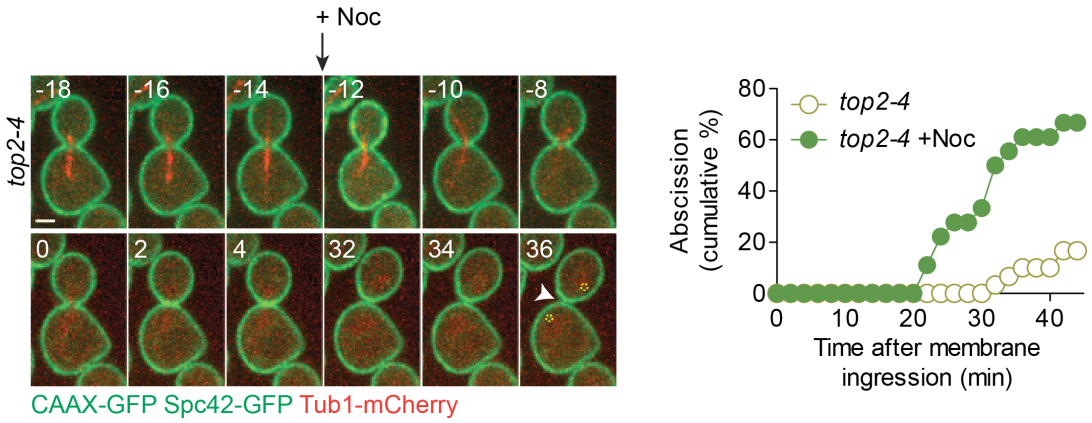

Figure 21: The anaphase spindle is essential for the NoCut response. Spindle (Tub1-mCherry) and plasma membrane dynamics (GFP-CAAX) visualized in *top2-4* cells. Nocodazole was added during anaphase (arrow). Maximal projections of the Tub1-mCherry channel and a single (medial) optical section of the membrane channel are shown for clarity. The position of spindle pole bodies labeled with Spc42-GFP and determined by examining all optical sections is marked with yellow circles in the last frame. Numbers indicate time in minutes; scale bars, 2 µm. 30 untreated cells and 18 nocodazole-treated cells from 1 experiment each were analyzed for abscission timing ($p < 0.001$, Mann-Whitney test).

4.6. Inactivation of Rad53 bypasses the NoCut response in condensin mutant cells

The experiments above show that Rad53 and Mre11 are required for the inhibition of abscission in response to condensin-defective bridges and suggest that spindle microtubules are also essential for this inhibition. Therefore we tested whether Rad53 and Mre11 contribute to the spindle stabilization observed in condensin mutant cells. Inactivation of Rad53 in the condensin mutant background still led to disassembly of the spindle after ring contraction (Fig. **22a**). Surprisingly, the *rad53-21* mutant alone showed a similar effect on spindle dynamics, which was also observed for *mre11*Δ cells (Fig. **22a**). However, this effect was not due to stabilization of the mitotic spindle, since spindle disassembly was not delayed relative to anaphase onset (Fig. **22b**). Rather contraction of the myosin ring was significantly advanced by the inactivation of Rad53 (Fig. **22c**).

These data have two implications. First, Rad53 and possibly Mre11 regulate the timing of cell cycle events at late stages of mitosis. Inactivation of Rad53 advances ring contraction and spindle disassembly, but since the disassembly occurs only after

ring contraction it suggests that the advancement in contraction leads to spindle breakage. Second, Rad53 and Mre11 are not part of the NoCut checkpoint, although their functions are required for establishment of a checkpoint response in the case of condensin-defective bridges. This further supports the requirement for spindle microtubules in the NoCut response.

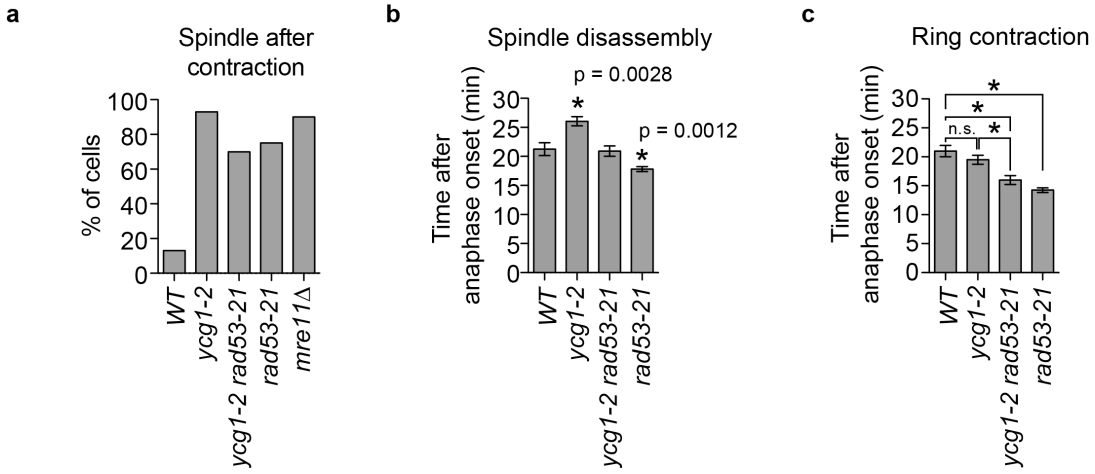

Figure 22: Mitotic spindle and myosin ring dynamics. (**a**) Percentage of cells in which spindle disassembly occurs after full myosin ring contraction. (**b,c**) Time of spindle disassembly (b) and time of ring contraction (c) relative to anaphase onset. Asterisks in (b,c) indicate statistical significant. In (b) *p* values relative to *WT* are shown. In (c) $p < 0.003$. n.s., not significant. Student's t-test.

4.7. APC^{Cdh1} counteracts Aurora B-dependent detection of chromatin bridges

How are spindles stabilized in cells with catenated / decondensed bridges? Spindle disassembly at the end of mitosis relies on degradation of spindle proteins dependent on the ubiquitin-ligase complex APC^{Cdh1}, including Ase1, Cin8 and Fin1 (Woodruff et al., 2010). Our finding that stabilized spindles in condensin mutant cells contain Ase1 and Cin8 (Fig. **20a, b**) opened the possibility that the Cdh1-dependent pathway of spindle disassembly is impaired in the presence of decondensed chromatin bridges. We thus tested whether Cdh1 depletion inhibits abscission either on its own, or in combination with dicentric chromosome bridges.

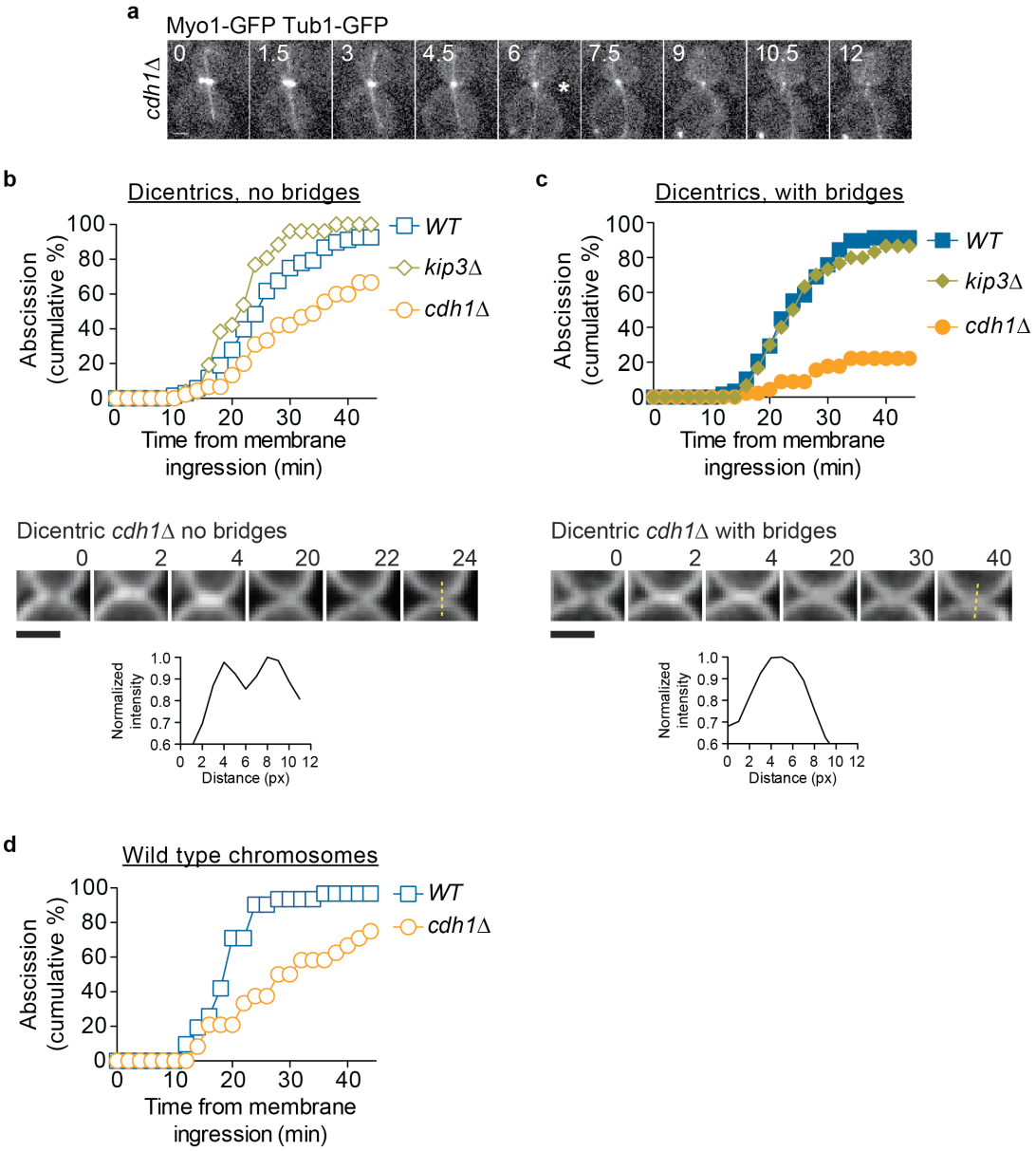

Figure 23: APC^{Cdh1} counteracts Aurora B dependent detection of chromatin bridges. (a) Anaphase spindle disassembly visualized through tubulin (Tub1-GFP) and myosin (Myo1-GFP) dynamics in a representative *cdh1*Δ cell. An asterisk marks full contraction of the myosin ring. 85% (26/30) of *cdh1*Δ cells disassembled the spindle after ring contraction. (**b-c**) Deletion of Cdh1, but not Kip3, inhibits abscission in cells with dicentric bridges. Dicentric cells from Fig. 17b (*WT*) are shown for comparison. Time series of membrane ingression and resolution in dicentric *cdh1*Δ cells with and without bridges is shown and fluorescence intensity was measured across the cleavage plane. Numbers indicate time in minutes. Scale bars, 2 µm. *n* = 26 (*kip3*Δ, no bridges), 30 (*kip3*Δ, with bridges), 45 (*cdh1*Δ, no bridges), 45 (*cdh1*Δ, with bridges). Abscission was delayed in *cdh1*Δ in the presence and absence of bridges ($p < 0.0001$, Mann-Whitney test). (**d**) Mild abscission delay after deletion of CDH1 in cells with normal chromosomes. Wild type cells from Fig. 17b (*WT*) are shown for comparison; *cdh1*Δ = 24 cells ($p < 0.0001$, Mann-Whitney test).

Deletion of *CDH1* stabilized anaphase spindles during Myo1 ring contraction as reported (Woodruff et al., 2010) (Fig. **23a**) and caused a mild abscission delay in cells with normal chromosomes, and in dicentric cells without bridges, as revealed by CAAX-GFP and Htb2-mCherry imaging (Fig. **23b, d**). This is consistent with the role of APC in promoting cytokinesis in cells with normal chromosome segregation (Tully et al., 2009). In contrast, *cdh1*Δ mutant cells strongly inhibited abscission specifically in the presence of dicentric bridges (Fig. **23b, c**). This bridge-specific abscission inhibition was mediated by Aurora B and by Ahc1, because both *cdh1*Δ *ipl1-321* and *cdh1*Δ *ahc1*Δ double mutants with dicentric bridges completed abscission with dynamics similar to those of *cdh1*Δ single mutants without bridges (Fig. **24a, b**). Thus dicentric bridges can trigger the NoCut response, provided that APC^{Cdh1} is inhibited.

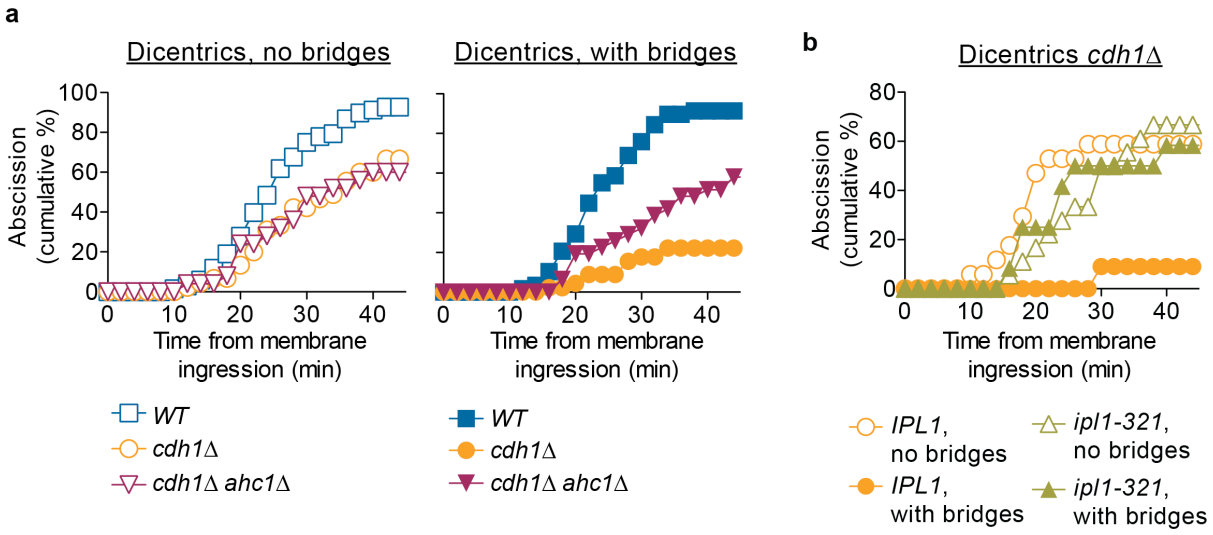

Figure 24: Inhibition of abscission in *cdh1*Δ cells with dicentric bridges is Ipl1- and Ahc1-dependent. (**a**) Cumulative percentage of abscission in dicentric cells of the indicated genotypes and categories. Wild-type and *cdh1*Δ dicentric cells (from Fig. 17d and Fig. 23b,c, respectively) are shown for comparison. (**b**) Cells were treated as in (a) but shifted to 37 ºC after release from G_1 to inactivate Ipl1. *n* = 25 cells (*cdh1*Δ *ahc1*Δ, no bridges); 31 (*cdh1*Δ *ahc1*Δ, with bridges); 17 cells (*IPL1 cdh1*Δ no bridges), 11 (*IPL1 cdh1*Δ with bridges), 18 (*ipl1-321 cdh1*Δ no bridges), 12 (*ipl1-321 cdh1*Δ with bridges). Abscission kinetics were considered significantly different between *cdh1*Δ, with bridges and *cdh1*Δ *ahc1*Δ, with bridges ($p < 0.0001$, Mann-Whitney) in (a); and between *cdh1*Δ, no bridges and *cdh1*Δ, with bridges ($p < 0.05$, Mann-Whitney test) in (b).

Interestingly, the APC^{Cdh1} substrate Iqg1, not involved inspindle stability, was timely removed from the actomyosin ring in condensin mutant cells (Fig. **25**) suggesting that not all APC^{Cdh1} substrates are involved in the NoCut response. Moreover, depletion of the kinesin-8 family member Kip3 (which promotes spindle disassembly through a mechanism independent of APC^{Cdh1} (Woodruff et al., 2010)) did not cause a delay in abscission in cells with dicentric chromosomes, irrespective of the presence of a chromosome bridge during membrane ingression (Fig. **23b, c**). This suggests that a specific inhibition of the APC-dependent pathway of spindle disassembly is required for NoCut. Together with the observation that anaphase spindles are required for abscission inhibition in the *top2* mutant (Fig. **21**), these results indicate that inhibition of APC^{Cdh1} –dependent spindle disassembly is essential for efficient detection of chromatin bridges by Aurora B, and abscission inhibition.

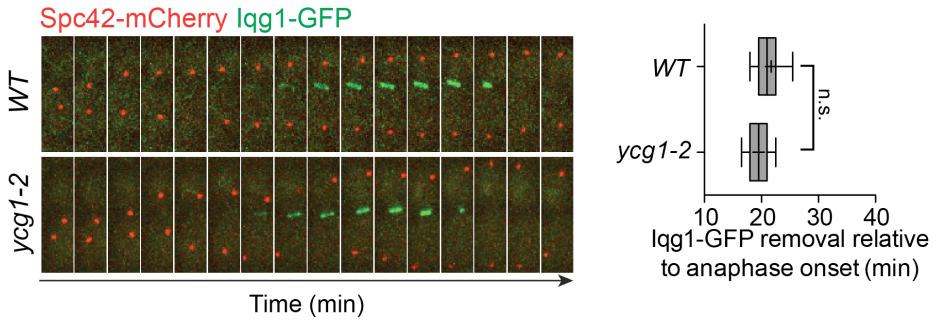

Figure 25: The APC-Cdh1 substrate Iqg1 is timely removed in condensin mutant cells. Visualization of Iqg1-GFP dynamics during spindle elongation (Spc42-mCherry) in wild type and *ycg1-2* cells; time interval is 1.5 minutes. The graphs show the time of disappearance from the bud neck relative to the start of spindle elongation. ns, $p > 0.5$ (Student's t-test). $n = 23$ cells (*WT*); 8 cells (*ycg1-2*).

5. Discussion

Defects during chromosome segregation activate the NoCut checkpoint, which delays abscission. Experiments in human cells and in yeast suggest that the presence of chromatin at the site of division activates Aurora B to induce a delay in abscission. This abscission delay was proposed to prevent damage of the segregating chromosomes (Norden et al., 2006; Mendoza et al., 2009; Carlton et al., 2012). However, different types of chromosome segregation defects have been shown to lead to DNA damage, which was dependent on cytokinesis (Janssen et al., 2011; Cuylen et al., 2013). Therefore, it remained to be understood how chromatin bridges are detected by the NoCut checkpoint, and whether inhibition of abscission prevents their damage.

The work presented here we shows that NoCut prevents DNA damage and promotes cellular viability, after replication stress. Replication stress, induced by treatment with HU, leads to formation of chromatin bridges and a NoCut-dependent abscission delay. Abolishing this delay causes DNA damage. This suggests that the NoCut checkpoint delays abscission to allow for proper segregation of these bridges.
Additionally, we have observed that NoCut is activated by chromatin bridges induced by inactivation of condensin or topoisomerase II (topo 2), but not by dicentric chromatin bridges. NoCut activation is accompanied by stabilization of the anaphase spindle and of spindle-associated proteins. We show that spindle stability is required for NoCut function. Interestingly, NoCut can respond to dicentric bridges after inactivation of the APC-Cdh1 pathway, possibly through stabilization of the anaphase spindle.

We propose that chromatin bridges induced by replication stress and by defects in condensation or decatenation activate the NoCut checkpoint. NoCut activation delays abscission and allows for bridge segregation, which prevents damage of the segregating chromosomes and promotes cellular viability.

5.1. A model for the detection of anaphase bridges by the NoCut checkpoint

The results presented in this work allow us to propose the following model (Fig. **26**). Anaphase bridges, induced by DNA replication stress, defects in condensation or in decatenation, generate a signal that impairs APC-Cdh1 function in late anaphase. As a result, the anaphase spindle is stabilized during cytokinesis, due to delayed degradation of spindle-stabilizing factors. Thanks to the stabilization of the spindle, chromatin bridges can be detected by Aurora B, which is bound to the spindle midzone (Fig. **26a**). Aurora B can subsequently delay abscission, prolonging the lifetime of the chromatin bridge, and providing time for its final resolution. On the other hand, dicentric chromosome bridges do not lead to stabilization of APC substrates, perhaps due to their proficient replication, condensation and decatenation. Therefore, they cannot be recognized by Aurora B and consequently abscission is not delayed, leading to chromosome breakage (Fig. **26b**).

Based on our results, this model has two major implications. Firstly, not all DNA bridges are alike. Even though all anaphase bridges can be sensed by Aurora B when in close proximity (Mendoza et al., 2009), the data show that not all bridges activate NoCut. Therefore, specific features on the anaphase bridges, such as unreplicated, decondensed or catenated DNA, might be required for NoCut activation. Additionally, this suggests that, in the case of dicentric bridges, failure to activate NoCut could be caused by an inability to transmit the signal from Aurora B that will promote the inhibition of abscission. In other words, for NoCut activation, Aurora B must be in the right place (the spindle midzone) and at the right time (during cytokinesis) to delay abscission. What regulates this is not completely understood, but our data suggest that a mechanism that promotes spindle disassembly might be involved. This brings us to the second implication of the model: the anaphase spindle is required for NoCut checkpoint signaling and needs to be stabilized during cytokinesis to allow for bridge detection by Aurora B. The results suggest that the stabilized APC substrates Ase1, Cin8 and possibly other spindle-associated proteins, are upstream on the NoCut signaling pathway. This is because inactivation of Ahc1 or of Ipl1 rescues the abscission delay imposed by

CDH1 deletion in cells with dicentric bridges. Therefore, we believe that NoCut activation requires two essential steps: first a chromatin-based signal induces stabilization of the spindle, through the APC-Cdh1 pathway; and second Aurora B at the spindle midzone, activated by a DNA bridge, signals to inhibit abscission.
Following this, once all chromosomes have been cleared away from the midzone Aurora B becomes inactive and abscission can then proceed. This is very similar to what has been observed in human cells, where Aurora B remains active in the presence of bridges and its inactivation is required for abscission to take place (Steigemann et al., 2009; Carlton et al., 2012; Thoresen et al., 2014).

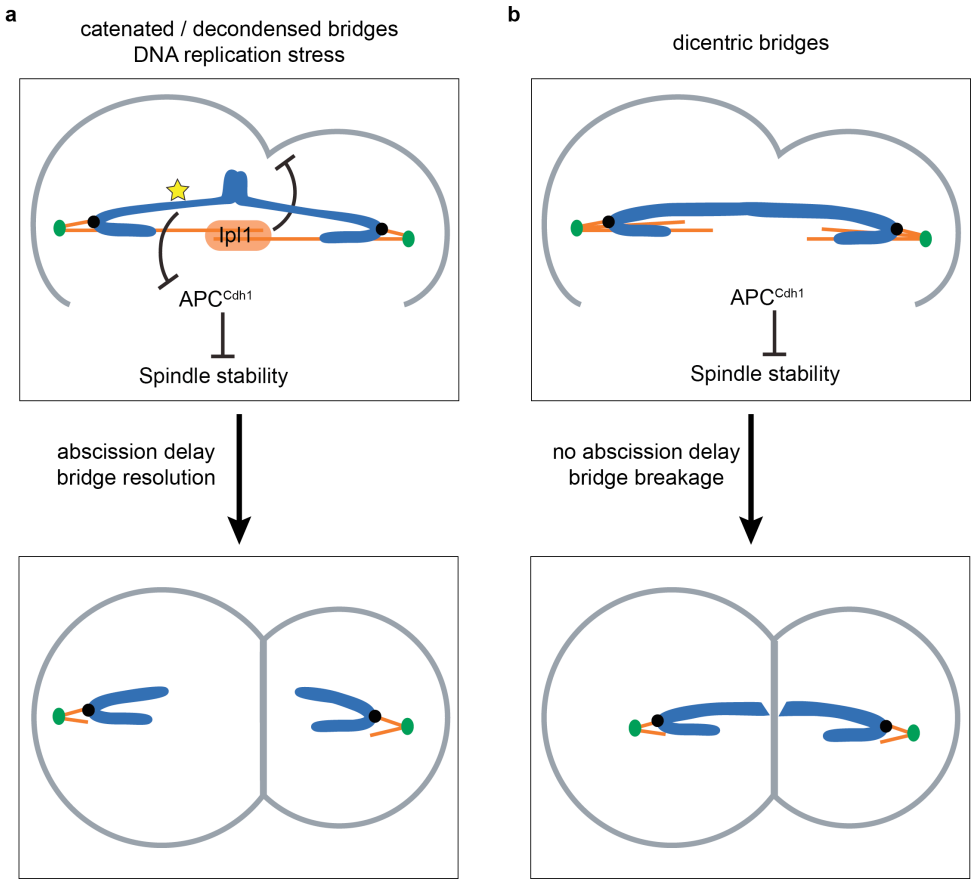

Figure 26: Detection of anaphase chromatin bridges depends on the type of segregation error. (**a**) A chromatin signal (yellow star) associated with defective condensation and/or decatenation of chromosomes (in blue) triggers stabilization of APC·Cdh1 substrates, delaying disassembly of the spindle (in orange) during actomyosin ring contraction (not depicted). The stabilized spindle acts as a platform for Ipl1 (orange oval), allowing it to detect lagging chromatin in the vicinity of the spindle midzone, and to inhibit abscission. This delay provides time for bridge resolution after DNA replication stress, possibly mediated by condensin or topo II. Abscission is completed after the bridge has been properly resolved. (**b**) Condensed, decatenated chromosome bridges do not cause stabilization of APC substrates. This leads to anaphase spindle disassembly during cytokinesis and prevents bridge recognition by Aurora B. Abscission is not delayed and the dicentric bridge breaks. Green and black circles represent spindle poles and kinetochores, and the plasma membrane is represented in grey.

5.2. The molecular origin of chromatin bridges determines the NoCut response

Anaphase bridges induced by HU-treatment, inactivation of condensin or topo 2 trigger the NoCut checkpoint to produce an abscission delay, whereas dicentric chromatin bridges do not activate NoCut. Therefore, the molecular origin of the bridge determines NoCut activation.

This leads to a very interesting question: Is there a DNA structure/signal that is detected by NoCut? Bridges induced by HU, and by inactivation of condensin or topo 2, might have a common factor that is recognized by NoCut. It is possible that HU-induced bridges have defects in condensation and/or decatenation. Since HU interferes with DNA replication it is possible that, while recovering from this stress, cells prolong replication with consequent delays in condensation and decatenation of the late replicating regions. In fact, condensation and replication are tightly associated processes. Replicative stress affects condensin-mediated sister chromatid separation in HeLa cells (Ono et al., 2013) and chromosome condensation is abnormal if DNA replication is inhibited in *C. elegans* embryos (Sonneville et al., 2015).

Alternatively, condensin and topo 2 functions might be required for proper DNA replication. Topo 2 was shown to be required for replication termination in eukaryotic chromosomes (Fachinetti et al., 2010) and we have observed that, in the case of condensin mutants, NoCut is triggered only when condensin inactivation is completed before mitosis (data not shown). This suggests that condensin has functions during DNA replication, which are possibly required for proper assembly of chromatin. Moreover, it suggests that the DNA structure or signal, in anaphase bridges, that triggers NoCut is generated during replication. Dicentric chromosomes, on the other hand, are presumably properly replicated, condensed and decatenated, which could explain why dicentric bridges are not detected by NoCut.

In agreement with this, spontaneous chromatin bridges in human cells inhibit abscission, whereas lagging chromosomes do not (Janssen et al., 2011). Also in

these cases, this could be explained by the different nature of the chromatin bridges, which might affect their detection by Aurora B.

One additional hypothesis to explain why NoCut is activated by some bridges but not by others is chromosome stretching. Decondensed and catenated chromosomes are stretched during anaphase, as observed by the increased distance between two loci in the same chromosome (Renshaw et al., 2010; Titos et al., 2014). If some of the features of condensin- and top2-defective bridges are present in HU-induced bridges, these could be stretched too. On the other hand, the dicentric chromosomes used in our experiments may not have been stretched during anaphase. As mentioned before, our dicentric chromosomes are the result of the fusion of the two longest chromosome arms of the budding yeast genome (chromosomes IV and XII), and therefore have a large inter-centromeric distance (2.8 Mb). These dicentric chromosomes did not affect cell cycle progression (Fig. **16c**). However, dicentric chromosomes with significantly shorter inter-centromeric distances (45 kb and 620 Kb) have been shown to affect spindle elongation (Yang et al., 1997; Lopez et al., 2015), but an effect on cytokinesis was not studied. Therefore, it would be interesting to use dicentric chromosomes of varied inter-centromeric distances and observe their effect on abscission. This should allow us to understand whether stretching of chromosomes during anaphase is sufficient to trigger a NoCut response.

In addition, our experiments also suggest that the nature of the bridge determines its fate. Chromatin bridges in condensin- and topo 2-mutant cells are impossible to resolve, unless the respective protein functions are restored. In fact, we have observed that even after a permanent inhibition of cytokinesis (by inactivation of the actomyosin ring component Iqg1) condensin-mutant bridges fail to resolve and either collapse into one cell and/or enter the next cycle without having finished nuclear division (Michael Maier and Manuel Mendoza, unpublished results). Therefore, we consider these bridges as irreparable. This category of bridges, in which we include dicentric bridges as well, get damaged in a cytokinesis-dependent manner, whether or not they activate NoCut. On the other hand, HU-induced bridges, which are presumably reparable, can be properly segregated when given sufficient time. This is clearly shown by our data: advancing abscission after an HU pulse increases the

percentage of cells with Mre11-GFP foci and the percentage of inviable cells, whereas delaying abscission in these cells decreases both Mre11 foci and inviability to levels comparable to their wild type counterparts (Fig. **7c** and **10c, d**).

Altogether, this suggests that the nature of the chromatin bridge independently determines the establishment of a NoCut response and the fate of the bridge. In other words, activation of NoCut in response to anaphase bridges does not necessarily prevent damage of the bridges. However, by delaying abscission, NoCut provides extra time to promote the resolution and segregation of anaphase bridges that, as HU-induced bridges, can be resolved. This may have important implications in human cells as well. Chromatin bridges caused by replication stress are associated with chromosome instability in animal cells, and the NoCut checkpoint might provide additional time for their resolution.

5.3. The mitotic spindle is an essential structure for the NoCut mechanism

Our results suggest that NoCut relies on the anaphase spindle to relay the signal that delays abscission in cells with chromatin bridges. It was previously proposed that Aurora B at the spindle midzone can sense the presence of chromatin (Mendoza et al., 2009). However, it was not clear how could Aurora B at the spindle regulate abscission, since the anaphase spindle disassembles before complete ring contraction.

We show that anaphase spindle stabilization correlates with and is required for NoCut activation. However, stabilization of the spindle alone is not sufficient to active NoCut, but if a dicentric bridge is present NoCut can be activated, provided that the APC-Cdh1 function is inhibited.
Accordingly, we see altered dynamics of spindle-associated APC-Cdh1 substrates. These substrates presumably promote efficient spindle stabilization, as anaphase spindles in *cdh1*Δ cells are more stable and remain assembled for longer when compared to deletion of the microtubule depolymerase Kip3 (spindle disassembly

relative to anaphase onset - *kip3*Δ: 21.9 ± 3.3 min; *cdh1*Δ: 26.7 ± 6.8 min), consistent with a previous study (Woodruff et al., 2010). This suggests that stabilization of spindle proteins , including Ase1 and Cin8, is required for the NoCut response.

How are APC substrates stabilized in response to chromatin bridges? The fact that the cytosolic substrate Iqg1 was not affected when NoCut was activated in a condensin mutant (Fig. **25c**), suggests that there is either a local inhibition of the APC, for instance in the nucleus but not in the cytosol, or that specific substrates are protected from degradation. In this respect, it would be interesting to follow additional APC substrates in NoCut-activating conditions to understand if only nuclear substrates are stabilized and whether this response is specific to spindle associated proteins. The mechanism of this stabilization remains unknown.

Activation of the DNA damage checkpoint has been shown to regulate spindle dynamics (Bachant, 2005; McKnight et al., 2014). However, our results suggest that the NoCut response is independent of the canonical DNA damage checkpoint. Inactivation of several checkpoint components did not affect the NoCut-dependent abscission delay induced by anaphase bridges. Interestingly, some of the mutants (*tel1*, *rad9* and *chk1*) delayed abscission even in untreated cells with functional condensin and topo 2. Due to their participation in the DNA damage checkpoint, deletion of these genes could lead to low levels of replicative stress, even in normal proliferating cells that have not been challenged. Therefore, we speculate that these mutations could be activating NoCut. We did not further explore the phenotype of these mutants. However, we could gain useful insights into the mechanism of the NoCut checkpoint by understanding whether the abscission delays in *tel1*, *rad9* and *chk1* cells are NoCut-dependent and if inactivation of NoCut could affect their viability.

Mutation of the DNA damage response proteins Rad53 or Mre11 in condensin mutants restored abscission almost back to wild type kinetics. This was surprising as deletion of these genes did not affect the phenotypes of topo 2 mutants or wild type cells after an HU pulse, which suggests that the requirement for Rad53 and Mre11 for the NoCut response might be specific to condensin mutant cells. We

hypothesized that inactivation of condensin could be generating a damage signal activating Rad53 and Mre11. However, we could not detect any sign of DNA damage in condensin-mutant cells before cytokinesis. After inactivation of condensin we observed Mre11-GFP and Ddc1-GFP foci and a slower migrating form of Rad53 was detected by western blot (all of these signs of DNA damage), but inhibition of cytokinesis abolished all of them (data not shown). This suggested that Rad53 and Mre11 have additional, checkpoint-independent functions, as have been described (Zhao et al., 2001; Gunjan and Verreault, 2003). Some of these functions, and possibly additional unknown functions, might be required for the NoCut response specifically after condensin inactivation.

One possible explanation for this comes from the effect of these proteins on cell cycle progression, namely on actomyosin ring and spindle dynamics. Our data suggests that advanced ring contraction caused by the *rad53-21* mutation could be the cause for an early spindle disassembly (Fig. **22**), both in wild type and condensin mutant backgrounds. The early disassembly of the spindle could prevent chromatin bridge detection in condensin mutant cells and abolish their delay in abscission. This is in agreement with the rescue of the abscission defects in topo 2 mutants, due to depolymerization of the spindle by nocodazole (Fig. **21**). However, this does not explain why *rad53-21* and *mre11*Δ mutations do not rescue abscission defects in HU-treated or *top2-4* cells.

The AAA-ATPase Cdc48/p97, a chaperone involved in protein degradation, has been shown to be required for spindle disassembly in *Xenopus* egg extracts, budding yeast and fission yeast (Cao et al., 2003; Lucena et al., 2015). Cdc48 interacts with Ase1 to promote its removal from the spindle and degradation by the proteasome. Interestingly, in *S. pombe* Cdc48 and the proteasome localize to the midzone in late anaphase (Lucena et al., 2015), which suggests a specific spatial regulation of Ase1 degradation by the proteasome. Moreover, Cdc48/p97 promotes extraction of ubiquitylated Aurora B from chromatin in human cells, which is required for proper chromosome segregation during anaphase and decondensation and nuclear envelope reformation in telophase (Ramadan et al., 2007; Dobrynin et al., 2011). This makes Cdc48/p97 an interesting candidate as a mediator of NoCut checkpoint function. Cdc48/p97 could regulate the proposed role of Aurora B/Ipl1 in anaphase

bridge detection and the selective stabilization of APC substrates when NoCut is activated. It would be worth testing whether Cdc48 inactivation activates NoCut in cells with dicentric bridges, in a similar way to CDH1 deletion.

5.4. The NoCut checkpoint prevents damage of anaphase bridges after DNA replication stress

We have shown that NoCut can protect from damage by delaying abscission and giving time for bridge resolution. However, as mentioned before, this is only possible in bridges that can be properly resolved and segregated, as is the case in bridges induced by DNA replication stress. When abscission occurs in the presence of anaphase bridges this leads to DNA damage and cell death. Therefore, by delaying abscission, the NoCut checkpoint promotes genome stability and cell viability.

However, irreparable anaphase bridges pose a challenge to the cell. We and others (Baxter and Diffley, 2008; Cuylen et al., 2013; Lopez et al., 2015) have observed that these bridges, which cannot be resolved and cleared away from the site of division, become damaged in a cytokinesis-dependent manner. Since some of these bridges (condensin- and top2-defective bridges) also activate NoCut this might seem paradoxical. Our data provides a possible explanation to this.
In most condensin- and top2-mutant cells abscission seems permanently inhibited, when inspected by fluorescence microscopy (Fig. **12c**). Our electron microscopy analysis confirms that abscission is impaired in these cells, as continuous channels can be seen connecting mother and daughter cells (Fig. **13**). However, analysis of late stages of cytokinesis suggests that these channels eventually close (Fig. **13c**). Additionally, these cells are able to form a new bud, which indicates that they start a new cycle, but with a delay relative to wild type cells (Fig. **12c**). These results suggest that NoCut promotes a delay in cytokinesis, rather than a complete inhibition. Therefore, by delaying cytokinesis NoCut provides extra time for segregation of DNA at the site of division. However, in the presence of irreparable bridges, as they cannot be resolved and properly segregated, they become damaged once cytokinesis occurs.

Damaged DNA, if irreparable, is lethal for the cell and losing or gaining genes can impair cellular viability. However, it has been shown that cells can cope with whole-chromosome aneuploidies (Sheltzer et al., 2011; Blank et al., 2015), and broken DNA fragments, in human cells, can lead to dramatic chromosomal rearrangements, through the process of chromothripsis, which has been proposed to be an early event in cancer development (Stephens et al., 2011). Therefore, from an evolutionary perspective, it might be advantageous to gain extra chromosomal fragments as a trade off for cellular viability.
Accordingly, our experiments show that, after an HU pulse, NoCut-mutant cells lose viability compared to NoCut-proficient cells, but most (~70%) still remain viable afterwards (Fig. **7c**). This suggests that, at least in some cells, viability is maintained even after chromosome damage is induced by the advancement of abscission. In all types of bridges we have analyzed segregation eventually occurs, again suggesting that the bridges are only transiently protected from damage. In this respect, it would be interesting to understand whether breaking irreparable chromosome bridges can be advantageous to the cell, possibly as a way of allowing for proliferation to be resumed. This could be tested by assessing cellular viability after transient inactivation of condensin or topo 2, for the duration of one cell cycle. Reactivation of these proteins after cytokinesis might allow at least a fraction of the cells to remain viable as opposed to inviability of the majority of cells when these proteins are permanently inactivated.

Interestingly, the advanced abscission in HU-treated, NoCut-mutant cells does not lead to an immediate proliferation arrest during the second cycle, when the DNA damage is first detected. After treatment with HU, most damage foci are short-lived (6 minutes on average), which suggests that the damage is being repaired shortly after its detection. Accordingly, in most cases these cells divide a few times to form a microcolony. This suggests that at least in some cases cell death is not a direct consequence of the observed damage but could be due to chromosomal rearrangements and/or accumulation of mutations during the following cycles.

5.4.1. How are chromatin bridges damaged?

Even though anaphase bridges become damaged after cytokinesis it is not clear what exactly causes the damage. We have observed that an increased percentage of NoCut-mutant cells, when treated with a pulse of HU, show Mre11-GFP foci after cytokinesis (Fig. **10c, d**). Interestingly, more than half of these foci appear only in the following S/G2 phase (53% of *ahc1*Δ and 74% of the *ipl1-321* cells containing foci). This suggests that, in the majority of cells, problems arise during DNA replication, which could simply mean that unfinished replication due to HU exposure is recognized and repaired in the following cycle. However, introducing a cytokinesis delay significantly reduces foci formation after cytokinesis (Fig. **10c, d**), which argues that DNA damage is rather a consequence of the timing of cytokinesis.

Actomyosin ring contraction is not affected by the presence of chromatin bridges (discussed in the next section), suggesting that chromatin bridges that persist at the site of division during cytokinesis are damaged by a late cytokinetic event. Since NoCut regulates abscission in response to chromatin bridges, this further suggests that abscission itself and/or an event occurring concomitantly with abscission induces damage to chromatin bridges. In human cells, ESCRT complexes have an essential role in abscission. The ESCRT-III subunit CHMP4C has been proposed to form helical spirals at the abscission site and to drive membrane ingression through constriction of the spiral (Elia et al., 2013). As ESCRTs can induce constriction they might be able to provide the necessary force to break DNA remaining at the site of division. In budding yeast, the mechanism that specifically controls abscission is not known, and ESCRTs seem to have only a minor role in enhancing the efficiency of cytokinesis (McMurray et al., 2011). Nevertheless, it should be explored whether these proteins have a role in promoting DNA bridge resolution at the site of cytokinesis.

5.4.2. How is abscission controlled by the NoCut checkpoint?

Our data show that the presence of anaphase bridges does not affect myosin ring contraction. Neither the timing of its onset nor its contraction period are delayed (Fig. **11a**), which is consistent with previous data (Cuylen et al., 2013; Lopez et al., 2015).

In contrast to this, live cell microscopy of HU-treated wild type cells and of condensin and topo 2 mutants shows a delay or inhibition of plasma membrane resolution - our readout for abscission. This suggests that ring contraction and abscission are separable events. Moreover, electron microscopy imaging of condensin and topo 2 mutants revealed an incomplete closure of the mother-bud channel (Fig. **13**), which suggests that the myosin ring is not responsible for this final step in cytokinesis. This resembles mammalian cytokinesis where the actomyosin ring promotes cleavage furrow ingression to form the intercellular bridge but becomes dispensable afterwards for abscission, when ESCRT subunits take the lead (Guizetti et al., 2011). Therefore, it is likely that as in mammalian cells, the actomyosin ring contracts to an extent, driving ingression of the plasma membrane, but leaves a channel connecting the two cells, and once it disassembles leaves space for abscission to be completed by an yet unidentified mechanism that will finally seal the channel. This is supported by the fact that impairing disassembly of the actomyosin ring affects completion of cytokinesis (Tully et al., 2009).

The mechanism of abscission is controlled by NoCut, presumably through substrates of the Aurora B/Ipl1 kinase, as in human cells (Steigemann et al., 2009; Carlton et al., 2012; Thoresen et al., 2014). The Boi1 and Boi2 proteins have been proposed to be such substrates (Norden et al., 2006; Mendoza et al., 2009), but their role on the regulation of abscission is not entirely clear. One other target of the checkpoint to inhibit abscission could be the cytokinetic protein Cyk3. In fact, deletion of CYK3 seems to specifically delay abscission (Fig. **9c**)(Onishi et al., 2013) and unpublished data from our lab shows that Cyk3 recruitment to the bud neck is impaired in condensin mutant cells (Arun Kumar and Manuel Mendoza). Cyk3 has no known sites for phosphorylation by Aurora B/Ipl1 and interactions with NoCut genes have not been described. However, it would be interesting to test if Cyk3 is regulated by the NoCut pathway to inhibit abscission, by analyzing to what extent abscission is delayed in NoCut mutants when CYK3 is deleted and if Cyk3 has specific interaction partners during NoCut activation.

Finally, as mentioned before, ESCRT proteins have been shown to have only a minor role in budding yeast cytokinesis, but their participation in the NoCut signaling pathway remains a possibility. In fact, deletion of the ESCRT subunit Snf7 was

shown to improve cell proliferation of cells with defects in cytokinesis due to septin mutation (McMurray et al., 2011). This suggests that, at least in some cases, yeast ESCRTs can have an inhibitory role in cytokinesis and could therefore be a target of the NoCut checkpoint to delay abscission in response to DNA bridges.

Together these results provide the first evidence that the NoCut checkpoint preserves cellular viability in the presence of DNA bridges. Moreover, we propose a possible mechanism for how chromatin bridges are detected by NoCut. Using live cell microscopy, we gained insight into how different events in late mitosis, such as spindle disassembly and cytokinesis, have to be coordinated to produce a functional NoCut response. We propose that stabilization of the anaphase spindle, through the APC-Cdh1 pathway, is essential for recognition of anaphase bridges by the NoCut checkpoint.

6. Conclusion

From the work presented here we conclude the following:

- The NoCut checkpoint can prevent damage of anaphase bridges and promote cell viability. DNA replication stress induces the formation of anaphase bridges and a NoCut-dependent abscission delay. Inactivation of NoCut, after replication stress, advances abscission, increases DNA damage after cytokinesis and decreases cell viability.

- NoCut responds differently to different types of chromatin bridges. Replication stress-induced bridges, as well as decondensed and catenated bridges activate the NoCut checkpoint, whereas bridges from dicentric chromosomes do not.

- The anaphase spindle microtubules are required for the NoCut response. We observed that inactivation of condensin or topoisomerase II and DNA replication stress delay the disassembly of the anaphase spindle. Moreover, inducing depolymerization of the spindle microtubules during anaphase rescued the topoisomerase II mutant abscission delay.

- APC-Cdh1 counteracts detection of chromatin bridges by the NoCut checkpoint. We observed that spindle-associated, APC-Cdh1 substrates are stabilized in condensin mutant cells. Inactivation of APC-Cdh1 function, in the presence of dicentric bridges, leads to a NoCut-dependent abscission delay.

7. Future directions

- We have uncovered a mechanism that allows for the detection of chromatin bridges by the NoCut checkpoint. However, it is still not known how these bridges are sensed and how do they trigger NoCut. By testing several known DNA-binding proteins we hope to understand which are the factors required for sensing of anaphase bridges by the NoCut checkpoint.

- Our experiments suggest that APC-Cdh1 activity is at least transiently impaired to allow for NoCut activation. How its activity is regulated in the context of NoCut is not known. A better characterization of the APC-Cdh1 substrates should be done, in NoCut-activating conditions. To understand if there's local inhibition of APC-Cdh1 activity or a specific protection of some of its substrates, we should test these proteins for post-translational modifications.

- The Ipl1 kinase has a central role in the NoCut checkpoint. It can sense the presence of DNA bridges at the site of division and it promotes inhibition of abscission, in the presence of those bridges. However, the effectors and/or substrates of Ipl1 that are relevant for NoCut signaling are not known. This has been the focus of most NoCut studies in human cells and therefore it would be interesting to: firstly, test if the homologues of the human targets of Aurora B also have a role in budding yeast NoCut; and secondly, search for new targets of Ipl1, to expand our understanding of how abscission is regulated by the NoCut checkpoint.

- Ultimately we will test whether some of our findings are also applicable to human cells. Specifically, we would like to understand whether the NoCut checkpoint in human cells detects chromatin bridges caused by replication stress, as this is a common feature of cancer cells.

8. References

Adams, A.E., D.I. Johnson, R.M. Longnecker, B.F. Sloat, and J.R. Pringle. 1990. CDC42 and CDC43, two additional genes involved in budding and the establishment of cell polarity in the yeast Saccharomyces cerevisiae. *The Journal of Cell Biology*. 111:131–142.

Akiyoshi, B., K.K. Sarangapani, A.F. Powers, C.R. Nelson, S.L. Reichow, H. Arellano-Santoyo, T. Gonen, J.A. Ranish, C.L. Asbury, and S. Biggins. 2010. Tension directly stabilizes reconstituted kinetochore-microtubule attachments. *Nature*. 468:576–579. doi:10.1038/nature09594.

Arias, E.E., and J.C. Walter. 2005. PCNA functions as a molecular platform to trigger Cdt1 destruction and prevent re-replication. *Nat. Cell Biol.* 8:84–90. doi: 10.1038/ncb1346.

Bachant, J. 2005. The yeast S phase checkpoint enables replicating chromosomes to bi-orient and restrain spindle extension during S phase distress. *The Journal of Cell Biology*. 168:999–1012. doi:10.1083/jcb.200412076.

Baladron, V., S. Ufano, E. Duenas, A.B. Martin-Cuadrado, F. del Rey, and C.R. Vazquez de Aldana. 2002. Eng1p, an Endo-1,3- -Glucanase Localized at the Daughter Side of the Septum, Is Involved in Cell Separation in Saccharomyces cerevisiae. *Eukaryotic Cell*. 1:774–786. doi:10.1128/EC.1.5.774-786.2002.

Barral, Y., V. Mermall, M.S. Mooseker, and M. Snyder. 2000. Compartmentalization of the cell cortex by septins is required for maintenance of cell polarity in yeast. *MOLCEL*. 5:841–851.

Baxter, J. 2015. “Breaking Up Is Hard to Do”: The Formation and Resolution of SisterChromatid Intertwines. *Journal of Molecular Biology*. 427:590–607. doi: 10.1016/j.jmb.2014.08.022.

Baxter, J., and J.F.X. Diffley. 2008. Topoisomerase II Inactivation Prevents the Completion of DNA Replication in Budding Yeast. *Molecular Cell*. 30:790–802. doi:10.1016/j.molcel.2008.04.019.

Bi, E., P. Maddox, D.J. Lew, E.D. Salmon, J.N. McMillan, E. Yeh, and J.R. Pringle. 1998. Involvement of an actomyosin contractile ring in Saccharomyces cerevisiae cytokinesis. *The Journal of Cell Biology*. 142:1301–1312.

Blanco, M.G., J. Matos, and S.C. West. 2014. Dual Control of Yen1 Nuclease Activity and Cellular Localization by Cdk and Cdc14 Prevents Genome Instability. *Molecular Cell*. 54:94–106. doi:10.1016/j.molcel.2014.02.011.

Blank, H.M., J.M. Sheltzer, C.M. Meehl, and A. Amon. 2015. Mitotic entry in the presence of DNA damage is a widespread property of aneuploidy in yeast. *Molecular Biology of the Cell*. 26:1440–1451. doi:10.1091/mbc.E14-10-1442.

Bowers, B., G. Levin, and E. Cabib. 1974. Effect of polyoxin D on chitin synthesis and septum formation in Saccharomyces cerevisiae. *J. Bacteriol.* 119:564–575.

Burgess, D.R., and F. Chang. 2005. Site selection for the cleavage furrow at cytokinesis. *Trends in Cell Biology*. 15:156–162. doi:10.1016/j.tcb.2005.01.006.

Buvelot, S., S.Y. Tatsutani, D. Vermaak, and S. Biggins. 2003. The budding yeast Ipl1/Aurora protein kinase regulates mitotic spindle disassembly. *The Journal of Cell Biology*. 160:329–339. doi:10.1083/jcb.200209018.

Caballe, A., D.M. Wenzel, M. Agromayor, S.L. Alam, J.J. Skalicky, M. Kloc, J.G. Carlton, L. Labrador, W.I. Sundquist, and J. Martin-Serrano. 2015. ULK3 regulates cytokinetic abscission by phosphorylating ESCRT-III proteins. *eLife*. 4. doi:10.7554/eLife.06547.

Cao, K., R. Nakajima, H.H. Meyer, and Y. Zheng. 2003. The AAA-ATPase Cdc48/p97 regulates spindle disassembly at the end of mitosis. *Cell*. 115:355–367.

Capalbo, L., E. Montembault, T. Takeda, Z.I. Bassi, D.M. Glover, and P.P. D'Avino. 2012. The chromosomal passenger complex controls the function of endosomal sorting complex required for transport-III Snf7 proteins during cytokinesis. *Open Biol*. 2:120070. doi:10.1098/rsob.120070.

Carlton, J.G., A. Caballe, M. Agromayor, M. Kloc, and J. Martin-Serrano. 2012. ESCRT-III Governs the Aurora B-Mediated Abscission Checkpoint Through CHMP4C. *Science*. 336:220–225. doi:10.1126/science.1217180.

Carlton, J.G., and J. Martin-Serrano. 2007. Parallels between cytokinesis and retroviral budding: a role for the ESCRT machinery. *Science*. 316:1908–1912. doi:10.1126/science.1143422.

Casamayor, A., and M. Snyder. 2002. Bud-site selection and cell polarity in budding yeast. *Curr. Opin. Microbiol.* 5:179–186.

Chan, K.L., P.S. North, and I.D. Hickson. 2007. BLM is required for faithful chromosome segregation and its localization defines a class of ultrafine anaphase bridges. *The EMBO Journal*. 26:3397–3409. doi:10.1038/sj.emboj.7601777.

Chan, K.L., T. Palmai-Pallag, S. Ying, and I.D. Hickson. 2009. Replication stress induces sister-chromatid bridging at fragile site loci in mitosis. *Nat. Cell Biol.* 11:753–760. doi:10.1038/ncb1882.

Chant, J., and I. Herskowitz. 1991. Genetic control of bud site selection in yeast by a set of gene products that constitute a morphogenetic pathway. *Cell*. 65:1203–1212.

Chant, J., K. Corrado, J.R. Pringle, and I. Herskowitz. 1991. Yeast BUD5, encoding a putative GDP-GTP exchange factor, is necessary for bud site selection and interacts with bud formation gene BEM1. *Cell*. 65:1213–1224.

Chin, C.F., A.M. Bennett, W.K. Ma, M.C. Hall, and F.M. Yeong. 2011. Dependence of Chs2 ER export on dephosphorylation by cytoplasmic Cdc14 ensures that septum formation follows mitosis. *Molecular Biology of the Cell*. 23:45–58. doi: 10.1091/mbc.E11-05-0434.

Cid, V.J., L. Adamiková, M. Sánchez, M. Molina, and C. Nombela. 2001. Cell cycle control of septin ring dynamics in the budding yeast. *Microbiology (Reading, Engl.)*. 147:1437–1450. doi:10.1099/00221287-147-6-1437.

Cimini, D., B. Howell, P. Maddox, A. Khodjakov, F. Degrassi, and E.D. Salmon. 2001. Merotelic Kinetochore Orientation Is a Major Mechanism of Aneuploidy in Mitotic Mammalian Tissue Cells. *The Journal of Cell Biology*. 153:517–528. doi:10.1083/jcb.113.5.1091.

Ciosk, R., W. Zachariae, C. Michaelis, A. Shevchenko, M. Mann, and K. Nasmyth. 1998. An ESP1/PDS1 complex regulates loss of sister chromatid cohesion at the metaphase to anaphase transition in yeast. *Cell*. 93:1067–1076.

Clemente-Blanco, A., M. Mayan-Santos, D.A. Schneider, F. Machín, A. Jarmuz, H. Tschochner, and L. Aragón. 2009. Cdc14 inhibits transcription by RNA polymerase I during anaphase. *Nature*. 457:219–222. doi:10.1038/nature07652.

Cohen-Fix, O., J.M. Peters, M.W. Kirschner, and D. Koshland. 1996. Anaphase initiation in Saccharomyces cerevisiae is controlled by the APC-dependent degradation of the anaphase inhibitor Pds1p. *Genes & Development*. 10:3081–3093.

Connell, J.W., C. Lindon, J.P. Luzio, and E. Reid. 2008. Spastin Couples Microtubule Severing to Membrane Traffic in Completion of Cytokinesis and Secretion. *Traffic*. 10:42–56. doi:10.1111/j.1600-0854.2008.00847.x.

Cuylen, S., J. Metz, A. Hruby, and C.H. Haering. 2013. Short Article. *Developmental Cell*. 27:469–478. doi:10.1016/j.devcel.2013.10.018.

Cvrcková, F., C. De Virgilio, E. Manser, J.R. Pringle, and K. Nasmyth. 1995. Ste20-like protein kinases are required for normal localization of cell growth and for cytokinesis in budding yeast. *Genes & Development*. 9:1817–1830.

D'Amours, D., and S.P. Jackson. 2002. The mre11 complex: at the crossroads of dna repair and checkpoint signalling. *Nat. Rev. Mol. Cell Biol.* 3:317–327. doi: 10.1038/nrm805.

Desai, A., and T.J. Mitchison. 1997. Microtubule polymerization dynamics. *Annu. Rev. Cell Dev. Biol.* 13:83–117. doi:10.1146/annurev.cellbio.13.1.83.

Diffley, J.F., J.H. Cocker, S.J. Dowell, and A. Rowley. 1994. Two steps in the assembly of complexes at yeast replication origins in vivo. *Cell*. 78:303–316.

Dobbelaere, J., and Y. Barral. 2004. Spatial Coordination of Cytokinetic Events by Compartmentalization of the Cell Cortex. *Science*. 305:393–396. doi:10.1126/science.1099892.

Dobbelaere, J., M.S. Gentry, R.L. Hallberg, and Y. Barral. 2003. Phosphorylation-dependent regulation of septin dynamics during the cell cycle. *Developmental Cell*. 4:345–357.

Dobrynin, G., O. Popp, T. Romer, S. Bremer, M.H.A. Schmitz, D.W. Gerlich, and H. Meyer. 2011. Cdc48/p97-Ufd1-Npl4 antagonizes Aurora B during chromosome segregation in HeLa cells. *Journal of Cell Science*. 124:1571–1580. doi:10.1242/jcs.069500.

Dong, Y. 2003. Formin-dependent actin assembly is regulated by distinct modes of Rho signaling in yeast. *The Journal of Cell Biology*. 161:1081–1092. doi: 10.1083/jcb.200212040.

Dungrawala, H., K.L. Rose, K.P. Bhat, K.N. Mohni, G.G. Glick, F.B. Couch, and D. Cortez. 2015. The Replication Checkpoint Prevents Two Types of Fork Collapse without Regulating Replisome Stability. *MOLCEL*. 1–14. doi: 10.1016/j.molcel.2015.07.030.

Eissler, C.L., G. Mazón, B.L. Powers, S.N. Savinov, L.S. Symington, and M.C. Hall. 2014. The Cdk/Cdc14 Module Controls Activation of the Yen1 Holliday Junction Resolvaseto Promote Genome Stability. *Molecular Cell*. 54:80–93. doi:10.1016/j.molcel.2014.02.012.

Elia, N., C. Ott, and J. Lippincott-Schwartz. 2013. Incisive Imaging and Computation for Cellular Mysteries:Lessons from Abscission. *Cell*. 155:1220–1231. doi: 10.1016/j.cell.2013.11.011.

Elia, N., R. Sougrat, T.A. Spurlin, J.H. Hurley, and J. Lippincott-Schwartz. 2011. Dynamics of endosomal sorting complex required for transport (ESCRT) machinery during cytokinesis and its role in abscission. *Proceedings of the National Academy of Sciences*. 108:4846–4851. doi:10.1073/pnas.1102714108.

Fabbro, M., B.-B. Zhou, M. Takahashi, B. Sarcevic, P. Lal, M.E. Graham, B.G. Gabrielli, P.J. Robinson, E.A. Nigg, Y. Ono, and K.K. Khanna. 2005. Cdk1/Erk2- and Plk1-Dependent Phosphorylation of a Centrosome Protein, Cep55,

Is Required for Its Recruitment to Midbody and Cytokinesis. *Developmental Cell*. 9:477–488. doi:10.1016/j.devcel.2005.09.003.

Fachinetti, D., R. Bermejo, A. Cocito, S. Minardi, Y. Katou, Y. Kanoh, K. Shirahige, A. Azvolinsky, V.A. Zakian, and M. Foiani. 2010. Replication Termination at Eukaryotic Chromosomes Is Mediated by Top2 and Occursat Genomic Loci Containing Pausing Elements. *MOLCEL*. 39:595–605. doi:10.1016/j.molcel. 2010.07.024.

Fang, X., J. Luo, R. Nishihama, C. Wloka, C. Dravis, M. Travaglia, M. Iwase, E.A. Vallen, and E. Bi. 2010. Biphasic targeting and cleavage furrow ingression directed by the tail of a myosin II. *The Journal of Cell Biology*. 191:1333–1350. doi:10.1073/pnas.95.23.13652.

Fasulo, B., C. Koyama, K.R. Yu, E.M. Homola, T.S. Hsieh, S.D. Campbell, and W. Sullivan. 2012. Chk1 and Wee1 kinases coordinate DNA replication, chromosome condensation, and anaphase entry. *Molecular Biology of the Cell*. 23:1047–1057. doi:10.1091/mbc.E11-10-0832.

Finnigan, G.C., E.A. Booth, A. Duvalyan, E.N. Liao, and J. Thorner. 2015. The Carboxy-Terminal Tails of Septins Cdc11 and Shs1 Recruit Myosin-II Binding Factor Bni5 to the Bud Neck in Saccharomyces cerevisiae. *Genetics*. 200:821–840. doi:10.1534/genetics.115.176503.

Flescher, E.G., K. Madden, and M. Snyder. 1993. Components required for cytokinesis are important for bud site selection in yeast. *The Journal of Cell Biology*. 122:373–386.

Floyd, S., N. Whiffin, M.P. Gavilan, S. Kutscheidt, M. De Luca, C. Marcozzi, M. Min, J. Watkins, K. Chung, O.T. Fackler, and C. Lindon. 2013. Spatiotemporal organization of Aurora-B by APC/CCdh1 after mitosis coordinates cell spreading through FHOD1. *Journal of Cell Science*. 126:2845–2856. doi: 10.1242/jcs.123232.

Germann, S.M., V. Schramke, R.T. Pedersen, I. Gallina, N. Eckert-Boulet, V.H. Oestergaard, and M. Lisby. 2013. TopBP1/Dpb11 binds DNA anaphase bridges to prevent genome instability. *The Journal of Cell Biology*. 204:45–59. doi:10.1111/j.1432-1033.1997.00794.x.

Gershony, O., T. Pe'er, M. Noach-Hirsh, N. Elia, and A. Tzur. 2014. Cytokinetic abscission is an acute G1 event. *Cell Cycle*. 13:3436–3441. doi: 10.4161/15384101.2014.956486.

Gillis, A.N., S. Thomas, S.D. Hansen, and K.B. Kaplan. 2005. A novel role for the CBF3 kinetochore-scaffold complex in regulating septin dynamics and cytokinesis. *The Journal of Cell Biology*. 171:773–784. doi:10.1083/jcb. 200507017.

Graziano, B.R., H.Y.E. Yu, S.L. Alioto, J.A. Eskin, C.A. Ydenberg, D.P. Waterman, M. Garabedian, and B.L. Goode. 2014. The F-BAR protein Hof1 tunes formin

activity to sculpt actin cables during polarized growth. *Molecular Biology of the Cell*. 25:1730–1743. doi:10.1091/mbc.E14-03-0850.

Guizetti, J., L. Schermelleh, J. Mantler, S. Maar, I. Poser, H. Leonhardt, T. Muller-Reichert, and D.W. Gerlich. 2011. Cortical Constriction During Abscission Involves Helices

of ESCRT-III–Dependent Filaments

. *Science*. 331:1612–1616. doi:10.1126/science.1198443.

Gunjan, A., and A. Verreault. 2003. A Rad53 kinase-dependent surveillance mechanism that regulates histone protein levels in S. cerevisiae. *Cell*. 115:537–549.

Gupta, M.L., P. Carvalho, D.M. Roof, and D. Pellman. 2006. Plus end-specific depolymerase activity of Kip3, a kinesin-8 protein, explains its role in positioning the yeast mitotic spindle. *Nat. Cell Biol.* 8:913–923. doi:10.1038/ncb1457.

Guse, A., M. Mishima, and M. Glotzer. 2005. Phosphorylation of ZEN-4/MKLP1 by Aurora B Regulates Completion of Cytokinesis. *Current Biology*. 15:778–786. doi:10.1016/j.cub.2005.03.041.

Hallett, M.A., H.S. Lo, and A. Bender. 2002. Probing the importance and potential roles of the binding of the PH-domain protein Boi1 to acidic phospholipids. *BMC Cell Biol*. 3:16.

Hildebrandt, E.R., and M.A. Hoyt. 2001. Cell cycle-dependent degradation of the Saccharomyces cerevisiae spindle motor Cin8p requires APC(Cdh1) and a bipartite destruction sequence. *Molecular Biology of the Cell*. 12:3402–3416.

Hills, S.A., and J.F.X. Diffley. 2014. DNA Replication and Oncogene-Induced Review Replicative Stress. *Current Biology*. 24:R435–R444. doi:10.1016/j.cub.2014.04.012.

Hoffelder, D.R., L. Luo, N.A. Burke, S.C. Watkins, S.M. Gollin, and W.S. Saunders. 2004. Resolution of anaphase bridges in cancer cells. *Chromosoma*. 112:389–397. doi:10.1007/s00412-004-0284-6.

Holland, A.J., and D.W. Cleveland. 2009. Boveri revisited: chromosomal instability, aneuploidy and tumorigenesis. 1–10. doi:10.1038/nrm2718.

Holm, C., T. Goto, J.C. Wang, and D. Botstein. 1985. DNA topoisomerase II is required at the time of mitosis in yeast. *Cell*. 41:553–563.

Hu, F., Y. Wang, D. Liu, Y. Li, J. Qin, and S.J. Elledge. 2001. Regulation of the Bub2/Bfa1 GAP complex by Cdc5 and cell cycle checkpoints. *Cell*. 107:655–665.

Idrissi, F.-Z., H. Grötsch, I.M. Fernández-Golbano, C. Presciatto-Baschong, H. Riezman, and M.-I. Geli. 2008. Distinct acto/myosin-I structures associate with

endocytic profiles at the plasma membrane. *The Journal of Cell Biology*. 180:1219–1232. doi:10.1083/jcb.200708060.

Ira, G., A. Pellicioli, A. Balijja, X. Wang, S. Fiorani, W. Carotenuto, G. Liberi, D. Bressan, L. Wan, N.M. Hollingsworth, J.E. Haber, and M. Foiani. 2004. DNA end resection, homologous recombination and DNA damage checkpoint activation require CDK1. *Nature*. 431:1011–1017. doi:10.1038/nature02964.

Janke, C., M.M. Magiera, N. Rathfelder, C. Taxis, S. Reber, H. Maekawa, A. Moreno-Borchart, G. Doenges, E. Schwob, E. Schiebel, and M. Knop. 2004. A versatile toolbox for PCR-based tagging of yeast genes: new fluorescent proteins, more markers and promoter substitution cassettes. *Yeast*. 21:947–962. doi:10.1002/yea.1142.

Janssen, A., M. van der Burg, K. Szuhai, G.J.P.L. Kops, and R.H. Medema. 2011. Chromosome Segregation Errors as a Cause of DNA Damage and Structural Chromosome Aberrations. *Science*. 333:1895–1898. doi:10.1126/science.1210214.

Jaspersen, S.L., J.F. Charles, and D.O. Morgan. 1999. Inhibitory phosphorylation of the APC regulator Hct1 is controlled by the kinase Cdc28 and the phosphatase Cdc14. *Current Biology*. 9:227–236.

Juang, Y.L. 1997. APC-Mediated Proteolysis of Ase1 and the Morphogenesis of the Mitotic Spindle. *Science*. 275:1311–1314. doi:10.1126/science.275.5304.1311.

Kamei, T., K. Tanaka, T. Hihara, M. Umikawa, H. Imamura, M. Kikyo, K. Ozaki, and Y. Takai. 1998. Interaction of Bnr1p with a novel Src homology 3 domain-containing Hof1p. Implication in cytokinesis in Saccharomyces cerevisiae. *J. Biol. Chem.* 273:28341–28345.

Kimura, K., O. Cuvier, and T. Hirano. 2001. Chromosome Condensation by a Human Condensin Complex inXenopus Egg Extracts. *Journal of Biological Chemistry*. 276:5417–5420. doi:10.1074/jbc.C000873200.

Kitamura, E., K. Tanaka, Y. Kitamura, and T.U. Tanaka. 2007. Kinetochore microtubule interaction during S phase in Saccharomyces cerevisiae. *Genes & Development*. 21:3319–3330. doi:10.1101/gad.449407.

Kiyomitsu, T., and I.M. Cheeseman. 2013. Cortical Dynein and Asymmetric Membrane Elongation Coordinately Position the Spindle in Anaphase. *Cell*. 154:391–402. doi:10.1016/j.cell.2013.06.010.

Kotwaliwale, C.V., S.B. Frei, B.M. Stern, and S. Biggins. 2007. A Pathway Containing the Ipl1/Aurora Protein Kinase and the Spindle Midzone Protein Ase1 Regulates Yeast Spindle Assembly. *Developmental Cell*. 13:433–445. doi:10.1016/j.devcel.2007.07.003.

Kremer, J.R., D.N. Mastronarde, and J.R. McIntosh. 1996. Computer visualization of three-dimensional image data using IMOD. *Journal of Structural Biology*. 116:71–76. doi:10.1006/jsbi.1996.0013.

Kuranda, M.J., and P.W. Robbins. 1991. Chitinase is required for cell separation during growth of Saccharomyces cerevisiae. *J. Biol. Chem.* 266:19758–19767.

Labib, K. 2010. How do Cdc7 and cyclin-dependent kinases trigger the initiation of chromosome replication in eukaryotic cells? *Genes & Development*. 24:1208–1219. doi:10.1101/gad.1933010.

Lafaurie-Janvore, J., P. Maiuri, I. Wang, M. Pinot, J.-B. Manneville, T. Betz, M. Balland, and M. Piel. 2013. ESCRT-III assembly and cytokinetic abscission are induced by tension release in the intercellular bridge. *Science*. 339:1625–1629. doi:10.1126/science.1233866.

Lavoie, B.D. 2004. In vivo requirements for rDNA chromosome condensation reveal two cell-cycle-regulated pathways for mitotic chromosome folding. *Genes & Development*. 18:76–87. doi:10.1101/gad.1150404.

Lavoie, B.D., E. Hogan, and D. Koshland. 2002. In vivo dissection of the chromosome condensation machinery: reversibility of condensation distinguishes contributions of condensin and cohesin. *The Journal of Cell Biology*. 156:805–815. doi:10.1083/jcb.200109056.

Lee, P.R., S. Song, H.S. Ro, C.J. Park, J. Lippincott, R. Li, J.R. Pringle, C. De Virgilio, M.S. Longtine, and K.S. Lee. 2002. Bni5p, a Septin-Interacting Protein, Is Required for Normal Septin Function and Cytokinesis in Saccharomyces cerevisiae. *Molecular and Cellular Biology*. 22:6906–6920. doi:10.1128/MCB.22.19.6906-6920.2002.

Lippincott, J. 2000. Nuclear Envelope Fission Is Linked to Cytokinesis in Budding Yeast. *Experimental Cell Research*. 260:277–283. doi:10.1006/excr.2000.5021.

Lippincott, J., and R. Li. 1998a. Sequential assembly of myosin II, an IQGAP-like protein, and filamentous actin to a ring structure involved in budding yeast cytokinesis. *The Journal of Cell Biology*. 140:355–366.

Lippincott, J., and R. Li. 1998b. Dual function of Cyk2, a cdc15/PSTPIP family protein, in regulating actomyosin ring dynamics and septin distribution. *The Journal of Cell Biology*. 143:1947–1960.

Lippincott, J., K.B. Shannon, W. Shou, R.J. Deshaies, and R. Li. 2001. The Tem1 small GTPase controls actomyosin and septin dynamics during cytokinesis. *Journal of Cell Science*. 114:1379–1386.

Liu, D., G. Vader, M.J.M. Vromans, M.A. Lampson, and S.M.A. Lens. 2009. Sensing chromosome bi-orientation by spatial separation of aurora B kinase from kinetochore substrates. *Science*. 323:1350–1353. doi:10.1126/science.1167000.

Lopez, V., N. Barinova, M. Onishi, S. Pobiega, J.R. Pringle, K. Dubrana, and S. Marcand. 2015. Cytokinesis breaks dicentric chromosomes preferentially at

pericentromeric regions and telomere fusions. *Genes & Development*. 29:322–336. doi:10.1101/gad.254664.114.

Louvion, J.F., B. Havaux-Copf, and D. Picard. 1993. Fusion of GAL4-VP16 to a steroid-binding domain provides a tool for gratuitous induction of galactose-responsive genes in yeast. *Gene*. 131:129–134.

Lucena, R., N. Dephoure, S.P. Gygi, D.R. Kellogg, V.A. Tallada, R.R. Daga, and J. Jiménez. 2015. Nucleocytoplasmic transport in the midzone membrane domain controls yeast mitotic spindle disassembly. *The Journal of Cell Biology*. 209:387–402. doi:10.1371/journal.pbio.0050170.

Mackay, D.R., M. Makise, and K.S. Ullman. 2010. Defects in nuclear pore assembly lead to activation of an Aurora B-mediated abscission checkpoint. *The Journal of Cell Biology*. 191:923–931. doi:10.1093/emboj/20.20.5703.

Maddox, P.S., K.S. Bloom, and E.D. Salmon. 2000. The polarity and dynamics of microtubule assembly in the budding yeast Saccharomyces cerevisiae. *Nat. Cell Biol.* 2:36–41. doi:10.1038/71357.

Masai, H., S. Matsumoto, Z. You, N. Yoshizawa-Sugata, and M. Oda. 2010. Eukaryotic Chromosome DNA Replication: Where, When, and How? *Annu. Rev. Biochem.* 79:89–130. doi:10.1146/annurev.biochem.052308.103205.

McClintock, B. 1941. The Stability of Broken Ends of Chromosomes in Zea Mays. *Genetics*. 26:234–282.

McKnight, K., H. Liu, and Y. Wang. 2014. Replicative Stress Induces Intragenic Transcription of the ASE1 Genethat Negatively Regulates Ase1 Activity. *Current Biology*. 24:1101–1106. doi:10.1016/j.cub.2014.03.040.

McMurray, M.A., C.J. Stefan, M. Wemmer, G. Odorizzi, S.D. Emr, and J. Thorner. 2011. Genetic interactions with mutations affecting septin assembly reveal ESCRT functions in budding yeast cytokinesis. *Biological Chemistry*. 392. doi: 10.1515/BC.2011.091.

Meitinger, F., M.E. Boehm, A. Hofmann, B. Hub, H. Zentgraf, W.D. Lehmann, and G. Pereira. 2011. Phosphorylation-dependent regulation of the F-BAR protein Hof1 during cytokinesis. *Genes & Development*. 25:875–888. doi:10.1101/gad.622411.

Mendoza, M., C. Norden, K. Durrer, H. Rauter, F. Uhlmann, and Y. Barral. 2009. A mechanism for chromosome segregation sensing by the NoCut checkpoint. *Nat. Cell Biol.* 11:477–483. doi:10.1038/ncb1855.

Mirchenko, L., and F. Uhlmann. 2010. Dephosphorylation Prevents Mitotic Checkpoint ReengagementDue to Loss of Tension at Anaphase OnsetRepor t. *Curr. Biol.* 20:1396–1401. doi:10.1016/j.cub.2010.06.023.

Mishra, M., J. Kashiwazaki, T. Takagi, R. Srinivasan, Y. Huang, M.K. Balasubramanian, and I. Mabuchi. 2013. In vitro contraction of cytokinetic ring depends on myosin II but not on actin dynamics. 1–15. doi:10.1038/ncb2781.

Mohl, D.A., M.J. Huddleston, T.S. Collingwood, R.S. Annan, and R.J. Deshaies. 2009. Dbf2-Mob1 drives relocalization of protein phosphatase Cdc14 to the cytoplasm during exit from mitosis. *The Journal of Cell Biology*. 184:527–539. doi:10.1126/science.282.5394.1721.

Morgan, D.O. 2007. The Cell Cycle. New Science Press. 1 pp.

Neurohr, G., A. Naegeli, I. Titos, D. Theler, B. Greber, J. Diez, T. Gabaldon, M. Mendoza, and Y. Barral. 2011. A Midzone-Based Ruler Adjusts Chromosome Compaction to Anaphase Spindle Length. *Science*. 332:465–468. doi: 10.1126/science.1201578.

Neurohr, G. 2012. A Midzone-Based Ruler Adjusts Chromosome Compaction to Anaphase Spindle Length. UPF.

Nishihama, R., J.H. Schreiter, M. Onishi, E.A. Vallen, J. Hanna, K. Moravcevic, M.F. Lippincott, H. Han, M.A. Lemmon, J.R. Pringle, and E. Bi. 2009. Role of Inn1 and its interactions with Hof1 and Cyk3 in promoting cleavage furrow and septum formation in S. cerevisiae. *The Journal of Cell Biology*. 185:995–1012. doi:10.1083/jcb.200604094.

Norden, C., M. Mendoza, J. Dobbelaere, C.V. Kotwaliwale, S. Biggins, and Y. Barral. 2006. The NoCut pathway links completion of cytokinesis to spindle midzone function to prevent chromosome breakage. *Cell*. 125:85–98. doi:10.1016/j.cell.2006.01.045.

Oh, Y., J. Schreiter, R. Nishihama, C. Wloka, and E. Bi. 2013. Targeting and functional mechanisms of the cytokinesis-related F-BAR protein Hof1 during the cell cycle. *Molecular Biology of the Cell*. 24:1305–1320. doi:10.1091/mbc.E12-11-0804.

Onishi, M., N. Ko, R. Nishihama, and J.R. Pringle. 2013. Distinct roles of Rho1, Cdc42, and Cyk3 in septum formation and abscission during yeast cytokinesis. *The Journal of Cell Biology*. 202:311–329. doi:10.1074/jbc.M402292200.

Ono, T., D. Yamashita, and T. Hirano. 2013. Condensin II initiates sister chromatid resolution during S phase. *The Journal of Cell Biology*. 200:429–441. doi: 10.1083/jcb.201208008.dv.

Palani, S., F. Meitinger, M.E. Boehm, W.D. Lehmann, and G. Pereira. 2012. Cdc14-dependent dephosphorylation of Inn1 contributes to Inn1-Cyk3 complex formation. *Journal of Cell Science*. 125:3091–3096. doi:10.1242/jcs.106021.

Pereira, G. 2003. Separase Regulates INCENP-Aurora B Anaphase Spindle Function Through Cdc14. *Science*. 302:2120–2124. doi:10.1126/science.1091936.

Perkins, G., L.S. Drury, and J.F. Diffley. 2001. Separate SCF(CDC4) recognition elements target Cdc6 for proteolysis in S phase and mitosis. *The EMBO Journal*. 20:4836–4845. doi:10.1093/emboj/20.17.4836.

Petersen, B.O., J. Lukas, C.S. Sørensen, J. Bartek, and K. Helin. 1999. Phosphorylation of mammalian CDC6 by cyclin A/CDK2 regulates its subcellular localization. *The EMBO Journal*. 18:396–410. doi:10.1093/emboj/18.2.396.

Piatti, S., T. Böhm, J.H. Cocker, J.F. Diffley, and K. Nasmyth. 1996. Activation of S-phase-promoting CDKs in late G1 defines a “point of no return” after which Cdc6 synthesis cannot promote DNA replication in yeast. *Genes & Development*. 10:1516–1531.

Pinsky, B.A., C. Kung, K.M. Shokat, and S. Biggins. 2005. The Ipl1-Aurora protein kinase activates the spindle checkpoint by creating unattached kinetochores. *Nat. Cell Biol.* 8:78–83. doi:10.1038/ncb1341.

Pinto, I.M., B. Rubinstein, A. Kucharavy, J.R. Unruh, and R. Li. 2012. Actin Depolymerization Drives Actomyosin Ring Contraction during Budding Yeast Cytokinesis. *Developmental Cell*. 22:1247–1260. doi:10.1016/j.devcel.2012.04.015.

Pobiega, S., and S. Marcand. 2010. Dicentric breakage at telomere fusions. *Genes & Development*. 24:720–733. doi:10.1101/gad.571510.

Queralt, E., C. Lehane, B. Novak, and F. Uhlmann. 2006. Downregulation of PP2ACdc55 Phosphatase by Separase Initiates Mitotic Exit in Budding Yeast. *Cell*. 125:719–732. doi:10.1016/j.cell.2006.03.038.

Ramadan, K., R. Bruderer, F.M. Spiga, O. Popp, T. Baur, M. Gotta, and H.H. Meyer. 2007. Cdc48/p97 promotes reformation of the nucleus by extracting the kinase Aurora B from chromatin. *Nature*. 450:1258–1262. doi:10.1038/nature06388.

Rancati, G., N. Pavelka, B. Fleharty, A. Noll, R. Trimble, K. Walton, A. Perera, K. Staehling-Hampton, C.W. Seidel, and R. Li. 2008. Aneuploidy Underlies Rapid Adaptive Evolution of Yeast Cells Deprivedof a Conserved Cytokinesis Motor. *Cell*. 135:879–893. doi:10.1016/j.cell.2008.09.039.

Renshaw, M.J., J.J. Ward, M. Kanemaki, K. Natsume, F.J. Nédélec, and T.U. Tanaka. 2010. Condensins Promote Chromosome Recoiling during Early Anaphase to Complete Sister Chromatid Separation. *Developmental Cell*. 19:232–244. doi:10.1016/j.devcel.2010.07.013.

Richman, T.J., M.M. Sawyer, and D.I. Johnson. 1999. The Cdc42p GTPase is involved in a G2/M morphogenetic checkpoint regulating the apical-isotropic switch and nuclear division in yeast. *J. Biol. Chem.* 274:16861–16870.

Sacristan, C., and G.J.P.L. Kops. 2015. Joined at the hip: kinetochores, microtubules, and spindle assembly checkpoint signaling. *Trends in Cell Biology*. 25:21–28. doi:10.1016/j.tcb.2014.08.006.

Sadian, Y., C. Gatsogiannis, C. Patasi, O. Hofnagel, R.S. Goody, M. Farkašovský, and S. Raunser. 2013. The role of Cdc42 and Gic1 in the regulation of septin filament formation and dissociation. *eLife*. 2:e01085. doi:10.7554/eLife.01085.

Sagot, I., S.K. Klee, and D. Pellman. 2002. Yeast formins regulate cell polarity by controlling the assembly of actin cables. *Nat. Cell Biol.* 4:42–50. doi:10.1038/ncb719.

Sanchez, Y., J. Bachant, H. Wang, F. Hu, D. Liu, M. Tetzlaff, and S.J. Elledge. 1999. Control of the DNA damage checkpoint by chk1 and rad53 protein kinases through distinct mechanisms. *Science*. 286:1166–1171.

Sanchez-Diaz, A., V. Marchesi, S. Murray, R. Jones, G. Pereira, R. Edmondson, T. Allen, and K. Labib. 2008. Inn1 couples contraction of the actomyosin ring to membrane ingression during cytokinesis in budding yeast. *Nat. Cell Biol.* 10:395–406. doi:10.1038/ncb1701.

Saunders, W.S., and M.A. Hoyt. 1992. Kinesin-related proteins required for structural integrity of the mitotic spindle. *Cell*. 70:451–458.

Schiel, J.A., K. Park, M.K. Morphew, E. Reid, A. Hoenger, and R. Prekeris. 2011. Endocytic membrane fusion and buckling-induced microtubule severing mediate cell abscission. *Journal of Cell Science*. 124:1769–1769. doi:10.1242/jcs.092007.

Schmidt, M., B. Bowers, A. Varma, D.-H. Roh, and E. Cabib. 2002. In budding yeast, contraction of the actomyosin ring and formation of the primary septum at cytokinesis depend on each other. *Journal of Cell Science*. 115:293–302.

Schuyler, S.C., J.Y. Liu, and D. Pellman. 2003. The molecular function of Ase1p: evidence for a MAP-dependent midzone-specific spindle matrix. *The Journal of Cell Biology*. 160:517–528. doi:10.1083/jcb.200210021.

Schwab, M., A.S. Lutum, and W. Seufert. 1997. Yeast Hct1 is a regulator of Clb2 cyclin proteolysis. *Cell*. 90:683–693.

Severin, F., B. Habermann, T. Huffaker, and T. Hyman. 2001. Stu2 promotes mitotic spindle elongation in anaphase. *The Journal of Cell Biology*. 153:435–442.

Shaw, J.A., P.C. Mol, B. Bowers, S.J. Silverman, M.H. Valdivieso, A. Durán, and E. Cabib. 1991. The function of chitin synthases 2 and 3 in the Saccharomyces cerevisiae cell cycle. *The Journal of Cell Biology*. 114:111–123.

Sheltzer, J.M., H.M. Blank, S.J. Pfau, Y. Tange, B.M. George, T.J. Humpton, I.L. Brito, Y. Hiraoka, O. Niwa, and A. Amon. 2011. Aneuploidy Drives Genomic Instability in Yeast. *Science*. 333:1026–1030. doi:10.1126/science.1206412.

Shou, W., J.H. Seol, A. Shevchenko, C. Baskerville, D. Moazed, Z.W. Chen, J. Jang, A. Shevchenko, H. Charbonneau, and R.J. Deshaies. 1999. Exit from mitosis is triggered by Tem1-dependent release of the protein phosphatase Cdc14 from nucleolar RENT complex. *Cell*. 97:233–244.

Simoneau, A., X. Robellet, A.-M. Ladouceur, and D. D'Amours. 2014. Cdk1-dependent regulation of the Mre11 complex couples DNA repair pathways to cell cycle progression. *Cell Cycle*. 13:1078–1090. doi:10.4161/cc.27946.

Sloat, B.F., A. Adams, and J.R. Pringle. 1981. Roles of the CDC24 gene product in cellular morphogenesis during the Saccharomyces cerevisiae cell cycle. *The Journal of Cell Biology*. 89:395–405.

Sonneville, R., G. Craig, K. Labib, A. Gartner, and J.J. Blow. 2015. Both Chromosome Decondensation and Condensation Are Dependent on DNA Replication in C. elegans Embryos. *CellReports*. 12:405–417. doi:10.1016/j.celrep.2015.06.046.

Speck, C., and B. Stillman. 2007. Cdc6 ATPase activity regulates ORC x Cdc6 stability and the selection of specific DNA sequences as origins of DNA replication. *J. Biol. Chem.* 282:11705–11714. doi:10.1074/jbc.M700399200.

St-Pierre, J., M. Douziech, F. Bazile, M. Pascariu, É. Bonneil, V. SauvE, H. Ratsima, and D.D. Amours. 2009. Polo Kinase Regulates Mitotic Chromosome Condensation by Hyperactivationof Condensin DNA Supercoiling Activity. *MOLCEL*. 34:416–426. doi:10.1016/j.molcel.2009.04.013.

Stegmeier, F., R. Visintin, and A. Amon. 2002. Separase, polo kinase, the kinetochore protein Slk19, and Spo12 function in a network that controls Cdc14 localization during early anaphase. *Cell*. 108:207–220.

Steigemann, P., C. Wurzenberger, M.H.A. Schmitz, M. Held, J. Guizetti, S. Maar, and D.W. Gerlich. 2009. Aurora B-Mediated Abscission Checkpoint Protects against Tetraploidization. *Cell*. 136:473–484. doi:10.1016/j.cell.2008.12.020.

Stephens, P.J., C.D. Greenman, B. Fu, F. Yang, G.R. Bignell, L.J. Mudie, E.D. Pleasance, K.W. Lau, D. Beare, L.A. Stebbings, S. McLaren, M.-L. Lin, D.J. McBride, I. Varela, S. Nik-Zainal, C. Leroy, M. Jia, A. Menzies, A.P. Butler, J.W. Teague, M.A. Quail, J. Burton, H. Swerdlow, N.P. Carter, L.A. Morsberger, C. Iacobuzio-Donahue, G.A. Follows, A.R. Green, A.M. Flanagan, M.R. Stratton, P.A. Futreal, and P.J. Campbell. 2011. Massive Genomic Rearrangement Acquired in a Single Catastrophic Eventduring Cancer Development. *Cell*. 144:27–40. doi:10.1016/j.cell.2010.11.055.

Stewénius, Y., L. Gorunova, T. Jonson, N. Larsson, M. Höglund, N. Mandahl, F. Mertens, F. Mitelman, and D. Gisselsson. 2005. Structural and numerical chromosome changes in colon cancer develop through telomere-mediated anaphase bridges, not through mitotic multipolarity. *Proc. Natl. Acad. Sci. U.S.A.* 102:5541–5546. doi:10.1073/pnas.0408454102.

Stracker, T.H., and J.H.J. Petrini. 2011. The MRE11 complex: starting from the ends. *Nat. Rev. Mol. Cell Biol.* 12:90–103. doi:10.1038/nrm3047.

Tanaka, H., Y. Katou, M. Yagura, K. Saitoh, T. Itoh, H. Araki, M. Bando, and K. Shirahige. 2009. Ctf4 coordinates the progression of helicase and DNA polymerase α. *Genes to Cells*. 14:807–820. doi:10.1111/j.1365-2443.2009.01310.x.

Tanaka, T.U., N. Rachidi, C. Janke, G. Pereira, M. Galova, E. Schiebel, M.J.R. Stark, and K. Nasmyth. 2002. Evidence that the Ipl1-Sli15 (Aurora kinase-INCENP) complex promotes chromosome bi-orientation by altering kinetochore-spindle pole connections. *Cell*. 108:317–329.

Tang, C.S.L., and S.I. Reed. 2002. Phosphorylation of the septin cdc3 in g1 by the cdc28 kinase is essential for efficient septin ring disassembly. *Cell Cycle*. 1:42–49. doi:10.4161/cc.1.1.99.

Thomas, S., and K.B. Kaplan. 2007. A Bir1p Sli15p kinetochore passenger complex regulates septin organization during anaphase. *Molecular Biology of the Cell*. 18:3820–3834. doi:10.1091/mbc.E07-03-0201.

Thoresen, S.B., C. Campsteijn, M. Vietri, K.O. Schink, K. Liestøl, J.S. Andersen, C. Raiborg, and H. Stenmark. 2014. ANCHR mediates Aurora-B-dependent abscission checkpoint control through retention of VPS4. *Nat. Cell Biol.* doi:10.1038/ncb2959.

Tian, C., Y. Wu, and N. Johnsson. 2014. Stepwise and cooperative assembly of a cytokinetic core complex in yeast Saccharomyces cerevisiae. *Journal of Cell Science*. doi:10.1242/jcs.153429.

Titos, I., T. Ivanova, and M. Mendoza. 2014. Chromosome length and perinuclear attachment constrain resolution of DNA intertwines. *The Journal of Cell Biology*. 206:719–733. doi:10.1534/genetics.111.128710.

Tolliday, N., L. VerPlank, and R. Li. 2002. Rho1 directs formin-mediated actin ring assembly during budding yeast cytokinesis. *Curr. Biol.* 12:1864–1870.

Tolliday, N., M. Pitcher, and R. Li. 2003. Direct evidence for a critical role of myosin II in budding yeast cytokinesis and the evolvability of new cytokinetic mechanisms in the absence of myosin II. *Molecular Biology of the Cell*. 14:798–809. doi:10.1091/mbc.E02-09-0558.

Tully, G.H., R. Nishihama, J.R. Pringle, and D.O. Morgan. 2009. The anaphase-promoting complex promotes actomyosin-ring disassembly during cytokinesis in yeast. *Molecular Biology of the Cell*. 20:1201–1212. doi:10.1091/mbc.E08-08-0822.

Uhlmann, F., D. Wernic, M.A. Poupart, E.V. Koonin, and K. Nasmyth. 2000. Cleavage of cohesin by the CD clan protease separin triggers anaphase in yeast. *Cell*. 103:375–386.

Vallen, E.A., J. Caviston, and E. Bi. 2000. Roles of Hof1p, Bni1p, Bnr1p, and myo1p in cytokinesis in Saccharomyces cerevisiae. *Molecular Biology of the Cell*. 11:593–611.

VerPlank, L., and R. Li. 2005. Cell cycle-regulated trafficking of Chs2 controls actomyosin ring stability during cytokinesis. *Molecular Biology of the Cell*. 16:2529–2543. doi:10.1091/mbc.E04-12-1090.

Visintin, R., E.S. Hwang, and A. Amon. 1999. Cfi1 prevents premature exit from mitosis by anchoring Cdc14 phosphatase in the nucleolus. *Nature*. 398:818–823. doi:10.1038/19775.

Visintin, R., K. Craig, E.S. Hwang, S. Prinz, M. Tyers, and A. Amon. 1998. The phosphatase Cdc14 triggers mitotic exit by reversal of Cdk-dependent phosphorylation. *Molecular Cell*. 2:709–718.

Wang, H., D. Liu, Y. Wang, J. Qin, and S.J. Elledge. 2001. Pds1 phosphorylation in response to DNA damage is essential for its DNA damage checkpoint function. *Genes & Development*. 15:1361–1372. doi:10.1101/gad.893201.

Wang, J.C. 2002. Cellular roles of dna topoisomerases: a molecular perspective. *Nat. Rev. Mol. Cell Biol.* 3:430–440. doi:10.1038/nrm831.

Weiss, E.L. 2002. The Saccharomyces cerevisiae Mob2p-Cbk1p kinase complex promotes polarized growth and acts with the mitotic exit network to facilitate daughter cell-specific localization of Ace2p transcription factor. *The Journal of Cell Biology*. 158:885–900. doi:10.1083/jcb.200203094.

Weiss, E.L. 2012. Mitotic Exit and Separation of Mother and Daughter Cells. *Genetics*. 192:1165–1202. doi:10.1534/genetics.112.145516.

Winey, M., and E.T. O'Toole. 2001. The spindle cycle in budding yeast. *Nat. Cell Biol.* 3:E23–7. doi:10.1038/35050663.

Winey, M., C.L. Mamay, E.T. O'Toole, D.N. Mastronarde, T.H. Giddings, K.L. McDonald, and J.R. McIntosh. 1995. Three-dimensional ultrastructural analysis of the Saccharomyces cerevisiae mitotic spindle. *The Journal of Cell Biology*. 129:1601–1615.

Wood, J.S., and L.H. Hartwell. 1982. A dependent pathway of gene functions leading to chromosome segregation in Saccharomyces cerevisiae. *The Journal of Cell Biology*. 94:718–726.

Woodbury, E.L., and D.O. Morgan. 2006. Cdk and APC activities limit the spindle-stabilizing function of Fin1 to anaphase. *Nat. Cell Biol.* 9:106–112. doi: 10.1038/ncb1523.

Woodruff, J.B., D.G. Drubin, and G. Barnes. 2010. Mitotic spindle disassembly occurs via distinct subprocesses driven by the anaphase-promoting complex, Aurora B kinase, and kinesin-8. *The Journal of Cell Biology*. 191:795–808. doi:10.1083/jcb.201006028.

Yang, D., N. Rismanchi, B. Renvoisé, J. Lippincott-Schwartz, C. Blackstone, and J.H. Hurley. 2008. Structural basis for midbody targeting of spastin by the ESCRT-III protein CHMP1B. *Nat Struct Mol Biol*. 15:1278–1286. doi:10.1038/nsmb.1512.

Yang, S.S., E. Yeh, E.D. Salmon, and K. Bloom. 1997. Identification of a mid-anaphase checkpoint in budding yeast. *The Journal of Cell Biology*. 136:345–354.

Zhang, J., C. Kong, H. Xie, P.S. McPherson, S. Grinstein, and W.S. Trimble. 1999. Phosphatidylinositol polyphosphate binding to the mammalian septin H5 is modulated by GTP. *Curr. Biol.* 9:1458–1467.

Zhao, W.-M., A. Seki, and G. fang. 2006. Cep55, a microtubule-bundling protein, associates with centralspindlin to control the midbody integrity and cell abscission during cytokinesis. *Molecular Biology of the Cell*. 17:3881–3896. doi:10.1091/mbc.E06-01-0015.

Zhao, X., A. Chabes, V. Domkin, L. Thelander, and R. Rothstein. 2001. The ribonucleotide reductase inhibitor Sml1 is a new target of the Mec1/Rad53 kinase cascade during growth and in response to DNA damage. *The EMBO Journal*. 20:3544–3553. doi:10.1093/emboj/20.13.3544.

Zhao, X., E.G. Muller, and R. Rothstein. 1998. A suppressor of two essential checkpoint genes identifies a novel protein that negatively affects dNTP pools. *MOLCEL*. 2:329–340.

Ziman, M., D. Preuss, J. Mulholland, J.M. O'Brien, D. Botstein, and D.I. Johnson. 1993. Subcellular localization of Cdc42p, a Saccharomyces cerevisiae GTP-binding protein involved in the control of cell polarity. *Molecular Biology of the Cell*. 4:1307–1316.

Zimniak, T., K. Stengl, K. Mechtler, and S. Westermann. 2009. Phosphoregulation of the budding yeast EB1 homologue Bim1p by Aurora/Ipl1p. *The Journal of Cell Biology*. 186:379–391. doi:10.1091/mbc.E07-06-0536.

Zimniak, T., V. Fitz, H. Zhou, F. Lampert, S. Opravil, K. Mechtler, P. Stolt-Bergner, and S. Westermann. 2012. Spatiotemporal Regulationof Ipl1/Aurora Activityby Direct Cdk1 Phosphorylation. *Current Biology*. 22:787–793. doi:10.1016/j.cub.2012.03.007.

9. Acknowledgements

This work would not have been possible without the help of many people and institutions. I was fortunate to meet many interesting and interested people along the way who helped me become a better scientist. To those with whom I had the opportunity to learn from and discuss science my heartfelt thank you.

I am very grateful to my PhD supervisor Manuel Mendoza, for the opportunity to work in an exciting and challenging project. Thank you for introducing me to science, with many fruitful discussions; for the patience in teaching me and for giving me the freedom to explore (some times crazy) ideas.

I would like to thank my PhD committee: Fernando Monje-Casas, Pedro Carvalho and Pia Cosma, for the support, advice and useful feedback on the project.

Thank you in advance to the PhD defense panel: Doctors Ethel Queralt, Isabelle Vernos and Jeremy Carlton, for the interest and critical reading of this thesis.

I would like to express my gratitude to the people who have collaborated with me to make this work possible: Alex, Arun, Gabriel and Michael; Charlotta, Fatima, Neus, Maribel Geli and Jordi Torres-Rosell.

I acknowledge the staff of the Advance Light Microscopy Unit, for their assistance to the many many hours of imaging I did.

To the CRG, which besides a great location provided a great scientific environment and helped in my development. I would also like to thank the labs in the Cell and Developmental Biology department for the useful discussions during data clubs.

To the past and the current members of the Mendoza lab. Aina, Alex, Andrea, Anne, Arun, Francesca, Gabriel, Ibrahim, Iris, Michael, Nicola, Petra, Ping, Trini and Tsveti, thank you so much for making these years really special. I feel lucky to have found such smart, warm and friendly people. Thank you for all the scientific discussions I had with each one of you and for all the times you made me see things differently. Also thank you for all the fun we had, particularly for the past-6 o'clock daily stupidity. Thank you for trusting me and caring about me.
In particular I would like to thank to: Trini, tu eres el alma del labo. Muchíssimas grácias por toda la ayuda y la amistad; and to the NoCut team, Andrea and Nicola, for our fantastic discussions and for "The first-ever-worldwide NoCut meeting".

Obrigado à minha família. À minha esposa Carolina, aos meus queridos pais Álvaro e Teresa e ao meu irmão Ricardo por todo o apoio que me deram durante estes anos. Por serem o meu "porto de abrigo" e por acreditarem sempre em mim.